Design and Synthesis of Metal-Organic Frameworks for Selective Sensing Applications

A thesis

Submitted in partial fulfillment of the requirements

Of the degree of

Doctor of Philosophy

By

Sanjog S. Nagarkar

ID: 20103056

INDIAN INSTITUTE OF SCIENCE EDUCATION AND RESEARCH, PUNE

2015

Dedicated to...

My Beloved Father
& my Inspiration
Late Mr. Sunil L. Nagarkar

CERTIFICATE

Certified that the work incorporated in the thesis entitled "***Design and Synthesis of Metal-Organic Frameworks for Selective Sensing Applications"*** submitted by **Mr. Sanjog S. Nagarkar** was carried out by the candidate, under my supervision. The work presented here or any part of it has not been included in any other thesis submitted previously for the award of any degree or diploma from any other university or institution.

Date:

Dr. Sujit K. Ghosh
(Research Supervisor)

DECLARATION

I Mr. **Sanjog S. Nagarkar** declare that, this written submission represents my ideas in my own words and where others' ideas have been included; I have adequately cited and referenced the original sources. I also declare that I have adhered to all principles of academic honesty and integrity and have not misrepresented or fabricated or falsified any idea / data / fact / source in my submission. I understand that violation of the above will be cause for disciplinary action by the Institute and can also evoke penal action from the sources which have thus not been properly cited or from whom proper permission has not been taken when needed.

Date:

Mr. Sanjog S. Nagarkar

(ID: 20103056)

Acknowledgements

I would like to express my special appreciation and thanks to my advisor Dr. Sujit K. Ghosh, sir you have been a tremendous mentor for me. I would also like to thank you for believing in me, encouraging my research and for allowing me to grow as a researcher. I cannot forget the freedom which you have given to me to work and explore new research ideas. I could not have imagined better advisor and mentor for my doctoral studies. Your advice regarding research as well as my career has been priceless. Thank you very much sir for making me capable and I believe this experience will be helpful in future also.

I sincerely thank Director, Prof. K. N. Ganesh for providing state of the art research facilities and financial support during my research stay at IISER-Pune. I am also thankful to the CSIR, India for research fellowship during my research work at IISER-Pune.

I am very grateful to my Research Advisory Committee (RAC) members, Dr. Pankaj Poddar (National Chemical Laboratory, Pune) and Dr. R. Boomi Shankar (IISER-Pune) for their valuable suggestions and continual support during RAC meetings. I am deeply grateful to the entire Department of Chemistry at IISER Pune, all the faculty members especially to Dr. Partha Hazra, Dr. Nirmalya Ballav and Dr. Seema Varma for valuable suggestions during this work. I also would like to thank Dr. Asha and group from NCL-Pune for help during fluorescence measurements.

I am really lucky to have wonderful lab mates who have played a very crucial role in my day to day life during my research tenure. I also thanks to my lab mates Biplab Joarder, Biplab Manna, Avishek, Soumya, Aamod, Partha, Arif. I cannot forget the former member of our lab Remya, Mahendra, Abhijeet, Amitosh, Amrit, Shweta and Bharat. I also want to thank our new lab members with whom I worked for short duration in the lab but really helped me by their own way including Naveen, Shivani, Kriti and Amit. The "SKG laboratory" always supported me morally and scientifically during my entire research stay at IISER, Pune and will always remain an unforgettable episode in my entire life.

I deeply thankful to Archana for her help during single crystal X-ray analysis and Swati, Prashant, Nilesh and Anil for their help during various instrumental analyses.

I am grateful to Mayuresh, Mahesh and Nitin for administrative and official support. Special thanks go to Prof. V S Rao and Mr. Prabhas Patankar for their valuable support.

I enjoyed and shared my achievements and failures during research work with my friends. I am grateful to my friends Dnyaneshwar, Anupam, Satish, Gopalkrishna, Shekhar, Abhigyan, Sachin, Prakash, Nitin, Arvind, Santosh, Mahesh, Indu, Arun, and Pramod. Thank you all for your friendship, stimulating advice, positive criticism and support which encouraged me and played pivotal role in shaping my life during these past five years.

I would offer my sincere thanks to Sudarshana mam for her valuable guidance at early stage of the research which certainly helped me over these 5 years.

I would like to thank my parents and my family. I am indebted to my mother for giving endless support, unconditional love and encouragement. I owe much to her for her support to overcome difficulties I have encountered. The values and virtues she has instilled in me have made me achieve whatever I have achieved so far. I hope with my hard work and dedication, I would be able to translate their dreams into reality.

Finally, my deepest appreciation and love devoted to my dear wife, Snehal. The time, when I thought I would never get to this page, you were always there to encourage me and believing in me. I am grateful to her for her sacrifices, patience and support for us to have such a beautiful life.

I am so grateful to all of the amazing people that have directly or indirectly helped me along the way.

Sanjog S. Nagarkar

Table of Contents

List of Symbols and Abbreviations

°C	Degree Celsius
1,3-DNB	1,3-dinitrobenzene
^{1}H NMR	Proton nuclear magnetic resonance spectroscopy
2,4-DNP	2,4-dinitrophenol
2,4-DNT	2,4-dinitrotoluene
2,6-DNT	2,6-dinitrotoluene
Å	Angstrom
cm^{-1}	Centimeter inverse
CO	Carbon monoxide
Cys	Cysteine
D_2O	Deuterium oxide
DMEM	Dulbecco's modified eagle's medium
DMF	Dimethyl formamide
DMNB	2,3-dimethyl-2,3-dinitrobutane
DMSO	Dimethyl sulfoxide
DMSO-d6	Dimethyl sulfoxide deuterated
FT-IR	Fourier transformed infrared spectroscopy
GSH	Glutathione
H_2S	Hydrogen sulfide
HeLa	Type of cells taken from Henrietta Lacks
HEPES	4-(2-hydroxyethyl)piperazine-1-ethanesulfonic acid
HF	Hydrofluoric Acid
Hz	Hertz
K	Kelvin
MeCN	Acetonitrile
MeOH	Methanol
mg	Milligram(s)
MHz	Megahertz
mM	Milimole(s)
mol	Moles

MTT	3-(4,5-dimethylthiazol-2-yl)-2,5-diphenyltetrazolium bromide
N	Normality
NB	Nitrobenzene
NM	Nitromethane
nm	nanometer
NO	Nitric oxide
NP	Nitrophenol
PBS	Phosphate buffer saline
PXRD	Powder X-Ray diffraction
RDX	1,3,5-trinitro-1,3,5-triazacyclohexane
SC-XRD	Single-crystal X-ray diffraction
SEM	Scanning Electron Microscopy
TGA	Thermogravimetric analysis
THF	Tetrahydrofuran
TNP	2,4,6-trinitrophenol
TNT	2,4,6-trinitrotoluene
t_R	Reaction time
UV-Vis	Ultra violate-visible
α	Alpha
β	Beta
γ	Gamma
λ	Lambda

Synopsis

Thesis Title: "**Design and Synthesis of Metal-Organic Frameworks for Selective Sensing Applications**"

Selective sensing is inevitable in variety of areas including household/occupational safety, industrial process management, healthcare, food quality control, communication, environmental monitoring, homeland security and natural sciences. Variety of materials are being explored for selective sensing applications. Despite recent progress, development of new efficient sensors are required to address the key challenges like low cost, sensitivity, selectivity, fast detection, false response. The present thesis comprises of studies towards the design, synthesis and evaluation of Metal-Organic Frameworks (MOFs) for selective sensing applications in four chapters.

Chapter 1: Introduction

In this chapter we have presented brief introduction about Metal-Organic Frameworks (MOFs) and implications of MOFs as sensing material. MOFs have emerged as a new class of inorganic-organic hybrid porous material combining properties arising from both organic and inorganic materials (Figure **1**). The advances in design, synthesis and functionalization of MOFs in predictable manner along with high porosity, crystalline nature have made MOFs an attractive material for several applications like, gas storage,

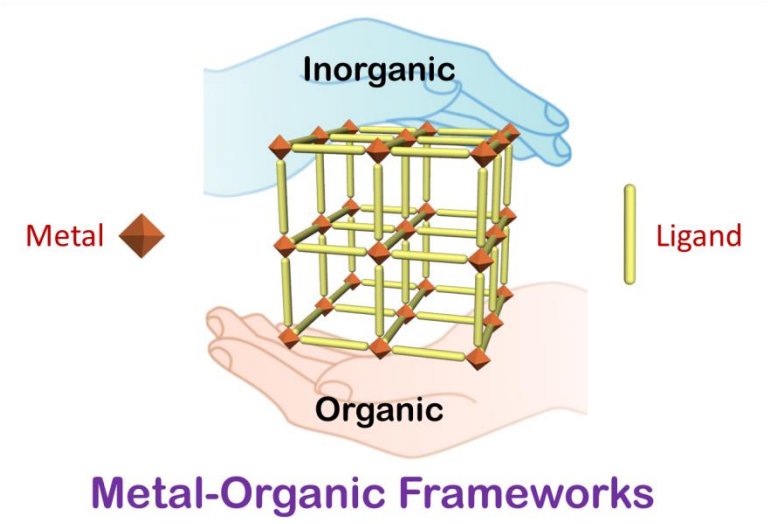

Figure 1: Self-assembly of metal ions/clusters and organic ligand forming of Metal-Organic Framework (MOF).

separation, heterogeneous catalysis, magnetism, biomedical, reaction vessel, solid-state proton conduction, and sensing. The crystalline nature, tailorable structures and/or topology, permanent porosity, systematically tunable electronic structures, and a wide range of physicochemical properties of MOF are advantageous as sensing material. However this potential material is not systematically studied for sensing applications. Despite the topical advancements, there is wide scope for the improvement in MOF performance and endeavoring new applications yet to be explored.

Selective and fast detection of nitro explosives like TNT, TNP has become one of the most persistent issues concerning homeland security, military applications, forensic investigations and environmental analysis. Apart from explosive nature they are also known for the toxic effects. During synthesis, use and disposal, the explosive materials are released in to the soil and aquatic systems posing environmental issues. Among these, TNP has higher explosive power in similar class of explosives. Apart from explosive nature TNP also causes skin/eye irritation, headache, anemia, liver injury, male infertility. Despite availability of sophisticated instruments for sensitive and accurate detection, the lack of portability, associated high cost of operation limits their routine use. Thus the development of efficient sensor material for TNP detection along with constant monitoring of soil and aquatic system is highly demanded.

H_2S, a conventionally known toxic gas, is recently identified as biological signaling molecule in organism ranging from bacteria to mammals. The abnormal levels of H_2S are reported to be related to diseases like Alzheimer's disease, diabetes, Down's syndrome, cancer. Therefore continuous monitoring of H_2S production, distribution and removal in biological system is highly desirable to gain knowledge about H_2S effects and its underlying mechanism. Hence the development of H_2S sensor is important for industrial as well as biomedical applications, but the highly volatile and reactive nature of H_2S makes it a daunting task.

The objective of the thesis is to design and synthesize MOFs for the selective, sensitive and prompt detection of nitro explosive TNP and biologically important H_2S. Fluorescence-based detection is employed owing to its high sensitivity, simplicity, short response time, its ability to be employed in solution/solid phase and noninvasive nature. Selective detection of target analyte (TNP/H_2S) in presence of respective competing molecules, employment of different functionalities for enhanced sensing efficiency and improvements in detection limit and response time are considered.

Chapter 2: Design and Synthesis of Fluorescent Metal-Organic Framework for Selective Nitro Explosive TNP Sensing

Chapter 2 describes, the selective detection of the nitro explosive TNP by a 3 dimensional porous fluorescent metal-organic framework $[Cd(L_1)_{0.5}(L_2)]\cdot G_x$ (**1**) (H_2L_1 = 2,6-napthalenedicarboxylic acid, HL_2 = 4-pyridinecarboxylic acid). Addition of TNP quenches fluorescence of activated MOF **1'** to 78% while all the other competing nitro analytes like TNT, 2,4-DNT, 2,6-DNT, 1,3-DNB, NB, DMNB, NM, and RDX showed negligible quenching effect (Figure **2**). The detection limit was determined to be 900 ppm. Compound **1'** exhibited selective detection of TNP, even in the presence of other nitro compounds in both aqueous and organic solutions. The binding constant for TNP was found to be 3.5×10^{-4} M^{-1}, which is comparable to known organic polymers and is ~30 times greater than for TNT and RDX. The selectivity is ascribed to electron and energy transfer mechanisms, as well as electrostatic interactions between TNP and the fluorophore. The selectivity for TNP is achieved by accessible Lewis basic sites, (pyridyl groups) present in MOF **1'**. The results demonstrate a promising approach to achieve highly selective TNP sensing in MOFs and provide a new insight into the design of MOF-based explosive sensors, which are likely to be useful under more realistic conditions in the near future. (*Angew. Chem. Int. Ed.* **2013,** *52*, 2881-2885)

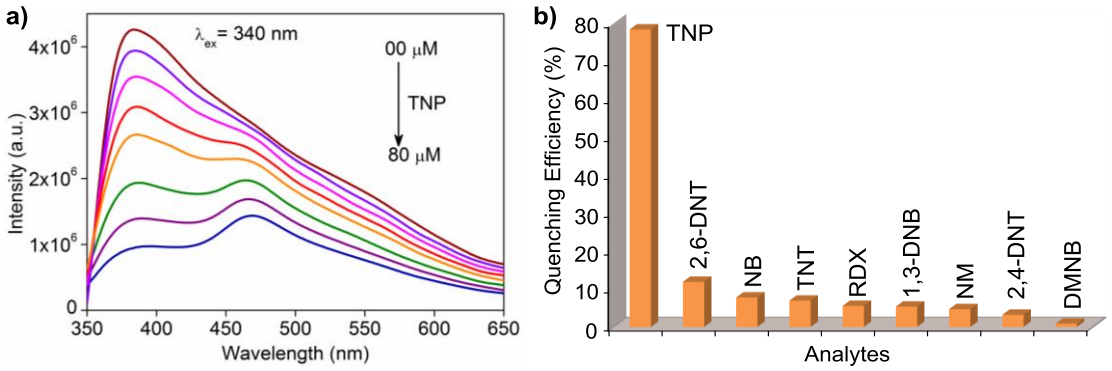

Figure 2: (a) Effect on the emission spectra of **1'** dispersed in MeCN upon incremental addition of a TNP solution. (b) Percentage of fluorescence quenching obtained for different analytes at room temperature.

Chapter 3: Aqueous Phase Selective Nitro Explosive TNP Sensing by Fluorescent Metal-Organic Framework with Guest Accessible Secondary Functional Group

For in-field selective detection of nitro explosive TNP present in soil and ground water, probe working in aqueous media is highly desirable. Although MOFs have been employed for liquid phase explosive detection, to the best of our knowledge MOF based probe has not been explored for selective detection of nitro explosives TNP in aqueous media before this work. TNP is known to interact selectively with Lewis basic sites providing tool for TNP selectivity. In this chapter we have studied hydrolytically stable, environment friendly, porous MOFs consisting of Lewis basic sites (pyridyl and amine) for selective TNP sensing.

Section A: Fluorescent MOF with Guest Accessible Pyridyl Moieties for Selective Sensing of Nitro Explosive TNP in an Aqueous Phase

In this section (A), we described $Zr_6O_4(OH)_4(L_3)_6$ (**2**, UiO-67@N) (H_2L_3 = 2-phenylpyridine-5,4'-dicarboxylic acid) with Lewis basic free pyridyl sites for selective TNP sensing (Figure **3**). The hydrolytically stable activated MOF **2'** is highly porous composed of non-toxic Zr(IV) metal centers. The MOF **2'** exhibits fluorescence quenching upon addition of TNP (73 %), even in the presence of competing nitro analytes in aqueous media. The **2'** respond to TNP in few seconds and the detection limit was calculated to be 0.6 ppm. Fitting of Stern-Volmer plot gave binding constant of 2.9×10^4 M^{-1}. Occurrence of both electron and energy transfer processes, in addition to electrostatic interaction between the Lewis basic pyridyl moieties in **2'** and TNP, ascribed to the unprecedented

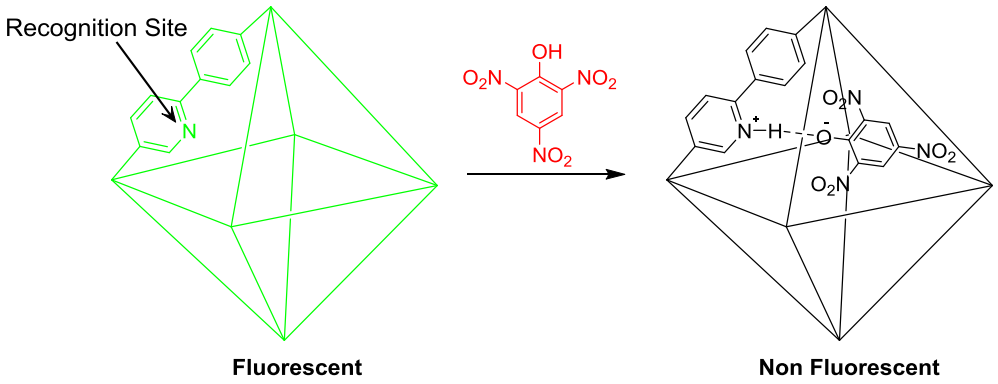

Figure 3: Schematic representation of selective detection of TNP by luminescent MOF **2'** with guest accessible pyridyl groups.

selective fluorescence quenching. (*Chem. Commun.* **2014,** *50,* 8915-8918)

Section B: Fluorescent MOF with Guest Accessible Amine Moieties for Selective Sensing of Nitro Explosive TNP in an Aqueous Phase

In this section (B), we described $Zr_6O_4(OH)_4(L_4)_6$ (**3**, UiO-68@NH_2) (H_2L_4 = 2'-amino-[1,1':4',1"-terphenyl]-4,4"-dicarboxylic acid) with Lewis basic free amine sites for selective TNP sensing (Figure **4**). Addition of TNP to activated MOF **3'** exhibits significant fluorescence quenching (86%), while all other competing analyte gave poor quenching response in aqueous media. The selectivity is consistent even in the presence of competing nitro analytes in aqueous media. Prompt detection of TNP was observed with detection limit of 0.4 ppm and binding constant of 5.8×10^4 M^{-1} as derived from Stern-Volmer plot. Occurrence of both electron and energy transfer processes, in addition to electrostatic interaction between the Lewis basic amine moieties in **3'** and TNP, assigned to the unprecedented selective fluorescence quenching. (*Dalton Trans.* **2015,** DOI: 10.1039/C5DT00397K)

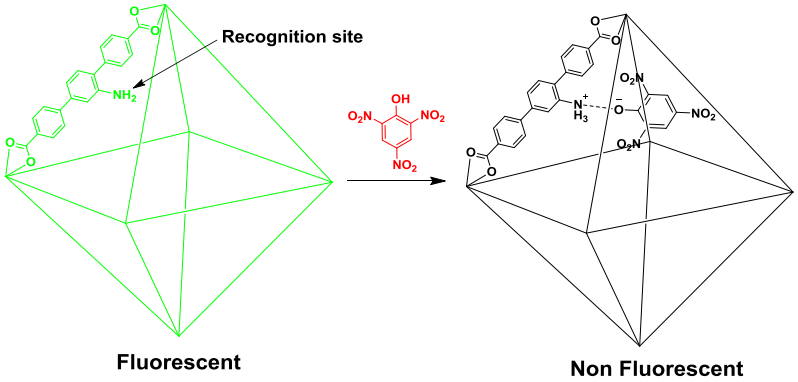

Figure 4: Schematic representation of selective detection of TNP by luminescent MOF **3'** with guest accessible amine groups.

Chapter 4: Metal-Organic Framework as Reaction based Fluorescence Turn-on Probe for H_2S Sensing

H_2S, a traditionally considered toxic gas has emerged as a biological signaling molecule after NO and CO. The abnormal levels of H_2S in cells are known to be related to Alzheimer's disease, diabetes, Down's syndrome, and cancer. Thus the elucidation of molecular mechanism of H_2S in physiological and pathological processes is an active area of current research. But volatile and reactive nature of H_2S makes the accurate detection of

H_2S a intimidating task. Fluorescence based detection systems are advantageous because of their high sensitivity, simplicity, short response time, non-invasive nature, real-time monitoring and precludes other sample processing. In this chapter we have presented functional MOF as reaction based turn-on probe for H_2S sensing.

Section A: Azide ($-N_3$) Functionalized Metal-Organic Framework as Reaction based Fluorescence Turn-on Probe for H_2S Sensing

In this section (A), we have utilized azide ($-N_3$) functionalized MOF $Zr_6O_4(OH)_4(L_6)_6$ (**5**, UiO-66@N_3) (H_2L_6 = 2-azido-benzene-1,4-dicarboxylic acid) as reaction based fluorescence turn-on probe for H_2S detection. The activated MOF **5'** is weakly fluorescent and in presence of H_2S, the azide ($-N_3$) functionality undergo H_2S mediated reduction to fluorescent amine ($-NH_2$) (UiO-66@NH_2, **4**) (Figure **5**) giving rise to florescence turn-on response. **5'** show fast ($t_{1/2}$ = 13.6 s) and selective turn-on response towards H_2S even in presence of potentially competing biomolecules under physiological conditions. The H_2S detection limit under physiology mimicking condition was found to be 118 μM. The cytotoxicity of **5'** was determined by MTT assay which shows **5'** is less toxic to cells. The live cell imaging studies demonstrated that probe can sense the H_2S in live cells. (*Sci. Rep.* **2014,** doi:10.1038/srep07053)

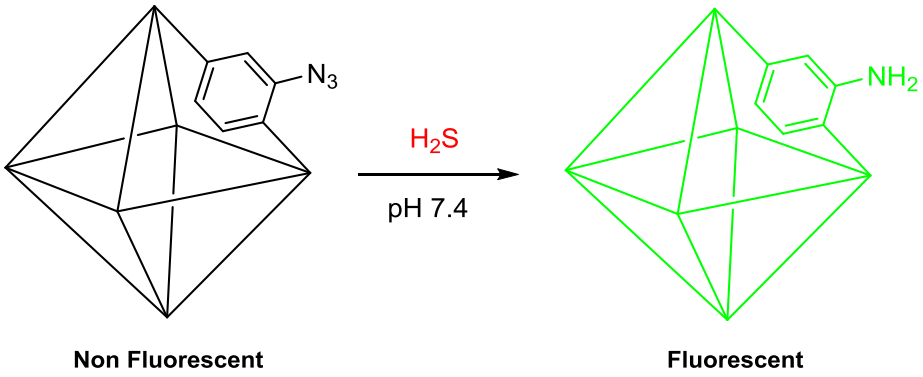

Figure 5: H_2S mediated reduction of $-N_3$ in MOF **5'** to $-NH_2$ upon addition of Na_2S under physiological pH giving rise to fluorescence turn-on response.

Section B: Nitro ($-NO_2$) Functionalized Metal-Organic Framework as Reaction based Fluorescence Turn-on Probe for H_2S Sensing

Similar to azide group, nitro (-NO_2) group also undergo H_2S mediated reduction to amine (-NH_2). In this section (B), we report nitro (-NO_2) functionalized MOF $Zr_6O_4(OH)_4(L_7)_6$ (**6**, UiO-66@NO_2) (H_2L_7 = 2-nitro-benzene-1,4-dicarboxylic acid) as reaction based fluorescence turn-on probe for H_2S detection. The activated **6'** is weakly fluorescent and in presence of H_2S the nitro (-NO_2) functionality undergo H_2S mediated reduction to fluorescent amine (-NH_2) (UiO-66@NH_2, **4**) (Figure **6**) giving rise to florescence turn-on response. **6'** exhibit selective turn-on response towards H_2S and reaction competes in 460 s with $t_{1/2}$ = 36 s. The selectivity was obtained even in presence of potentially competing biomolecules under physiological conditions. The H_2S detection limit under physiology mimicking condition was found to be 188 μM. Similar to azide functionalized probe (**5'**) the **6'** is also expected to sense the H_2S in live cells. (*Chem. Eur. J.* **2015,** Manuscript Accepted)

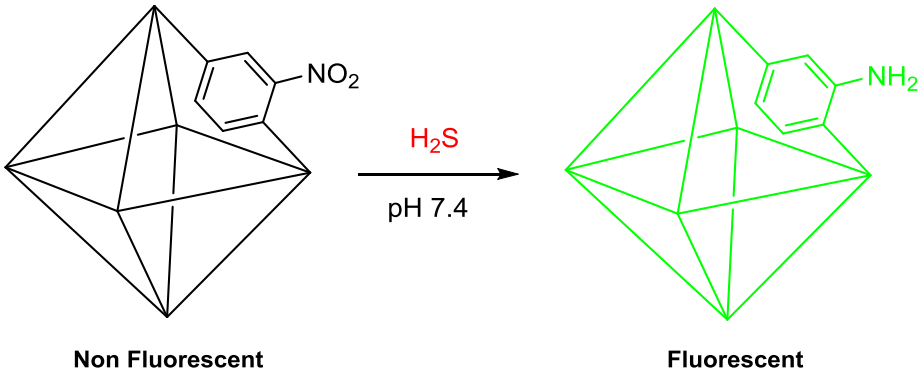

Figure 6: H_2S mediated reduction of -NO_2 in MOF to -NH_2 upon addition of Na_2S under physiological pH giving rise to fluorescence turn-on response.

List of Publications:

1. **Nagarkar, S. S.**; Chaudhari A. K.; Ghosh, S. K. *Inorg. Chem.* **2012,** *51,* 572-576.
2. **Nagarkar, S. S.**; Chaudhari, A. K.; Ghosh, S. K. *Cryst. Growth Des.* **2012,** *51,* 572-576.
3. **Nagarkar, S. S.**; Das, R.; Poddar, P.; Ghosh, S. K. *Inorg. Chem.* **2012,** *51,* 8317-8321.
4. **Nagarkar, S. S.**; Joarder, B.; Chaudhari, A. K.; Mukherjee, S.; Ghosh, S. K. *Angew. Chem. Int. Ed.* **2013,** *52,* 2881-2885.
5. **Nagarkar, S. S**; Desai, A. V.; Ghosh, S. K. *Chem. Asian J.* **2014,** *9,* 2358-2376.
6. **Nagarkar, S. S.**; Unni, S.; Sharma, A.; Kurungot, S.; Ghosh, S. K. *Angew. Chem. Int. Ed.* **2014,** *53,* 2638-2642.
7. **Nagarkar, S. S.**; Desai, A. V.; Ghosh, S. K. *Chem. Commun.* **2014,** *50,* 8915-8918.
8. **Nagarkar, S. S.**; Saha, T.; Desai, A. V.; Talukdar, P.; Ghosh, S. K. *Sci. Rep.* **2014,** doi:10.1038/srep07053.
9. **Nagarkar, S. S.**; Ghosh, S. K. *J. Chem. Sci.* **2015,** DOI: 10.1007/s12039-015-0820-3.
10. **Nagarkar, S. S.**; Desai, A. V.; Samanta, P.; Ghosh, S. K. *Dalton Trans.* **2015,** DOI: 10.1039/C5DT00397K.
11. **Nagarkar, S. S.**; Desai, A. V.; Ghosh, S. K. *Chem. Eur. J.* **2015,** Accepted Manuscript.
12. **Nagarkar, S. S.**; Anothumakkool, B.; Desai, A. V.; Shirolkar, M. M.; Kurungot, S.; Ghosh, S. K. (Submitted).
13. **Nagarkar, S. S.**; Anothumakkool, B.; Desai, A. V.; Kurungot, S.; Ghosh, S. K. (Submitted).
14. **Nagarkar, S.S.**; Desai, A. V.; Samanta, P.; Ghosh, S. K. (Manuscript Under Preparation).
15. Chaudhari, A. K.; **Nagarkar, S. S.**; Joarder, B.; Ghosh, S. K. *Cryst. Growth Des.* **2013,** *13,* 3716-3721.
16. Chaudhari, A. K.; **Nagarkar, S. S.**; Joarder, B.; Mukherjee, S.; Ghosh, S. K. *Inorg. Chem.* **2013,** *52,* 12784-12789.
17. Gupta, A. K.; **Nagarkar, S. S.**; Boomishankar; R. *Dalton Trans.* **2013,** *42,* 10964-10970.

18. Joarder, B.; Chaudhari, A. K.; **Nagarkar, S. S.**; Manna, B. Ghosh, S. K. *Chem. Eur. J.* **2013,** *19*, 11178-11183.
19. Chaudhari, A. K.; Mukherjee, S.; **Nagarkar, S. S.**; Joarder, B.; Ghosh, S. K.; *CrystEngComm* **2013,** *15*, 9465-9471.
20. Surya, S. G.; **Nagarkar, S. S.**; Sonar, P.; Ghosh, S. K.; Rao, V. R. (Submitted).

Chapter 1

Introduction

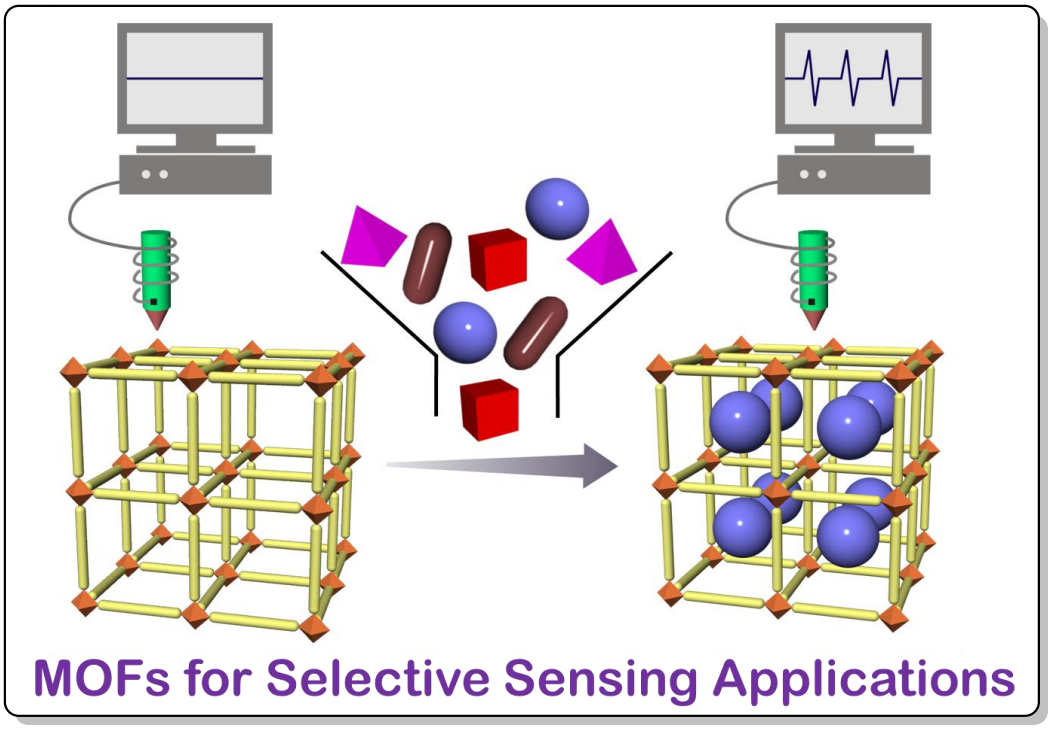

1.1 Porous Materials:

Porous materials have always attracted the attention of chemists, physicists, material scientists and chemical engineers because they are very useful for applications in the field of gas storage, purification of water and oil, catalysis, drug delivery, sensing, etc.[1] Porous materials allow guest molecules to diffuse inside the matrix and once incorporated, physical and chemical transformations of the guests may take place owing to confinement effect.

Porous materials are classified based on the pore size of the material as per IUPAC notation.[2] i) Microporous materials have pore diameters of < 2 nm, ii) Mesoporous materials have pore diameters between 2 nm to 50 nm, and iii) Macroporous materials have pore diameters of > 50 nm. Porous materials are omnipresent for example bone, lungs, coral, sandstone, sea sponge, egg shell, etc. are naturally occurring porous materials, while ceramic, bricks, concrete, sponges, bread, etc. are artificial porous materials. The porous materials are in demand since ancient time, charcoal a porous carbon material is widely used for water purification and medicinal purposes.[3] The processed carbon material like activated carbon is used as sorbent in industrial applications.[4] The broad pore size and disordered pore structure are few limitations of carbon material.[5] The emergence of inorganic porous material zeolite with uniform pore structures in 1950 has accelerated the industrial revolution and technological achievements.[6] However, small pore size and small number of naturally occurring/synthetic Zeolites limits their application.[7] Thus the discovery of new efficient porous materials with large and controlled sorption ability is scientifically and technologically appealing. The development of material depends upon progressive changes made in material during interactive cycle of design, implementation and evaluation, thus the continuous efforts are being made to synthesize novel porous materials.

1.2 Metal-Organic Frameworks (MOFs):

The traditionally known porous materials are either organic or inorganic, very recently Metal-Organic Frameworks (MOFs), have emerged as new class of inorganic-organic hybrid porous material combining properties arising from both organic and inorganic materials. MOFs are porous crystalline solids formed by self-assembly of inorganic nodes (metal ion/clusters) and organic ligands connecting these inorganic nodes

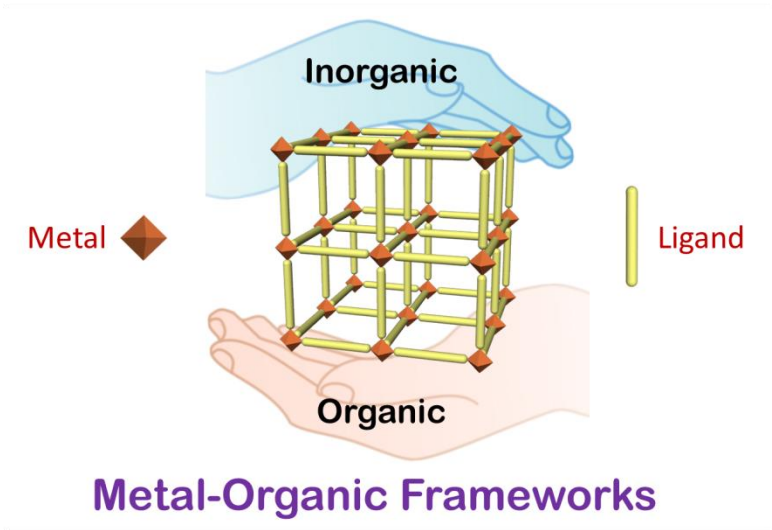

Figure 1.1: Formation of Metal-Organic Framework (MOF) by self-assembly of metal ions/clusters and organic ligand.

at regular intervals forming extended framework (Figure **1.1**).[8] MOFs has seen exponential growth in terms of synthesis, characterization and studies not only in terms of number of research articles but also in terms of scope of the material.[9]

1.2.1 Crystalline Nature:

Most of the MOFs are synthesized as single crystals or as a crystalline powder. The crystalline nature of MOFs allows precise determination of structure and positions of atoms with sub-nanometer level accuracy. The detailed knowledge about structure permits easy structure property correlation. The crystalline MOF have utilized for characterization of structure and relative stereochemistry of ordered guest molecules present in MOF matrix on a nanogram scale, providing new tool for characterization.[10] The crystalline nature also provides an opportunity to monitor solid-state reactions, which are otherwise difficult to monitor. Although crystalline nature of MOF provides several advantages, recently, Prof. Cheetham et al. reported amorphous MOFs with weak X-ray diffraction as advantageous material for certain applications.[11]

1.2.2 Designable Architecture:

Another hallmark characteristic of MOFs is designable architecture. MOF offer design flexibly in pore size, shape, dimensionality, free functionality etc. in predictable manner without compromising the underlying topology.[12] Following Robson's building block strategy, the combinations of diverse geometries of the organic linkers and

coordination modes/numbers of the inorganic metal node enables design of MOFs according to targeted properties. MOF pores are typically of microporous character (< 2 nm) however the pore size of MOF can be tuned from few angstroms to few nanometers by judicious choice of building unit. Recently, Multivariate MOFs (MTV-MOFs) have been developed where multiple functionalities are incorporated in single MOF is also a new strategy to design the MOF with complex functionalities in controlled manner.[13] The designable architecture facilitates the tuning of MOF performance and is a key to extensive utilization for various potential applications in assorted areas.

1.2.3 Ordered Extended Structure:

As mentioned earlier the MOFs are composed of inorganic nodes connected by organic ligands at periodic intervals giving rise to framework structure in possible symmetric manner. The ligands and metals are held at regular intervals and thus the uniform distribution of channels with consistent size and shape can be easily achieved with nanometer level accuracy over long range. The orderedness also enables arrangement of the active functionalities in MOF pores in periodic manner enabling improved host-guest interaction and efficient performance.

1.2.4 Permanent Porosity:

The most imperative property of MOFs is their porous nature. During MOF synthesis the extra framework spaces are generally occupied by molecules used during MOF synthesis. These guest molecules are then removed without breaking MOF framework to access the porous matrix of MOF. The porosity is commonly examined by low pressure gas adsorption analysis. The free volume in MOFs is reported to be up to 90% with enormous internal surface areas, extending beyond 6000 m^2/g which is higher than those of traditional porous materials such as zeolites and carbons.[9a,14]

1.2.5 Host-Guest Interactions:

The high porosity permits accumulation of guest molecules in MOF matrix and act as pre-concentrator.[15] The guest molecules can interact with host MOF giving rise to interesting host guest properties than found in bulk. The host-guest interactions may lead to change in the chemical/physical properties of either host/guest or the overall host-guest system.[16] Common host-guest interactions include π···π, C-H···π, ionic interactions, H bonding, etc.[17] During host-guest interactions, the overall MOF structure may change

(dynamic or soft MOFs) or remain same (rigid MOFs). These host-guest mediated changes have been utilized for applications like sensing, micro-mechanics, etc.[18]

1.3 Choices of Building Units:

As discussed earlier the MOFs are made up of metal ion/cluster/chain, organic ligand coordinating metal node and the guest molecules present in MOF pores. The overall MOF structure depends on the choice of building unit. Thus the MOF structure can be tuned by proper selection of building unit.

1.3.1 Central Metal Atom/Cluster/Chain:

Transition metal ions are commonly used as inorganic nodes in MOFs. However, almost all the di-, tri- tetravalent metal ions, ranging from alkali metals to lanthanide has been employed for MOF synthesis. Subject to metal ion and its oxidation state, the coordination number of metal varies from 2-7 (higher in case of Ln) giving rise to different geometries and their corresponding distorted forms.[19] In some cases *in-situ* formed polyatomic metal clusters also act as inorganic node (Figure **1.2**). The number of metal atoms in discrete cluster may vary from 2 to 13 which are connected to each other in 3D by organic linkers forming extended framework.[20] While some MOFs, instead of discrete metal clusters, contains infinite rode like metal oxide chains connected by organic ligands at regular intervals giving rise to framework structure.[21] Higher dimensionality of inorganic clusters/chains is favored upon increasing reaction temperature when all the other reaction parameters are same. Polyoxometalate with special physical and chemical

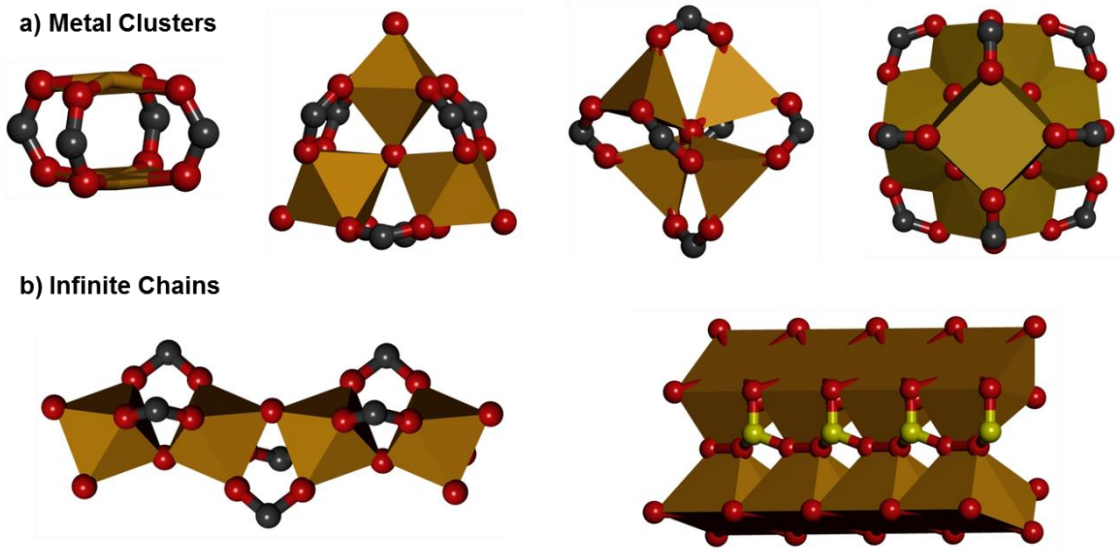

Figure 1.2: Representative examples of polyatomic Cluster/Chain present in MOFs.

properties have also been utilized as inorganic node during MOF synthesis.[22]

1.3.2 Ligands:

Ligands or organic 'struts' having pendent binding groups provide different possibilities of linkage to connect inorganic 'nodes' at regular intervals. The ability of binding group determines the overall stability of MOF, thus the design and selection of organic linker is very important. Linker also plays vital role in tuning the pore size of MOF, however great care must be taken while MOF synthesis as the longer ligands often result in interpenetrated structures with reduced porosity. Most commonly used linkers are anionic and neutral ligands nevertheless cationic ligands have also been used to synthesize the MOF (Figure **1.3**). The anionic ligands inherently favor binding to cationic metal centers. The typical anionic linkers are aliphatic/aromatic di-, tri-, tetra-, and hexacarboxylate molecules (Figure **1.3a**).[23] Non-symmetric ligands with combination of

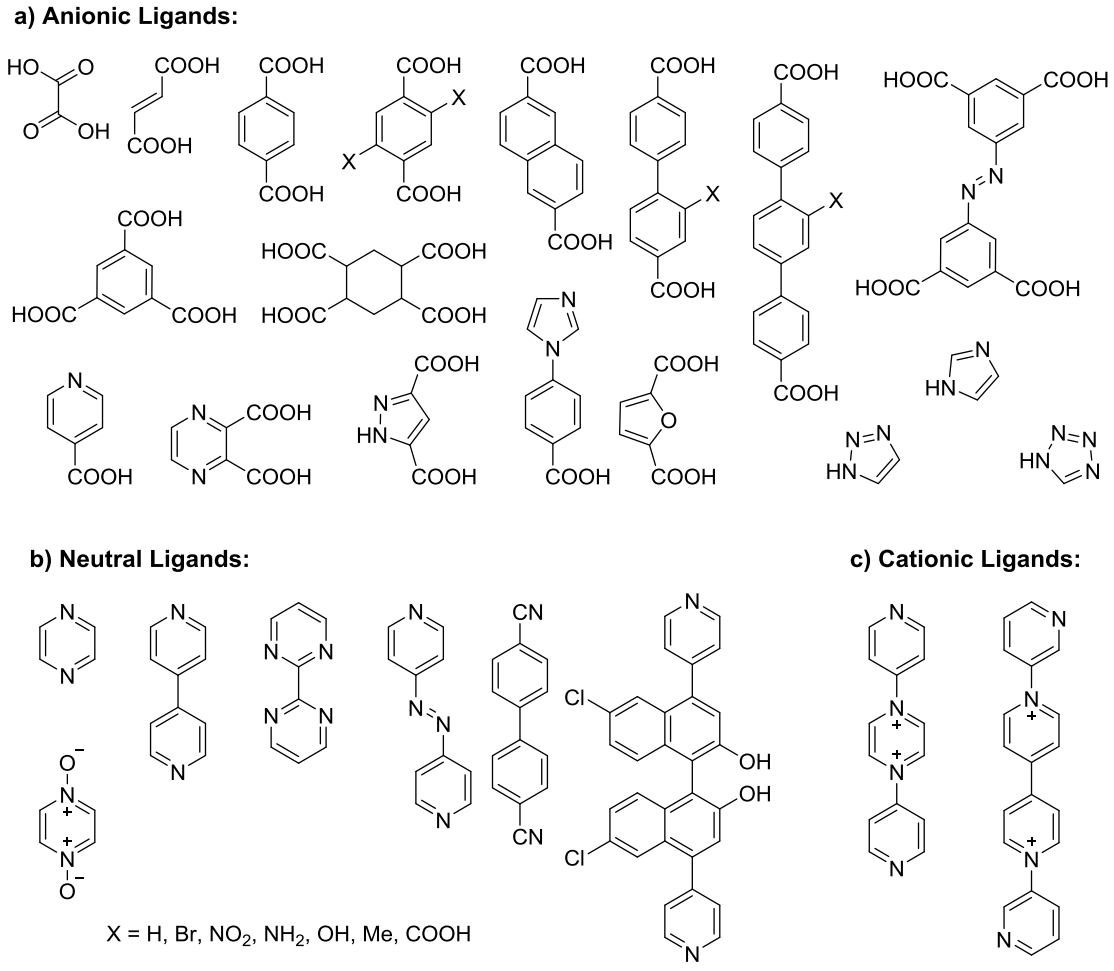

Figure 1.3: Representative examples of ligands used for MOF synthesis.

anionic and neutral coordinating groups have been employed for MOF synthesis. Neutral ligands mainly include polytopic N-heterocycle containing functionalities like pyridine, cyano with different spacers (Figure **1.3b**).[24] The coordination of neutral ligand to cationic metal centers generally yield cationic framework with anion/s in MOF matrix or anions coordinating/bridging the cationic metal units. Azolate-based ligands and their derivatives are used as anionic ligands as well.[25] Few cases viologen based cationic ligands with neutral coordinating groups have been used successfully for MOF synthesis (Figure **1.3c**).[26]

1.4 Synthesis of MOFs:

There are many material synthesis methods which have been used for MOF synthesis.

1.4.1 Conventional Methods:

The precipitation reaction followed by recrystallization or the slow evaporation of the solvent are well-known methods grow simple molecular or ionic crystals and have been utilized by Robson et al., in early days for synthesis. The other ambient temperature methods such as layering of reactant solutions, or slow diffusion are also used to grow high quality crystals from clear solutions that are large enough for single crystal X-ray crystallography.

Solvothermal synthesis is the most commonly employed MOF synthesis method. Solvothermal synthesis involves heating the mixture of ligand and metal salt in polar solvent such as water, alcohols, acetone, acetonitrile or dialkyl formamides in sealed vessels such as Teflon-lined stainless steel bombs or glass vials, under autogenous pressure.[27] The MOFs are commonly obtained as micrometer size single crystals, suitable for single crystal X-ray crystallographic analysis. Solvothermal synthesis often requires high temperature and longer reaction times. For kinetically more inert ions that are used in MOF synthesis, strong reaction conditions are required.

1.4.2 Recent Methods:

The synthetic methods that are energy efficient are not only desirable for commercial scale MOF production, but also for short crystallization time, narrow particle size distribution, facile morphology control, and efficient evaluation of process parameters.[28] In conventional solvothermal synthesis energy is transferred from

electrically heated hot system to reaction by convection. The energy can alternately be supplied by microwave irradiation, application of an electric potential, mechanically or through ultrasound.

Microwave-assisted synthesis relies on the interaction of electromagnetic waves with microwave-absorbing polar solvent molecules or ions in a solution.[29] The microwave-assisted synthesis enables fast and uniform heating during MOF synthesis. The fast reaction yields nanocrystalline product and thus is preferred to synthesize MOF thin films and nano MOF, especially for biomedical application.

Another efficient way to introduce energy during MOF synthesis is sonochemical synthesis. The ultrasound with a frequency between 20-10 kHz, interact with liquid producing high temperature and pressure by 'cavitation' process.[30] This favours formation of multiple high energy microreactors and hence the rapid MOF crystallization. The sonochemical synthesis is advantageous as it is easy, fast, energy-efficient, environmentally friendly, room temperature method, yet largely unexplored.

During MOF synthesis metal counter anions remains in mother liquor as by-products which may affect MOF performance and are major concern for industrial scale MOF production. Electrochemical synthesis MOF was established by researchers at BASF to exclude anions in MOF formation.[31] Metal anode act as source of metal ions via anode dissolution in reaction medium containing organic linker and conducting salt. This has been used for formation of films and patterned coatings of MOFs on desired substrate. As electrochemical synthesis process can run continuously, it is more appealing for industrial scale MOF synthesis.

Mechanical force is known to stimulate chemical reactions especially, in organic chemistry. Mechanically activated synthesis of MOF is an area of active interest due to its room temperature solvent free synthesis as against all the above methods.[32] Mechanochemical synthesis produces MOF as small particles using ball milling within few minutes. Poorly soluble metal oxides also can be used as source of metal ion with water as side product.

A reverse-phase microemulsion process has also been utilized for MOF synthesis with efficient particle size control.[33]

1.4.3 Morphology Control and Positioning MOF:

Manipulation of the size, shape and positioning of the MOF crystals is very important to optimize the physical properties of the solids for applications like smart membranes, catalytic coatings, chemical sensors, magnetic resonance imaging and drug delivery.[34] The compositional and process parameters like solvent, pH, counter anion, concentration, template used, and reaction temperature are known to affect the MOF synthesis.[35] Capping agents or modulators having the same chemical functionality as the multidentate linkers are added to reaction mixture to modulate size, morphology of MOF crystals.[36] We have recently reported effect of reaction temperature on the dimensionality of MOF structure.[37]

MOFs based thin films or membranes are synthesized following different synthetic conditions. MOF can be grown on functionalized substrates by immersing the substrate in the reaction solutions containing metal salts and linkers, known as direct synthesis or via layer-by layer growth, where functionalized substrate is dipped in alternately in metal and linker solutions in tandem process.[38]

Composites are another interesting material which combines the properties of constituent phases and permits tuning of the resultant properties. MOF composites can be obtained by dispersing MOF in organic or inorganic material matrix.[39]

1.4.4 Theoretical Screening:

The large number of available metal nodes and organic ligands, their possible combinations and reaction parameters can yield almost limitless MOF structures. The interesting diversity in MOF structures however on the other side poses daunting challenge to screen them as physical synthesis and testing of these MOFs is impractical. The recent development in computational chemistry enables the screening of reported MOFs and even hypothetical MOFs for adsorption of small molecules, separation, and probe effect of functional group on MOF performance.[40] The present approach is cost and time effective and getting captivating attention to uncover useful structure property correlationship.

1.5 Functionalization of MOFs:

The designable architecture along with synthetic flexibility in terms of choices of organic and inorganic components of MOFs provides ample opportunities to introduce desirable functionality. The functionality can be imparted to MOF prior to MOF synthesis

using functional building unit or after MOF synthesis by Post synthetic modification (PSM) methods.[41]

1.5.1 Functional Building Units:

The simplest way to impart functionality to MOF would be use of functional building units to synthesize the MOF also known as direct synthesis (Figure **1.4.a**). This ensures the complete and uniform incorporation of the functional group in MOF. In present approach the functionality can be incorporated by use of functional central metal atom which gives rise to metal based functionality or by use of functional ligand for ligand based functionality. Even the mixed ligand/metal approach can also be used for partial functionalization with preservation of topology also called as isomorphous mixed MOFs.[42] The functionality can also be introduced by use of solvent or guest molecules with functionality during synthesis which can acts as template or simple guest. But the need of unique synthetic protocol for each functionality limits its wide spread use.

1.5.2 Post Synthetic Methods:

Guest Exchange:

The MOFs are well known for their host-guest interactions. During synthesis the coordination space of MOF is generally filled by guest molecules like solvents. These molecules can be exchanged with the functional guest molecules without compromising the structural integrity of the material (Figure **1.4.b**).[43] This is also an efficient method of functionalization of MOFs. During guest exchange the MOF may retain the size/shape of the pore (rigid MOFs) or may change the size/shape in response to incoming guests (dynamic or flexible MOF). Also in the confined environment the guest do not interact with each other giving rise to unique properties compared to bulk sample.

Ion Exchange:

The ion exchange strategy is mainly employed to the ionic frameworks where the counter ions are present in the coordination space of MOF. Use of neutral coordinating ligands in MOF synthesis or formation of nonstoichiometric secondary building unit generally leads to the encapsulation of additional counter ions in the coordination space of MOF. These counter ions can be exchanged with the other ionic molecules (cations or

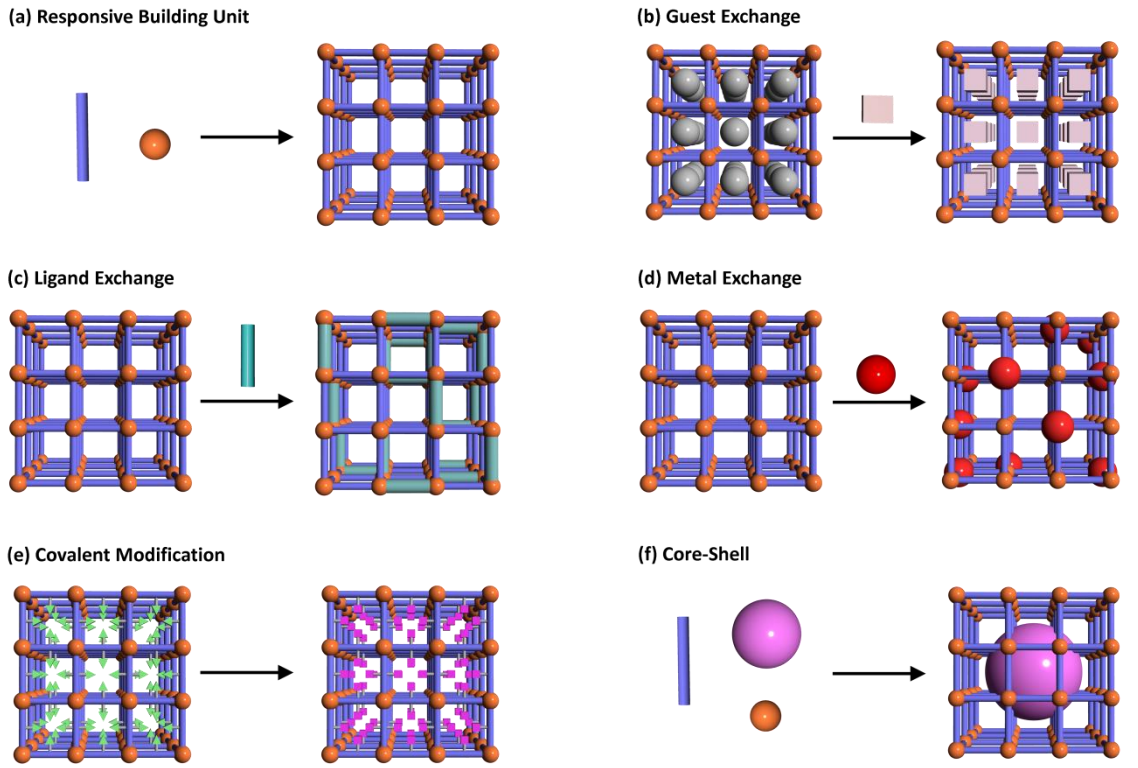

Figure 1.4: Different strategies adopted for functionalization of MOFs.

anions) by immersing the ionic MOF in the solution of ionic molecules while maintaining the crystalline framework (Figure **1.4.b**). Thus by exchanging these ions with functional ions we can functionalize MOF material. Due to ionic interaction between MOF and guest molecules potential leaching of the functional guests can be avoided.

Ancillary Ligand Exchange:

The ancillary ligands are coordinated to the central metal atom and removal of which doesn't affect the overall secondary building unit (SBU) or topology of MOF. Very first example of which is MOF-11 [Cu_2(ATC); ATC^{4-} = adamantane-1,3,5,7-tetracarboxylate] with Cu (II) paddle wheel structure and axially coordinated water molecules.[44a] On removal of coordinated water molecules, the coordinatively unsaturated site also called as open metal site is generated without loss in crystalline nature of the MOF. These labile ancillary ligands (generally solvent molecules) can be easily replaced by functionalized molecules (Figure **1.4.c**).[44b]

Ligand/Metal Exchange:

Functionality can also be introduced by postsynthetic exchange of ligand or metal.[45] The antecedent MOF is first synthesized and then the Ligand and/or Metal in

parent MOF is replaced or doped by new ligand L' with equivalent denticity or metal M' occupying equivalent metal site by soaking parent MOF (crystal or powder form) in solution (Figure **1.4.c-d**). This post synthetic ligand or metal exchange may lead to complete or partial exchange and exhibit intermediate properties between end members or even better than end members. This method is important especially, when the direct incorporation of active ligand is not possible.

Covalent Modification:

The periodic nature and long range ordering of the coordination bond between metal ions and coordinating ligands provides ample opportunities for covalent modification of MOFs. In this strategy the dormant functional group on linker is modified to active one without disturbing coordination bond and the overall structure of the MOF (Figure **1.4.e**).[46] These dormant functional groups can directly be incorporated (amine, hydroxide, alkynes, azides, etc.) or need prior activation before functionalization (protected groups). The latter approach of tandem modification is advantageous to avoid side reactions during synthesis of MOF. The common organic reactions used for covalent modifications are ring opening, click reaction, etc.[45,46]

1.5.3 Composites:

Composites are multicomponent materials with non-gaseous phase domains in with at least one type of continuous material.[47] Very recently, the composite approach has been adopted to functionalize the MOF where the hybridization of other class of functional material and MOF occur resulting in novel properties sometimes better than end members.[42] Core-shell structure is class of composite materials. The core-shell structures composed of two or more distinct phases where both the core and shell may be MOF (MOF on MOF) or one of them is MOF (Figure **1.4.f**). Pre-synthesized MOF can be used to make composite material or can be synthesized *in-situ* during composite formation. This approach allows the functionalization of the parent MOF through incorporation of additional functionality without affecting the inherent properties of MOF. The MOF itself can act as functional unit or as a protecting shell allowing specific functional group to interact with the functional core. Recently Prof. Suh and co-workers have reviewed the incorporation and applications of metal nanoparticles in MOFs.[48]

The wide varieties of functional molecules open a great avenue for imparting functionality to MOFs.

1.6 Applications of MOFs:

Advances in design, synthesis and functionalization of MOFs in predictable manner along with high porosity, crystalline nature have made MOFs an attractive material for various applications.[9a,49]

1.6.1 Gas Storage:

Hydrogen (H_2) and Methane (CH_4) are the leading candidates for upcoming clean fuels, but the safe and economical storage of these flammable gases is an issue. Porous materials are of interest to store these industrially important gases as they allow safer and economical way of gas storage. The high porosity and pore functionalization makes MOFs an attractive candidate for gas storage applications. Prof. Kitagawa et al. for the first time investigated CH_4 storage capacity of MOF employing $[Co_2(4,4'\text{-bipyridine})_3(NO_3)_4]$ MOF under high pressure;[50] while the H_2 storage ability of MOF was first established by Prof. Yaghi et al. employing $Zn_4O(BDC)_3$, (H_2BDC = 1,4-benzene dicarboxylic acid) MOF.[51] Since then MOFs have been extensively studied for storage of H_2 and CH_4. The highest CH_4 uptake of 212 mg/g at 290 K and 35 bar is reported for PCN-14 [$Cu_2(H_2O)_2(adip)\cdot 2DMF$, H_4adip = 5,5′-(9,10-Anthracenediyl)di-isophthalic Acid] MOF,[52] while the highest H_2 uptake till date of 9 wt% is observed for MOF NU-100 $[Cu_3(L)(H_2O)_3]_n$ (L = 1,3,5-tris[(1,3-carboxylicacid-5-(4-(ethynyl)phenyl))ethynyl]-benzene) at 77K and 56 bar.[53] Mercedes-Benz have already developed MOF based H_2 storage fuel tank for fuel cell-powered demonstration model, the F125.[54]

1.6.2 Separation:

The gas separation is also important in H_2 and CH_4 purifications, CO_2 capture from flue gases, CO removal for fuel cell technology, desulfurization of transportation fuels, and other technologies.[55] The gas separation ability of MOF generally depends up on both pore size and affinity of MOFs for analyte of interest. Selective adsorption of O_2 (kinetic diameter = 3.46 Å) over N_2 (3.64 Å) by MOF with pore size 3.5 × 3.5 Å is achieved by size exclusion.[56] Other than size exclusion the selective interactions between MOF and analyte is used to achieve separation.[57] Selective CO_2 capture from mixture of gases is important for carbon capture and storage (CCS) technology. Long et. al and Li et. al

reviewed the performance if MOFs with free functional groups like amine, alkali metals to achieve selective CO_2 capture over other gases.[58]

Separation and purification of solvents is also important for their potential applications. Apart from gases MOFs are also employed for adsorption based separation of vapors of liquid compounds.[59] Separation of water from alcohols is important in biofuel production. MOFs with high affinity site for water and smaller size are reported for potential water alcohol separation.[60] Separation C8 alkylaromatic isomeric compounds like o-xylene (oX), m-xylene (mX), p-xylene (pX), and ethylbenzene (EB) is achieved by flexible/dynamic MOF.[61] Recently Prof. Long et al. explored $Fe_2(BDP)_3$ (BDP^{2-} = 1,4-benzenedipyrazolate), MOF for separation of hexane isomers from equimolar mixture at 160 °C.[62]

As step towards application MOFs have also been employed as stationary phase in chromatographic and membrane separation applications.[63]

1.6.3 Catalysis:

Heterogeneous catalysis is one of the important applications of MOF envisioned.[64] As heterogeneous catalyst, MOF serve as an interesting material to study, as theoretically almost all the components of MOF can be utilizes for catalysis. The highly ordered and uniform metal center can act as an active catalytic site. The organic ligand connecting metal centers can also be utilized for organo-catalysis and/or functionalized with catalytically active site. Owing to uniform pore size, shape and environment, MOF can also act as good host material for active catalyst for heterogenization or avoid side reactions. MOF based catalysts have successfully been engaged for variety of reactions including but not limited to Knoevenagel condensation, Aerobic oxidation of olefin, Suzuki-Miyaura coupling, Friedel-Crafts alkylation, etc.[65] Finally, MOF itself can act as precursor for catalyst by framework decomposition.

1.6.4 Magnetism:

Magnetic materials are important in the areas of data storage devise, sensing, along with academic interest. The magnetic properties of material are susceptible to subtle changes in the structural arrangements. The magnetic MOFs can be synthesized using paramagnetic metal or open-shell organic ligands or both.[66] Designable architecture and predictable structures yield new properties and improve existing knowledge of structures

as well as their properties. The magnetic properties of MOFs can be modulated by external stimuli which can be utilized to develop new sensing materials.[67]

Recently, magnetocaloric materials are focus of intense research to develop efficient refrigeration technologies for liquid-helium temperatures.[68] The Gd(III) based magnetic MOFs have shown potential as magnetocaloric material as the magneto caloric effect (MEC) depend on Gd(III) density in material.[69]

1.6.5 Biomedical Applications:

The high porosity, fine tuning of pore size/shape and variety of tools available for MOF functionalization prompted their use in biomedical applications.[70] Owing to porous nature MOF can be loaded with active pharmaceutical ingredient and used for delivery application.[71] The active ingredient can itself be utilized to synthesize non-toxic MOF, and then formed MOF can be utilized as pro-drug. Following similar strategy nicotinic acid or vitamin B3 based iron MOF (Bio-MIL-1) was employed for delivery of vitamin B3.[72] The adsorptive property of MOFs have also been utilized for storage and delivery of gasotransmitter gases like Nitric Oxide (NO), Carbon Monoxide (CO) and Hydrogen Sulfide (H_2S).[73] Their release is commonly triggered by exposure to moisture. MOFs also become handy for diagnostics applications like Magnetic resonance imaging (MRI) where MOF can act as contrast agent. Gd(III) known to reduce proton relaxation is thus used as contrast agent. The Gd(III) based porous MOF have been studies as MRI contrast agents.[71a,74] X-ray computed tomography is another powerful diagnostic tool and can provide three-dimensional images with exceptional special resolution. The studies with Zn(II) and Cu(II) based MOFs with iodinated ligands have demonstrated potential of MOFs in X-ray computed tomography studies.[75]

1.6.6 Reaction Vessel:

The free volume in MOFs can be utilized as nano-reaction vessel to perform reactions. As we know the radical polymerization reactions are difficult to control and undergo rapid chain propagation without control of the stereoselectivity. Prof. Kitagawa et al. used the uniform nano-space of variety of MOFs for radical polymerization of vinyl monomers.[76] As against typical polymerization reaction better control over molecular weight, stereoregularity, reaction sites, copolymer composition and sequence was attained.

1.6.7 Solid-State Proton Conductor:

MOFs by virtue of its regular arrangements of voids, tailorable porosity, crystalline nature and greater control over MOFs microstructure has become an attractive material for use as solid-state proton conducting material.[77] The proton conducting MOFs are divided in two classes one operating below 100 °C in humid condition and the other operating above 100 °C under anhydrous conditions.[78] MOFs have demonstrated high conductivity values under humid condition and few cases is comparable to Nafion.[77-79] The reported anhydrous condition conductivities of MOFs are of the order of 10^{-3} S cm^{-1}.[79] In recent past we reported Zn(II) oxalate based MOF which exhibit high proton conduction in both humid and anhydrous conditions.[80]

1.6.8 Chemical Sensing:

Very recently, MOFs have been employed for chemical sensing application.[81] Host-guest interaction based changes in visible colour or luminescence are mainly used signal transduction mechanism in MOFs. The MOFs are also explored for the detection and identification of sub-atomic particles.[82] In few cases, change in refractive index of MOF, colloidal crystal containing MOFs, impedance analysis, electrochemical changes in MOFs were utilized for detection.[83] However MOFs have yet to be systematically investigated for sensing applications. There is wide scope for incorporation of new signal transduction mechanisms and the improvement in present MOF performance.[84] This dictates the urgent need of new designs and developments of MOF based chemical sensors.

1.7 Selective Sensing Applications:

Selective sensing is unavoidable in variety of areas including household/occupational safety, industrial process management, healthcare, food quality control, communication, environmental monitoring, homeland security and natural sciences. For example detection of anthropogenic toxic pollutants including products of combustion/chemical reactions as well as the leaks of harmful industrial gases/vapors is vital for household and occupational safety along with environmental monitoring.[85] Sensors are also important for industrial process management to get good quality product and utilizing the starting materials efficiently.[86] Additionally the sensors for detection of explosives and hazardous materials along with the deliberate emission of chemical warfare agents are decisive for homeland safety and environmental monitoring.[87] Sensors for

detection and monitoring of biomolecules are important for understanding cell chemistry and underlying mechanism in biological systems to address variety of clinical issues.[88] The sensors are essential in laboratory process management in natural sciences. Despite recent progress, development of new efficient sensing systems are required to address the key challenges like low cost, sensitivity, selectivity, fast detection, false response.

1.7.1 Explosive Detection:

The on-going rise in terrorist activities across the globe calls for efficient detection of life-threatening explosive materials, essential for homeland security, anti-terrorism activities and civilian safety.[89] Moreover, the analysis of explosives is also of interest in forensic research, detection of unexploded land mines. The explosives cover variety of compounds including nitro aromatics, nitramines, and peroxides (Figure **1.5**).[90] The nitro-organics like TNT (2,4,6-trinitrotoluene), TNP (2,4,6-trinitrophenol, common name Picric acid), 2,4-DNT (2,4,6-dinitrotoluene), etc. and nitramine like RDX (1,3,5-trinitro-1,3,5-triazacyclohexane) are the major components of the many landmines.[91] Apart from explosive nature these materials are also known as toxic environmental pollutant.[92] During synthesis, use and disposal, the explosive materials are released in to the soil and aquatic systems leading to contamination. Among these, TNP has higher explosive power in similar class of explosives. Apart from explosive nature TNP causes skin/eye irritation, headache, anemia, liver injury, male infertility and also known for mutagenic activity.[93]

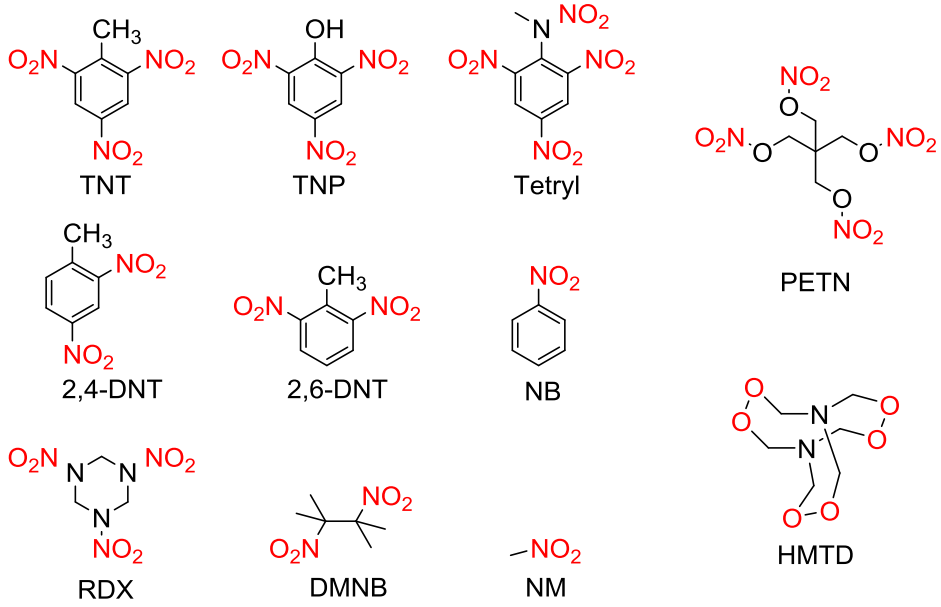

Figure 1.5: Selected explosives and explosive like compounds of interest for explosive detection.

Thus the development of efficient sensor material for TNP detection and constant monitoring of soil and aquatic system is highly demanded.

The current detection systems includes sophisticated instruments like Gas Chromatography (GC), Nuclear Quadruple Resonance (NQR), Energy Dispersive X-ray Diffraction (EDXRD), Plasma Desorption Mass Spectrometry (PDMS), Surface-Enhanced Raman Spectroscopy (SERS).[94] While, these methods demonstrate high sensitivity and accuracy, yet they suffer disadvantages like lack of portability, high cost, etc.[95] Thus the design and development of efficient explosive sensors with the goal being minimized cost, enhanced detection-limit, selectivity with improved portability and easy handling are in urgent need.

1.7.2 H_2S Detection:

H_2S a colorless, flammable gas released from geothermal and anthropogenic sources is well known toxic gas.[96] The exposure to H_2S leads to loss of sense of smell (olfactory paralysis) and causes headache; while prolong exposure may lead to death.[97] Recently, this toxic gas has also been identified as biologically signalling molecule (gasotransmitter) after Nitric Oxide (NO) and Carbon Monoxide (CO).[98] H_2S has also known to be associated with diseases like Alzheimer's disease, diabetes, Down's syndrome, cancer and thus can be utilized as potential drug target to treat these diseases.[99] The H_2S is also known for dilation of blood vessels, anti-inflammatory action and is used for signal transduction, immune response, energy production in organisms raging from bacteria to mammals.[100] Therefore to expand our knowledge about H_2S effects and underlying mechanism, continuous monitoring of H_2S production, distribution and removal in biological system is highly desirable. But real-time detection of H_2S in complex biological system is very difficult owing to highly volatile and reactive nature of H_2S.[101] Hence the development of H_2S sensor is important for industrial as well as biomedical applications.

1.7.3 Fluorescence based Methods:

The fluorescence based detection systems are getting increased attention due to high sensitivity and ability to detect even single molecule.[102] The short response time enables detection of highly reactive or short lived species. The fluorescence based detection systems provided design flexibility and can work in both solid as well as liquid

phase. The well-developed optics and detection technologies allow easy visualization of signal at low cost. The handy instrumentation like smart phone based fluorescence detection system or multichannel fluorescence detector system allows in-field use.[103] The noninvasive nature of system along with high sensitivity and remote monitoring makes it attractive candidate for biological imaging applications.

1.7.4 Advantages of MOFs as Sensing Material:

MOFs have become attractive candidate as sensing material and offer several advantages.[104] The performance of a sensory material generally depends upon the extent of interaction between probe and analyte, which in turn depend on concentration of analyte. The porous matrix of MOF act as host for incoming guest/analyte molecules and allow concentration of analyte in host matrix (pre-concentration effect) that produces amplified response.[15] The designable architecture in terms of size and shape of pore facilitate size exclusion or molecular sieving effect for improved selectivity. This also governs the sorption kinetics and thermodynamics and hence the response time. Additionally, the selectivity can also be improved by selective interactions with target analyte by secondary functional groups lining the pore surface. The electronic properties of MOFs can be fine-tuned by judicious selection of building units for enhanced performance. The restricted vibrational and rotational motions of ligand in MOF compared to free ligand give improved fluorescence and can be retained even at elevated temperatures.[105] The crystalline nature of MOF provide mechanistic insights and better structure-property correlation. The MOFs with biocompatible building units and high chemical stability can also be used for biological applications. Finally, the possibility of hybridization of MOF with different functional materials encourages the device fabrication.

1.7.5 MOFs for Explosive Sensing:

In 2009, Prof. Li et al. for the first time explored fluorescent MOF $Zn_2(bpdc)_2(bpee)\cdot 2DMF$, bpdc = 4,4'-biphenyldicarboxylate; bpee = 1,2-bis(4-pyridyl)ethylene) for vapor phase explosive detection.[106] Fast and efficient fluorescence quenching (turn-off) was observed in a reversible manner, when the fluorescent MOF was exposed to vapors of electron deficient nitro analytes. Since then many fluorescent MOFs were explored for vapor phase explosive detection,[107] however, the quenching performance was mainly governed by vapor pressure of analytes. To get more insights in

to the quenching mechanism, the same group carried out systematic investigation of fluorescent MOF response on exposure to both electron rich and electron deficient analytes.[108] The electron deficient analytes led to fluorescence quenching response while electron rich analytes resulted in enhancement in fluorescence intensity which was explained by excited state electron transfer process. Recently, we have also reported a 2D π-stacked luminescent MOF for vapor phase Nitrobenzene (NB) and (2,3-dimethyl-2,3-dinitrobutane) DMNB detection.[109]

Not only in vapor phase but the luminescent MOFs have also effectively used for liquid phase explosive detection. The liquid phase explosive detection is important for detection of buried/under water explosives and environmental monitoring. Prof. Qian et al. reported DNT and TNT detection in ethanol using lanthanide based nanoscale MOF $Eu_2(bdc)_3(H_2O)_2\cdot(H_2O)_2$ (H_2bdc = 1,4-benzenedicarboxylic acid). Prof. Mukherjee et al. utilized $[Zn_4O(L)_2(H_2O)_3]\cdot 3DMA\cdot 3EtOH\cdot 6H_2O$ (H_3L = 5-(4-carboxyphenylethynyl)isophthalic acid) MOF for TNT detection in ethanol.[111] Prof. Feng et al. investigated fluorescence performance of $[Zn_3(tdpat)(H_2O)_3]$ (H_6tdpat = 2,4,6-Tris(3,5-dicarboxyphenylamino)-1,3,5-triazine) towards NB in methanol.[112] Fluorescence quenching response of $[In_2L][NH_2(CH_3)_2]_2(DMF)_4(H_2O)_{16}$ (H_8L = tetrakis[(3,5-dicarboxyphenoxy)methyl]methane) was observed upon addition of electron rich and electron deficient analytes were studied by Prof. Chen et al.[113] There are few reports of MOF based probes for TNP sensing, however the selective detection of TNP in presence of TNT, RDX, DNT and related nitro analytes using MOF is rarely achieved.[107]

1.7.6 MOFs for H_2S Sensing:

In recent times MOFs are studied for storage and delivery of biologically important H_2S gas for industrial and biomedical applications.[114] As mentioned earlier the detection and continuous monitoring of H_2S in biological system is very important and fluorescence based detection systems can be very useful in this regards. Yet this functional material hasn't been studied for detection of H_2S especially in biological system. Fluorescence turn-on based systems are advantageous for biological imaging applications to avoid false response in pool of biomolecules as the detection occurs relative to black background. While we were working on MOF based fluorescence turn-on probe for H_2S, Prof. Wang et al. reported malonitrile functionalized MOF for the detection of H_2S and thiol containing amino acid Cysteine (Cys).[115]

1.8 Research Objective:

Despite recent reports of MOF based probes for the detection of nitro explosives, there is wide scope to develop new fluorescent MOFs for selective and sensitive nitro explosive TNP detection. The selectivity is important for successful detection; unfortunately reported MOFs did not show excellent selectivity. On the other hand, for real time application selective detection of targeted analyte in presence of other competing analytes is desired. Also there is scope for improvement in MOF sensing performance with regards to improved sensitivity and photophysical properties such as excitation and emission in visible region, water stability for aqueous phase explosive detection, biocompatibility for environmental monitoring.

The major objectives for improvements in nitro explosive sensing performance are:

(a) Selective detection of nitro explosive TNP in presence of competing nitro analytes.

(b) Use of specific chemical and physical interaction to achieve selectivity.

(c) Employing different functionalities for improved performance.

(d) Selective detection in aqueous phase.

(e) Excitation and emission wavelengths of probe should be in the visible range.

(f) Probes should be environment friendly.

Regarding H_2S detection MOF exhibiting fluorescence turn-on effect in response to H_2S is desirable. But the MOF which show turn-on response in response to targeted analytes are rare, and one which shows selectivity along with turn-on response are still rare. Also there are only limited number of MOF reports used for biological imaging applications. Thus there is plenty of scope for the improvement of MOF based turn-on probes for H_2S in terms of selectivity, sensitivity, fast response, detection limit, cell permeability and cytotoxicity.

The major objectives for improvements of H_2S sensing performance are:

(a) Selective detection of H_2S in presence of competing biomolecules.

(b) Use of specific chemical and physical interaction to achieve selectivity.

(c) Employing different functionalities for improved performance.

(d) Low cytotoxicity and possible application in live cell imaging.

1.9 References:

(1) (a) Navrotsky, A.; Trofymluk, O.; Levchenko, A. A. *Chem. Rev.* **2009,** *109,* 3885-3902. (b) Pera-Titus, M. *Chem. Rev.* **2014,** *114*, 1413-1492. (c) Valtchev, V.; Tosheva, L. *Chem. Rev.* **2013,** *113*, 6734-6760. (d) Wu, D.; Xu, F.; Sun, B.; Fu, R.; He, H.; Matyjaszewski, K. *Chem. Rev.* **2012,** *112*, 3959-4015. (e) Linares, N.; Silvestre-Albero, A. M.; Serrano, E.; Silvestre-Albero, J.; Garcia-Martınez, J. *Chem Soc. Rev.* **2014,** *43,* 7681-7717.

(2) Sing, K. S. W.; Everett, D. H.; Haul, R. A. W.; Moscou, L.; Pierotti, R. A.; Rouquerol, J.; Siemieniewska, T. *Pure and Applied Chemistry* **1985,** *57,* 603-619.

(3) (a) Kerihuel J. C. *J Wound Care.* **2010,** *19,* 208-215. (b) Brahmi, N.; Kouraichi, N.; Thabet, H.; Amamou, M. *Am. J. Emerg. Med.* **2006,** *24,* 440-443.

(4) (a) Manocha, L. M. *Sadhana* **2003,** *28,* 349-358. (b) Sakintuna, B.; Yürüm, Y. *Ind. Eng. Chem. Res.* **2005,** *44,* 2893-2902. (c) Yang, Y.; Chiang, K.; Burke, N. *Catal. Today* **2011,** *178,* 197-205.

(5) Meng, L.-Y.; Park, S.-J. *Bull. Korean Chem. Soc.* **2012,** *33,* 3749-3754.

(6) Yang, R. T. Wiley-Interscience, **2003**.

(7) Walton, K. S.; Abney, M. B.; Douglas LeVan, M. *Microporous Mesoporous Mater.* **2006,** *91,* 78-84.

(8) Batten, S. R.; Champness, N. R.; Chen, X.-M.; Garcia-Martinez, J.; Kitagawa, S.; Öhrström, L.; O'Keeffe, M.; Suh, M. P.; Reedijk, J. *Pure Appl. Chem.* **2013,** *85,* 1715-1724.

(9) (a) Furukawa, H.; Cordova, K. E.; O'Keeffe, M.; Yaghi, O. M. *Science* **2013,** *341,* 1230444 DOI: 10.1126/science.1230444. (b) Ferey, G. *Chem. Soc. Rev.* **2008,** *37,* 191-214.

(10) Inokuma, Y.; Yoshioka, S.; Ariyoshi, J.; Arai, T.; Hitora, Y.; Takada, K.; Matsunaga, S.; Rissanen, K.; Fujita, M. *Nature* **2013,** *495,* 461-466.

(11) Bennett, T. D.; Cheetham, A. K. *Acc. Chem. Res.* **2014,** *47,* 1555-1562.

(12) O'Keeffe, M.; Yaghi, O. M. *Chem. Rev.* **2012,** *112,* 675-702.

(13) Deng, H.; Doonan, C. J.; Furukawa, H.; Ferreira, R. B.; Towne, J.; Knobler, C. B.; Wang, B.; Yaghi, O. M. *Science* **2010,** *327,* DOI: 10.1126/science.1181761.

(14) Zhou, H.-C.; Long, J. R.; Yaghi, O. M. *Chem. Rev.* **2012,** *112,* 673-674.

(15) Xionga, R.; Odbadrakhb, K.; Michalkovac, A.; Lunaa, J. P.; Petrovac, T.; Keffera, D. J.; Nicholsond, D. M.; Fuentes-Cabrerae, M. A.; Lewisb, J. P.; Leszczynskic, J. *Sens. and Actuators B* **2010,** *148,* 459-468.

(16) (a) Stepanow, S.; Lingenfelder, M.; Dmitriev, A.; Spillmann, H.; Delvigne, E.; Lin, N.; Deng, X.; Cai, C.; Barth, J. V.; Kern, K. *Nat. Mater.* **2004,** *3,* 229-233. (b) Uemura, T.; Yanai, N.; Watanabe, S.; Tanaka, H.; Numaguchi, R.; Miyahara, M. T.; Ohta, Y.; Nagaoka, M.; Kitagawa, S. *Nat. Commun.* **2010,** doi:10.1038/ncomms1091. (c) Guo, Z.; Kobayashi, T.; Wang, L.-L.; Goh, T. W.; Xiao, C.; Caporini, M. A.; Rosay, M.; Johnson, D. D.; Pruski, M.; Huang, W. *Chem. Eur. J.* **2014,** *20,* 16308-16313.

(17) Horike, S.; Shimomura, S.; Kitagawa, S. *Nat. Chem.* **2009,** *1,* 695-704.

(18) (a) Yanai, N.; Kitayama, K.; Hijikata, Y.; Sato, H.; Matsuda, R.; Kubota, Y.; Takata, M.; Mizuno, M.; Uemura, T.; Kitagawa, S. *Nat. Mater.* **2011,** *10,* 787-793. (b) Halder, G. J.; Kepert, C. J.; Moubaraki, B.; Murray, K. S.; Cashion, J. D. *Science* **2002,** *298,* 1762-1765. (c) Takashima, Y.; Martinez, V. M.; Furukawa, S.; Kondo, M.; Shimomura, S.; Uehura, H.; Nakahama, M.; Sugimoto, K.; Kitagawa, S. *Nat. Commun.* **2011,** DOI: 10.1038/ncomms1170.

(19) Kitagawa, S.; Kitaura, R.; Noro, S.i. *Angew. Chem. Int. Ed.* **2004,** *43,* 2334-2375.

(20) Tranchemontagne, D. T.; Mendoza-Corte´s, J. L.; O'Keeffe, M.; Yaghi, O. M. *Chem. Soc. Rev.* **2009,** *38,* 1257-1283.

(21) (a) Loiseau, T.; Serre, C.; Huguenard, C.; Fink, G.; Taulelle, F.; Henry, M.; Bataille, T.; Ferey, G. *Chem. Eur. J.* **2004,** *10,* 1373-1382. (b) Volkringer, C.; Meddouri, M.; Loiseau, T.; Guillou, N.; Marrot, J.; Ferey, G.; Haouas, M.; Taulelle, F.; Audebrand, N.; Latroche, M. *Inorg. Chem.* **2008,** *47,* 11892-11901.

(22) Du, D.-Y.; Qin, J.-S.; Li, S.-L.; Su, Z.-M.; Lan, Y.-Q. *Chem. Soc. Rev.* **2014,** *43,* 4615-4632.

(23) (a) He, Y.; Li, B.; O'Keeffe, M.; Chen, B. *Chem. Soc. Rev.* **2014,** *43,* 5618-5656. (b) Smaldone, R. A.; Forgan, R. S.; Furukawa, H.; Gassensmith, J. J.; Slawin, A. M. Z.; Yaghi, O. M.; Stoddart, J. F. *Angew. Chem. Int. Ed.* **2010,** *49,* 8630-8634. (c) He, Y.; Furukawa, H.; Wu, C.; O'Keeffe M.; Chen, B. *CrystEngComm* **2013,**

15, 9328-9331. (d) Li, M.; Li, D.; O'Keeffe, M.; Yaghi, O. M. *Chem. Rev.* **2014,** *114*, 1343-1370.

(24) Lu, W.; Wei, Z.; Gu, Z.-Y.; Liu, T.-F.; Park, J.; Park, J.; Tian, J.; Zhang, M.; Zhang, Q.; Gentle III, T.; Boscha, M.; Zhou, H.-C. *Chem. Soc. Rev.* **2014,** *43*, 5561-5593.

(25) Zhang, J.-P.; Zhang, Y.-B.; Lin, J.-B.; Chen, X.-M. *Chem. Rev.* **2012,** *112*, 1001-1033.

(26) (a) Zhang, J.; Matsushita, M. M.; Kong, X. X.; Abe, J.; Iyoda, T. *J. Am. Chem. Soc.* **2001,** *123,* 12105-12106. (b) Matsushita, M. M.; Morikawa, M.; Kawai, T. Iyoda, T. *Mol. Cryst. Liq. Cryst.* **2000,** *343,* 87-96. (c) Davidson,G. J. E.; Loeb, S. J. *Angew. Chem. Int. Ed.* **2003,** *42,* 74-77.

(27) Rabenau, A. *Angew. Chem. Int. Ed. Engl.* **1985,** *24*, 1026-1040.

(28) (a) Stock, N.; Biswas, S. *Chem. Rev.* **2012,** *112*, 933-969. (b) Meek, S. T.; Greathouse, J. A.; Allendorf, M. D. *Adv. Mater.* **2011,** *23*, 249-267.

(29) (a) Klinowski, J.; Paz, F. A. A.; Rocha, J. *Dalton Trans.* **2011,** *40*, 321-330. (b) Schlesinger, M.; Schulze, S.; Hietschold, M.; Mehring, M. *Microporous Mesoporous Mater.* **2010,** *132*, 121-127.

(30) (a) Qiu, L.-G.; Li, Z.-Q.; Wu, Y.; Wang, W.; Xu, T.; Jiang, S. *Chem. Commun.* **2008,** 3642-3644. (b) Li, Z. Q.; Qiu, L. G.; Xu, T.; Wu, Y.; Wang, W.; Wu, Z. Y.; Jiang, X. *Mater. Lett.* **2009,** *63*, 78-80.

(31) (a) Mueller, U.; Puetter, H.; Hesse, M.; Wessel, H. WO 2005/049892. (b) Ameloot, R.; Pandey, L.; Van der Auweraer, M.; Alaerts, L.; Sels, B. F.; De Vos, D. E. *Chem. Commun.* **2010,** *46*, 3735-3737.

(32) (a) Pichon, A.; Lazuen-Garay, A.; James, S. L. *CrystEngComm* **2006,** *8*, 211-214. (b) Pichon, A.; James, S. L. *CrystEngComm* **2008,** *10*, 1839-1847.

(33) (a) Rieter, W. J.; Taylor, K. M. L.; An, H.; Lin, W.; Lin, W. *J. Am. Chem. Soc.* **2006,** *128*, 9024-9025. (b) Tanaka, D.; Henke, A.; Albrecht, K.; Moeller, M.; Nakagawa, K.; Kitagawa, S.; Groll, J. *Nat. Chem.* **2010,** *2*, 410-416.

(34) Renzo, F. D. *Catal. Today* **1998,** *41*, 37-40.

(35) (a) Horikoshi, R.; Mochida, T.; Kurihara, M.; Mikuriya, M. *Cryst. Growth Des.* **2005,** *5*, 243-249. (b) Ghosh, S.; Kitagawa, S. *CrystEngComm* **2008,** *10*, 1739-1742. (c) Sunatsuki, Y.; Ikuta, Y.; Matsumoto, N.; Ohta, H.; Kojima, M.; Iijima, S.; Hayami, S.; Maeda, Y.; Kaizaki, S.; Dahan, F.; Tuchagues, J.-P. *Angew. Chem.*,

Int. Ed. **2003,** *42,* 1614-1618. (d) Blake, A. J.; Champness, N. R.; Hubberstey, P.; Li, W.-S.; Withersby, M. A.; Schroder, M. *Coord. Chem. Rev.* **1999,** *183,* 117-138. (e) Zhang, J.-P.; Lin, Y.-Y.; Huang, X.-C.; Chen, X.-M. *Chem. Commun.* **2005,** 1258-1260. (f) Tanaka, D.; Kitagawa, S. *Chem. Mater.* **2008,** *20,* 922-931. (g) Nagarkar, S.S.; Chaudhari, A. K.; Ghosh, S. K. *Cryst. Growth Des.* **2012,** *12,* 572-576.

(36) (a) Cravillon, J.; Nayuk, R.; Springer, S.; Feldhoff, A.; Huber, K.; Wiebcke, M. *Chem. Mater.* **2011,** *23,* 2130-2141. (b) Chalati, T.; Horcajada, P.; Gref, R.; Couvreura, P.; Serre, C. *J. Mater. Chem.* **2011,** *21,* 2220-2227.

(37) Nagarkar, S. S.; Chaudhari, A. K.; Ghosh, S. K. *CrystGrowthDes* **2012,** *12,* 572-576.

(38) (a) Betard, A.; Fischer, R. A. *Chem. Rev.* **2012,** *112,* 1055-1083. (b) Falcaro, P.; Ricco, R.; Doherty, C. M.; Liang, K.; Hill, A. J.; Styles, M. J. *Chem. Soc. Rev.* **2014,** *43,* 5513-5560.

(39) (a) Bradshaw, D.; Garai, A.; Huo, J. *Chem. Soc. Rev.* **2012,** *41,* 2344-2381. (b) Zhua, Q.-L.; Xu, Q. *Chem. Soc. Rev.* **2014,** *43,* 5468-5512.

(40) Colon, Y. J.; Snurr, R. Q. *Chem. Soc. Rev.* **2014,** *43,* 5735-5749.

(41) Wanga, Z.; Cohen, S. M. *Chem. Soc. Rev.* **2009,** *38,* 1315-1329.

(42) (a) Foo, M. L.; Matsuda, R.; Kitagawa, S. *Chem. Mater.* **2014,** *26,* 310-322. (b) Burrows, A. D. *CrystEngComm* **2011,** *13,* 3623-3642.

(43) Beheshti, S.; Morsali, A. *RSC Adv.* **2014,** *4,* 41825-41830.

(44) (a) Chen, B.; Eddaoudi, M.; Reineke, T. M.; Kampf,J. W.; O'Keeffe, M.; Yaghi, O. M. *J. Am. Chem. Soc.* **2000,** *122,* 11559-11560. (b) Jeong, N. C.; Samanta, B.; Lee, C. Y.; Farha, O. K.; Hupp, J. T. *J. Am. Chem. Soc.* **2012,** *134,* 51-54.

(45) Tanabe, K. K.; Cohen, S. M. *Chem. Soc. Rev.* **2011,** *40,* 498-519.

(46) Cohen, S. M. *Chem. Rev.* **2012,** *112,* 970-1000.

(47) Ahmed, I.; Jhung, S. H. *Mater. Today* **2014,** *17,* 136-146.

(48) Moon, H. R.; Lim, D.-W.; Suh, M. P. *Chem. Soc. Rev.* **2013,** *42,* 1807-1824.

(49) Czaja, A. U.; Trukhanb, N.; Muller, U. *Chem. Soc. Rev.* **2009,** *38,* 1284-1293.

(50) Kondo, M.; Yoshitomi, T.; Seki, K.; Matsuzaka, H.; Kitagawa, S. *Angew. Chem. Int. Ed. Engl.* **1997,** *36,* 1725-1727.

(51) Rosi, N. L.; Eckert, J.; Eddaoudi, M.; Vodak, D. T.; Kim, J.; O'Keeffe, M.; Yaghi, O. M. *Science* **2003,** *300,* 1127-1129.

(52) Ma, S.; Sun, D.; Simmons, J. M.; Collier, C. D.; Yuan, D.; Zhou, H.-C. *J. Am. Chem. Soc.* **2008,** *130,* 1012-1016.

(53) Farha, O. M.; Yazaydın, A. O.; Eryazici, I.; Malliakas, C. D.; Hauser, B. G.; Kanatzidis, M. G.; Nguyen, S. T.; Snurr, R. Q.; Hupp, J. T. *Nat. Chem.* **2010,** *2,* 944-948.

(54) Mercedes-Benz F125; www.emercedesbenz.com/autos/mercedes-benz/concept-vehicles/mercedes-benz-f125-research-vehicle-technology.

(55) Li, J. R.; Kuppler, R. J.; Zhou, H.-C. *Chem. Soc. Rev.* **2009,** *38,* 1477-1504.

(56) Ma, S. Q.; Wang, X. S.; Collier, C. D.; Manis, E. S.; Zhou, H.-C. *Inorg. Chem.* **2007,** *46,* 8499-8501.

(57) Li, J. R.; Sculley, J.; Zhou, H.-C. *Chem. Rev.* **2012,** *112,* 869-932.

(58) (a) Sumida, K.; Rogow, D. L.; Mason, J. A.; McDonald, T. M.; Bloch, E. D.; Herm, Z.R.; Bae, T.-H.; Long, J. R. *Chem. Rev.* **2012,** *112,* 724-781. (b) Zhang, Z.; Zhao, Y.; Gong, Q.; Lib, Z.; Li, J. *Chem. Commun.* **2013,** *49,* 653-661.

(59) Voorde, B. V.; Bueken, B.; Denayerb, J.; Vos, D. D. *Chem. Soc. Rev.* **2014,** *43,* 5766-5788.

(60) Burtch, N.; Jasuja, H.; Walton, K. S. *Chem. Rev.* **2014,** *114,* 10575-10612.

(61) Alaerts, L.; Kirschhock, C. E.; Maes, M.; van der Veen, M.; Finsy, V.; Depla, A.; Martens, J.; Baron, G. V.; Jacobs, P.; Denayer, J. F. M.; Vos, D. E. D. *Angew. Chem. Int. Ed.* **2007,** *46,* 4293-4297.

(62) Herm, Z. R.; Wiers, B. M.; Mason, J. A.; Baten, J. M.; Hudson, M. R.; Zajdel, P.; Brown, C. M.; Masciocchi, N.; Krishna, R.; Long, J. R. *Science* **2013,** *340,* 960-964.

(63) (a) Han, S.; Wei, Y.; Valente, C.; Lagzi, I.; Gassensmith, J. J.; Coskun, A.; Stoddart, J. F.; Grzybowski, B. A. *J. Am. Chem. Soc.* **2010,** *132,* 16358-16361. (b) Xie, S.; Wang, B.; Zhang, X.; Zhang, J.; Zhang, M.; Yuan, L. *Chirality* **2014,** *26,* 27-32.

(64) (a) Zhao, M.; Ou, S.; Wu, C.-D. *Acc. Chem. Res.* **2014,** *47,* 1199-1207. (b) Dhakshinamoorthy, A.; Garcia, H. *Chem. Soc. Rev.* **2014,** *43,* 5750-5765. (c) Zhanga, T.; Lin, W. *Chem. Soc. Rev.* **2014,** *43,* 5982-5993. (d) Liu, J.; Chen, L.; Cui, H.; Zhang, J.; Zhang, L.; Su, C.-Y. *Chem. Soc. Rev.* **2014,** *43,* 6011-6061.

(65) Lee, J. Y.; Farha, O. K.; Roberts, J.; Scheidt, K. A.; Nguyen, S. T.; Hupp, J. T. *Chem. Soc. Rev.* **2009,** *38,* 1450-1459.

(66) (a) Kurmoo, M. *Chem. Soc. Rev.* **2009,** *38,* 1353-1379. (b) Blundell, S. J.; Pratt, F. L. *J. Phys.: Condens. Matter* **2004,** *16,* R771-R828. (c) Molecular Magnetism, New Magnetic Materials, ed. Itoh, K.; Kinoshita, M. Gordon Breach-Kodansha, Tokyo, **2000**.

(67) Coronado, E.; Espallargas, G. M. *Chem. Soc. Rev.* **2013,** *42*, 1525-1539.

(68) (a) Langley, S. K.; Chilton, N. F.; Moubaraki, B.; Hooper, T.; Brechin, E. K.; Evangelisti, M.; Murray, K. S. *Chem. Sci.* **2011,** *2*, 1166-1169. (b) Evangelisti, M.; Candini, A.; Affronte, M.; Pasca, E.; Jongh, L. J.; Scott, R. T. W.; Brechin, E. K. *Phys. Rev. B* **2009,** *79*, 104414-104420.

(69) Lorusso, G.; Palacios, M. A.; Nichol, G. S.; Brechin, E. K.; Roubeau, O.; Evangelisti, M. *Chem. Commun.* **2012,** *48*, 7592-7594.

(70) (a) Keskin, S.; Kızılel, S. *Ind. Eng. Chem. Res.* **2011,** *50*, 1799-812. (b) McKinlay, A. C.; Morris, R. E.; Horcajada, P.; Ferey, G.; Gref, R.; Couvreur, P.; Serre, C. *Angew. Chem. Int. Ed.* **2010,** *49*, 6260-6266.

(71) (a) Horcajada, P.; Chalati, T.; Serre, C.; Gillet, B.; Sebrie, C.; Baati, T.; Eubank, J. F.; Heurtaux, D.; Clayette, P.; Kreuz, C.; Chang, J.-S.; Hwang, Y. K.; Marsaud, V.; Bories, P.-N.; Cynober, L.; Gil, S.; Ferey, G.; Couvreur, P.; Gref, R. *Nat. Mater.* **2010,** *9*, 172-178. (b) Huxford, R. C.; Rocca, J. D.; Lin, W. *Curr. Opin. Chem. Bio.* **2010,** *14*, 262-268.

(72) Miller, S. R.; Heurtaux, D.; Baati, T.; Horcajada, P.; Greneche, J.-M.; Serre, C. *Chem. Commun.* **2010,** *46*, 4526-4528.

(73) (a) McKinlay, A. C.; Xiao, B.; Wragg, D. S.; Wheatley, P. S.; Megson, I. L.; Morris, R. E. *J. Am. Chem. Soc.* **2008,** *130*, 10440-10444. (b) Diring, S.; Wang, D. O.; Kim, C.; Kondo, M.; Chen, Y.; Kitagawa, S.; Kamei, K.-i.; Furukawa, S. *Nat. Commun.* **2013,** doi: 10.1038/ncomms3684. (c) Hamon, L.; Serre, C.; Devic, T.; Loiseau, T.; Millange, F.; Ferey, G.; Weireld, G. D. *J. Am. Chem. Soc.* **2009,** *131*, 8775-8777. (d) Allan, P. K.; Wheatley, P. S.; Aldous, D.; Mohideen, M. I.; Tang, C.; Hriljac, J. A.: Megson, I. L.; Chapman, K. W.; Weireld, G. D.; Vaesen, S.; Morris, R. E. *Dalton Trans.* **2012,** *41*, 4060-4066. (e) Bloch, E. D.; Hudson, M. R.; Mason, J. A.; Chavan, S.; Crocellà, V.; Howe, J. D.; Lee, K.; Dzubak, A. L.; Queen, W. L.; Zadrozny, J. M.; Geier, S. J.; Lin, L.-C.; Gagliardi, L.; Smit, B.; Neaton, J. B.; Bordiga, S.; Brown, C. M.; Long, J. R. *J. Am. Chem. Soc.* **2014,** *136*,

10752-10761. (f) DeCoste, J. B.; Peterson, G. W. *Chem. Rev.* **2014,** *114,* 5695-5727.

(74) (a) Rieter, W. J.; Taylor, K. M. L.; An, H.; Lin, W. *J. Am. Chem. Soc.* **2006,** *128,* 9024-9025. (b) Taylor, K. M. L.; Jin, A.; Lin, W. *Angew. Chem. Int. Ed.* **2008,** *47,* 7722-7725.

(75) Dekrafft, K. E.; Xie, Z. G.; Cao, G. H.; Tran, S.; Ma, L.; Zhou, O. Z.; Lin, W. *Angew. Chem. Int. Ed.* **2009,** *48,* 9901-9904.

(76) (a) Uemura, T.; Horike, S.; Kitagawa, S. *Chem.-Asian J.* **2006,** *1,* 36-44. (b) Uemura, T.; Yanaia, N.; Kitagawa, S. *Chem. Soc. Rev.* **2009,** *38,* 1228-1236.

(77) (a) Li, S.-L.; Xu, Q. *Energy Environ. Sci.* **2013,** *6,* 1656-1683. (b) Horike, S.; Umeyama, D.; Kitagawa, S. *Acc. Chem. Res.* **2013,** *46,* 2376-2384.

(78) Yoon, M.; Suh, K.; Natarajan, S.; Kim, K. *Angew. Chem. Int. Ed.* **2013,** *52,* 2688-2700.

(79) Ramaswamy, P.; Wong, N. E.; Shimizu, G. K. H. *Chem. Soc. Rev.* **2014,** *43,* 5913-5932.

(80) Nagarkar, S. S.; Unni, S. M.; Sharma, A.; Kurungot, S.; Ghosh, S. K. *Angew. Chem. Int. Ed.* **2014,** *53,* 2638-2642.

(81) Allendorf, M. D.; Bauer, C. A.: Bhaktaa, R. K.; Houka, R. J. T. *Chem. Soc. Rev.* **2009,** *38,* 1330-1352.

(82) Doty, F. P.; Bauer, C. A.; Skulan, A. J.; Grant, P. G.; Allendorf, M. D. *Adv. Mater.* **2009,** *21,* 95-101.

(83) (a) Lu, G.; Farha, O. K.; Kreno, L. E.; Schoenecker, P. M.; Walton, K. S.; Van Duyne, R. P.; Hupp, J. T. *Adv. Mater.* **2011,** *23,* 4449-4452. (b) Achmann, S.; Hagen, G.; Kita, J.; Malkowsky, I. M.; Kiener, C.; Moos, R. *Sensors* **2009,** *9,* 1574-1589. (c) Biemmi, E.; Darga, A.; Stock, N.; Bein, T. *Microporous Mesoporous Mater.* **2008,** *114,* 380-386. (d) Robinson, A. L.; Allendorf, M. D.; Stavila, V.; Thornberg, S. M. Materials Research Society Proceedings; San Francisco, CA, April 2011. (e) Allendorf, M. D.; Houk, R. J. T.; Andruszkiewicz, L.; Talin, A. A.; Pikarsky, J.; Choudhury, A.; Gall, K. A.; Hesketh, P. J. *J. Am. Chem. Soc.* **2008,** *130,* 14404-14405.

(84) Kreno, L. E.; Leong, K.; Farha, O. M.; Allendorf, M.; Duyne, R. P. V.; Hupp, J. T. *Chem. Rev.* **2012,** *112,* 1105-1125.

(85) (a) Barea, E.; Montoro, C.; Navarro, J. A. R. *Chem. Soc. Rev.* **2014,** *43,* 5419-5430. (b) Iversen, K. J.; Spencer, M. J. S. *J. Phys. Chem. C* **2013,** *117,* 26106-26118.

(86) Baldwin, E. A.; Bai, J.; Plotto, A.; Dea, S. *Sensors* **2011,** *11,* 4744-4766.

(87) (a) S.W. Thomas III, G. D. Joly, T. M. Swager, *Chem. Soc. Rev.* **2007,** *36,* 1339-1386. (b) Kim, K.; Tsay, O. G.; Atwood, D. A.; Churchill, D. G. *Chem. Rev.* **2011,** *111,* 5345-5403.

(88) (a) Domaille, D. W.; Que, E. L.; Chang, C. J. *Nat. Chem. Bio.* **2008,** *4,* 168-175. (b) Kumar, N.; Bhalla, V.; Kumar, M. *Coord. Chem. Rev.* **2013,** *257,* 2335-2347.

(89) Salinas, Y.; Martinez-Manez, R.; Marcos, M. D.; Sancenon, F.; Castero, A. M.; Parra, M.; Gil, S. *Chem. Soc. Rev.* **2012,** *41,* 1261-1296.

(90) Senesac, L.; Thundat, T. G. *Mater. Today* **2008,** *11,* 28-36.

(91) (a) McQuade, D. T.; Pullen, A. E.; Swager, T. M. *Chem. Rev.* **2000,** *100,* 2537-2574. (b) Sanchez, J. C.; Trogler, W. C. *J. Mater. Chem.* **2008,** *18,* 3143-3156.

(92) Steevens, J. A.; Duke, B. M.; Lotufo, G. R.; Bridges, T. S. *Environ. Toxicol. Chem.* **2002,** *21,* 1475-1482.

(93) (a) Thorne, P. G.; Jenkins, T. F. *Field Anal. Chem. Technol.* **1997,** *1,* 165-170. (b) Wyman, J. F.; Serve, M. P.; Honson, D. W.; Lee, L. H.; Uddin, D. E. *J. Toxicol. Environ. Health* **1992,** *37,* 313-327.

(94) (a) Eiceman, G. A.; Stone, J. A. *Anal. Chem.* **2004,** *76,* 390A-397A. (b) Håkansson, K..; Coorey, R. V.; Zubarev, R. A.; Talrose, V. L.; Håkansson, P. *J. Mass Spectrom.* **2000,** *35,* 337-346. (c) Sylvia, J. M.; Janni, J. A.; Klein, J. D.; Spencer, K. M. *Anal. Chem.* **2000,** *72,* 5834-5840. (d) Luggar, R. D.; Farquharson, M. J.; Horrocks, J. A.; Lacey, R. J. *X-Ray Spectrom.* **1998,** *27,* 87-94. (e) Hallowell, S. F. *Talanta* **2001,** *54,* 447-458.

(95) Toal, S. J.; Trogler, W. C. *J. Mater. Chem.* **2006,** *16,* 2871-2883.

(96) Pandey, S. K.; Kim, K.-H.; Tang, K.-T. *Trends Anal. Chem.* **2012,** *32,* 87-99.

(97) Reiffenstein, R. J.; Hulbert, W. C.; Roth, S. H. *Annu. Rev. Pharmacol. Toxicol.* **1992,** *32,* 109-134.

(98) Szabó, C. *Nat. Rev. Drug Discov.* **2007,** *6,* 917-935.

(99) (a) Eto, K.; Asada, T.; Arima, K.; Makifuchi, T.; Kimura, H. *Bio-chem. Biophys. Res. Commun.* **2002,** *293,* 1485-1488. (b) Kamoun, P.; Belardinelli, M.-C.; Chabli, A.; Lallouchi, K.; Chadefaux-Vekemans, B. *Am. J. Med. Genet.* **2003,**

116A, 310-311. (c) Yang, W.; Yang, G.; Jia, X.; Wu, L.; Wang, R. *J. Physiol.* **2005,** *569*, 519-531. (d) Szabo, C.; Coletta, C.; Chao, C.; Modis, K.; Szczesny, B.; Papapetropoulos, A.; Hellmich, M. R. *Proc. Natl. Acad. Sci. U.S.A.* **2013,** *110*, 12474-12479.

(100) (a) Lin, V. S., Lippert, A. R.; Chang, C. J. *Proc. Natl. Acad. Sci. U.S.A.* **2013,** *110*, 7131-7135. (b) Yang, G.; Wu, L.; Jiang, B.; Yang, W.; Qi, J.; Cao, K.; Meng, Q.; Mustafa, A. K.; Mu, W.; Zhang, S.; Snyder, S. H.; Wang, R. *Science* **2008,** *322*, 587-590.

(101) Peng, H.; Chen, W.; Burroughs, S.; Wang, B. *Curr. Org. Chem.* **2013,** *17*, 641-653.

(102) (a) Basabe-Desmonts, L.; Reinhoudta, D. N.; Crego-Calama, M. *Chem. Soc. Rev.* **2007,** *36*, 993-1017. (b) Khatua, S.; Orrit, M. *ACS Nano* **2013,** *7*, 8340-8343.

(103) (a) Wei, Q.; Qi, H.; Luo, W.; Tseng, D.; Ki, S. J.; Wan, Z.; Göröcs, Z.; Bentolila, L. A.; Wu, T.-T.; Sun, R.; Ozcan, A. *ACS Nano* **2013,** *7*, 9147-9155. (b) Xin, Y.; Wang, Q.; Liu, T.; Wang, L.; Lib, J.; Fang, Y. *Lab Chip* **2012,** *12*, 4821-4828.

(104) Cui, Y.; Yue, Y.; Qian, G.; Chen, B. *Chem. Rev.* **2012,** *112*, 1126-1162.

(105) Shustova, N. B.; Cozzolino, A. F.; Reineke, S.; Baldo, M.; Dinca, M. *J. Am. Chem. Soc.* **2013,** *135*, 13326-13329.

(106) Lan, A.; Li, K.; Wu, H.; Olson, D. H.; Emge, T. J.; Ki, W.; Hong, M.; Li, J. *Angew. Chem. Int. Ed.* **2009,** *48*, 2334-2338.

(107) (a) Hu, Z.; Deibert, B. J.; Li, J. *Chem. Soc. Rev.* **2014,** *43*, 5815-5840. (b) Banerjee, D.; Hu, Z.; Li, J. *Dalton Trans.* **2014,** *43*, 10668-10685.

(108) Pramanik, S.; Zheng, C.; Zhang, X.; Emge, T. J.; Li, J. *J. Am. Chem. Soc.* **2011,** *133*, 4153-4155.

(109) Chaudhari, A. K.; Nagarkar, S. S.; Joarder, B.; Ghosh, S. K. *Cryst. Growth Des.* **2013,** *13*, 3716-3721.

(110) Xu, H.; Liu, F.; Cui, Y.; Chen, B.; Qian, G. *Chem. Commun.* **2011,** *47*, 3153-3155.

(111) Gole, B.; Bar, A. K.; Mukherjee, P. S. *Chem. Commun.* **2011,** *47*, 12137-12139.

(112) Ma, D.; Li, B.; Zhou, X.; Zhou, Q.; Liu, K.; Zeng, G.; Li, G.; Shi, Z.; Feng, S. *Chem. Commun.* **2013,** *49*, 8964-8966.

(113) Xue, Y.-S.; He, Y.; Zhou, L.; Chen, F.-J.; Xu, Y.; Du, H.-B.; You, X.-Z.; Chen, B. *J. Mater. Chem. A* **2013,** *1*, 4525-4530.

(114) (a) Hamon, L.; Serre, C.; Devic, T.; Loiseau, T.; Millange, F.; Férey, G.; Weireld, G. D. *J. Am. Chem. Soc.* **2009,** *131*, 8775-8777. (b) Petit, C.; Mendoza, B.;

Bandosz, T. J. *ChemPhysChem* **2010,** *11,* 3678-3684. (c) Petit, C.; Bandosz, T. J. *Dalton Trans.* **2012,** *41,* 4027-4035. (d) Allan, P. K.; Wheatley, P. S.; Aldous, D.; Infas Mohideen, M.; Tang, C.; Hriljac, J. A.; Megson, I. L.; Chapman, K. W.; Weireld, G. D.; Vaesen, S.; Morris, R. E. *Dalton Trans.* **2012,** *41*, 4060-4066. (e) Gutierrez-Sevillano, J. J.; Martin-Calvo, A.; Dubbeldam, D.; Calero, S.; Hamad, S. *RSC Adv.* **2013,** *3,* 14737-14749. (f) Chavan, S.; Bonino, F.; Valenzano, L.; Civalleri, B.; Lamberti, C.; Acerbi, N,; Cavka, J. H.; Leistner, M.; Bordiga, S. *J. Phys. Chem. C* **2013,** *117,* 15615-15622. (g) Nickerl, G.; Leistner, M.; Helten, S.; Bon, V.; Senkovska, I.; Kaskel, S. *Inorg. Chem. Front.* **2014,** *1*, 325-330. (h) Liu, B.; Chen, Y. *Anal. Chem.* **2013,** *85,* 11020-11025.

(115) Li, H.; Feng, X.; Guo, Y.; Chen, D.; Li, R.; Ren, X.; Jiang, X.; Dong, Y.; Wang, B. *Sci. Rep.* **2014,** doi:10.1038/srep04366.

Chapter 2

Design and Synthesis of Fluorescent Metal Organic Framework for Selective Nitro Explosive TNP Sensing

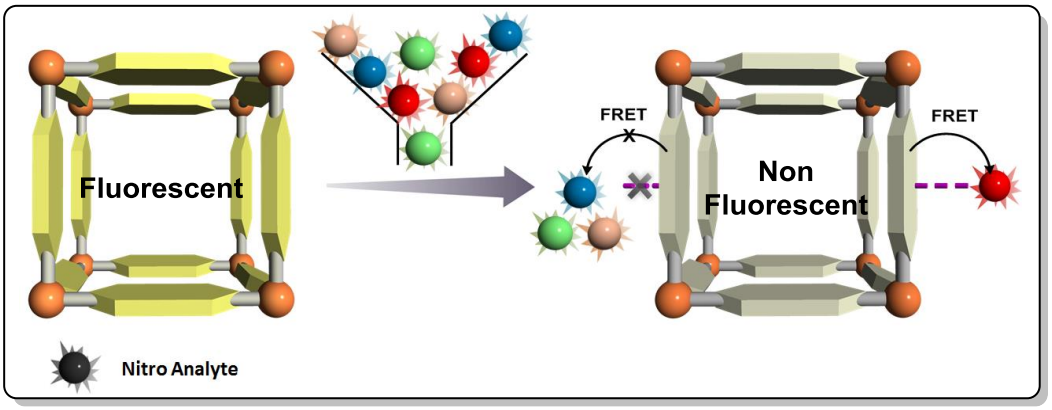

2.1 Introduction:

Rapid and selective detection of explosives has become one of the most pressing issues concerning homeland security, military applications, forensic investigations, and mine-field analysis.[1] Nitro aromatics such as 2,4,6-trinitrotoluene (TNT), 2,4-dinitrotoluene (2,4-DNT) and 2,4,6-trinitrophenol (TNP) are common ingredients of industrial explosives and found in many unexploded land mines worldwide.[1,2] The detection of nitro aromatics present in soil and groundwater is very crucial for tracing buried, underwater explosives and for environmental monitoring near ordnance bases.[3] Current high explosive detection methods include canines or sophisticated instruments that are expensive, complex and have portability issues during in-field use.[3] Fluorescence based detection is gaining increasing attention owing to its high sensitivity, simplicity, short response time and its ability to be employed both in solution and solid phase. Numerous π-electronrich fluorescent conjugated polymers have been synthesized and are used in the detection of trace amounts of nitro aromatics.[4]

Although extremely high sensitivity towards nitro aromatic explosives has been demonstrated, the quick and selective detection of nitro explosives is still an unexplored area. Selectivity is critical for fruitful detection in practical applications. The selective detection of TNT or TNP from a mixture by photo induced electron transfer (PET) is very difficult, as both of them have extremely strong electron affinity.[5] Targeting specific chemical and/or physical properties in addition to strong electron affinity can be a better approach to overcome this problem. The major focus of current research is on the detection of TNT, despite the superior explosive power of TNP.[6] Also, TNP is widely used in dyes, fireworks, matches, glass, and leather industries.[7] During commercial production and use, TNP is released into the environment, leading to the contamination of soil and aquatic systems. Additionaly, in mammalian metabolic processes, TNP transforms into picramic acid (2-amino-4,6-dinitrophenol), which has ten times more mutagenic activity than TNP.[8] Thus, there is an urgent need for efficient and reliable sensors for TNP.

Metal-organic frameworks (MOFs) are well known for their applications in molecular storage, separation, drug delivery and catalysis.[9] Detectable changes in luminescence by tuning the host-guest chemistry along with tailorable porosity and high surface area makes MOFs excellent candidates for sensing.[10] The use of a metal ions with a high complexation affinity and non-detrimental fluorescence, connected by a luminescent ligands can be a good strategy to synthesize fluorescent MOFs.[11] The

pioneering work of Prof. Li et al. and others have demonstrated the potential of luminescent MOFs in explosives detection.[12] These MOF materials exhibit fast, highly sensitive, and reversible nitro-explosives sensing. However, the selective detection of one of the nitro explosive in the presence of others has not been reported (Scheme **2.1**).

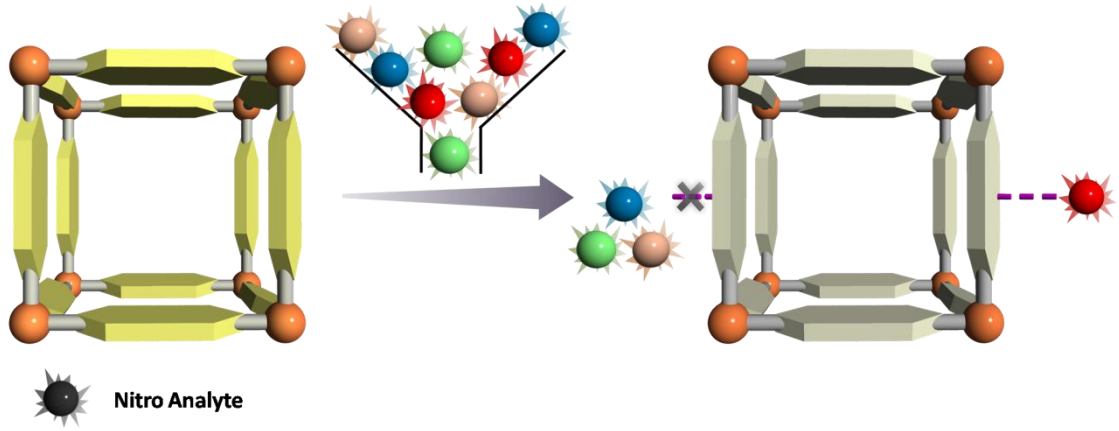

Scheme 2.1: MOF-based sensor for the selective detection of target nitro explosives in the presence of other nitro compounds.

In this chapter we present the selective detection of the nitro explosive TNP by a fluorescent metal-organic framework. For the first time, the selective detection of TNP in the presence of other nitro compounds has been demonstrated in MOFs. The selectivity for TNP is achieved by accessible Lewis basic sites, present in conjugated organic fluorophores, but no such report is known for MOF-based materials.[7,13]

2.2 Experimental Section:

Caution!: TNT, RDX and TNP are highly explosive and should be handled carefully and in small amounts. TNP (Common name Picric acid) forms shock-sensitive compounds with heavy metals.

2.2.1 Materials and Methods:

TNT and RDX were obtained from HEMRL Pune and used without further purification. All the other reagents and solvents were commercially available and used as received. FT-IR spectra were recorded on NICOLET 6700 FT-IR spectrophotometer using KBr pellets. Powder X-ray diffraction pattern (PXRD) were measured on Bruker D8 Advanced X-ray diffractometer at room temperature using Cu K_α radiation (λ = 1.5406 Å). Thermogravimetric analyses was recorded on a Perkin-Elmer STA 6000 TGA analyzer

under N_2 atmosphere with a heating rate of 10 °C/min. Fluorescence measurements were done using Horiba FluoroMax 4 with stirring. SEM image was obtained using FEI Quanta 3D dual beam ESEM and UV-Visble measurements using SPECTRASCAN UV-2600.

2.2.2 Synthesis of $[Cd(L_1)_{0.5}(L_2)]\cdot G_x$ (1):

$Cd(NO_3)_2\cdot 4H_2O$ (0.154 g), 2,6-napthalenedicarboxylic acid ($H_2\mathbf{L_1}$, 0.054 g), 4-pyridinecarboxylic acid ($H\mathbf{L_2}$, 0.061 g) were added to DMF-EtOH (1:1, 6 mL) and solution was then placed in a Teflon-lined autoclave. The autoclave was heated under autogenous pressure to 120 °C for 2 days and then cooled to room temperature over 24 h. Upon cooling, the compound **1** was obtained as brown colored single crystals in ~20% yield. Compound **1** can be also prepared with better yield (~45%) using DEF as solvent, which was used for further studies.

2.2.3 Single Crystal X-ray Structure Determination of 1:

Single-crystal X-ray data of **1** was collected at 150 K on a Bruker KAPPA APEX II CCD Duo diffractometer (50 kV, 30 mA) using graphite-monochromated Mo K_α radiation (λ = 0.71073 Å). Crystal was on nylon CryoLoops (Hampton Research) with Paraton-N (Hampton Research). The data integration and reduction were processed with SAINT software.[14] Multi-scan absorption correction was applied to the collected reflections. The structure was solved by the direct method using SHELXTL[15] and was refined on F^2 by full matrix least-squares technique using the SHELXL-97[16] program package within the WINGX[17] program. All non-hydrogen atoms were refined anisotropically. All hydrogen atoms were located in successive difference Fourier maps and they were treated as riding atoms using SHELXL default parameters. The structures were examined using the *Adsym* subroutine of PLATON[18] to ensure that no additional symmetry could be applied to the models. Identification of the guest entities within the voids of the frameworks was not possible by modeling electron densities due to the disordered nature contents of the large pores in the frameworks. The routine SQUEEZE was applied to the structures in order to remove diffuse electron density associated with badly disordered solvent molecules. Because of the poor crystal quality, the maximum residual electron density value is remaining high. Multiple crystals from different batches showed the same problem. Crystallographic data for compound **1** is listed in Table **2.A1** in Appendix.

2.2.4 Activation of Compound 1 (1'):

~50 mg compound **1** was immersed in 20 mL acetonitrile (MeCN) for two days and during two days the acetonitrile was replaced by fresh acetonitrile at regular time interval to get acetonitrile exchange sample. The acetonitrile exchanged sample was then heated at 120 °C under vacuum for 5 h to get activated (guest-free) compound **1'**.

2.2.5 Low Pressure Gas Sorption Measurements:

Low pressure gas sorption measurements were performed using BelSorpmax (Bel Japan). All of the gases used were of 99.999% purity. Prior to adsorption measurement, the guest-free sample **1'** was pretreated at 120 °C under vacuum for 5 h using BelPrepvacII and purged with N_2 on cooling. Between the experiments with various gases, the outgassing procedure was repeated for ~5 h. The N_2, H_2, Ar, and O_2 gas sorption isotherms were monitored at 77 K and 273 K. The adsorption isotherms for the CO_2 were measured at 195 K, 273 K. Surface area and pore size distribution were calculated using BelMaster analysis software.

2.2.6 Photophysical Measurements:

In typical experimental setup, 1 mg of **1'** is weighed and added to cuvette containing 2.5 mL of MeCN under stirring. The fluorescence spectra of **1'** was measured *in-situ* in 350-650 nm range with excitation wavelength of 340 nm upon incremental addition of freshly prepared analyte solutions. Solution was stirred at constant rate during experiment to maintain homogeneity of solution.

2.3 Results and Discussion:

2.3.1 Synthesis and X-ray Structure of 1:

Compound **1** was synthesized by solvothermal reaction of 2,6-naphthalenedicarboxylic acid ($H_2\mathbf{L_1}$), 4-pyridinecarboxylic acid ($H\mathbf{L_2}$), and $Cd(NO_3)_2{\cdot}4H_2O$ in DEF or DMF-EtOH mixture solvent as colorless crystals.[19] Single-crystal X-ray diffraction (SC-XRD) analysis revealed that **1** crystallizes in monoclinic crystal system, space group $P2_1/c$, and formulated as $[Cd(\mathbf{L_1})_{0.5}(\mathbf{L_2})]{\cdot}G_x$ (G = guest molecules). The asymmetric unit of **1** consists of one-half $\mathbf{L_1}$, one $\mathbf{L_2}$, and one Cd(II) ion and disorder solvents. Each metal ion exhibited seven coordinated distorted pentagonal bipyramidal geometry with NO_6 donor set, bonding from two bidentate carboxylate units

from two different ligands, two bridging carboxylate oxygen from another set of each ligand, and the seventh coordination was occupied by the nitrogen atom of one of the $\mathbf{L_2}$ ligand (Figure **2.1a**). These bridging bonds extended the metal centers to make a metal-carboxylate chain along the *c* axis. Other ends of both the ligands of the metal carboxylate chain were connected with four different metal carboxylate chains, and this continuous network formed the assembled three dimensional (3D) structure (Figure **2.1b**). The resultant 3D framework is porous and forms 1D channel along *c* axis, with the channel dimensions 9.5 × 7.8 $Å^2$. The cavities of the framework were occupied by disordered solvent molecules and PLATON analysis revealed that the 3D porous structure was composed of large voids of 1505.2 $Å^3$ that represent 34.9% per unit cell volume.

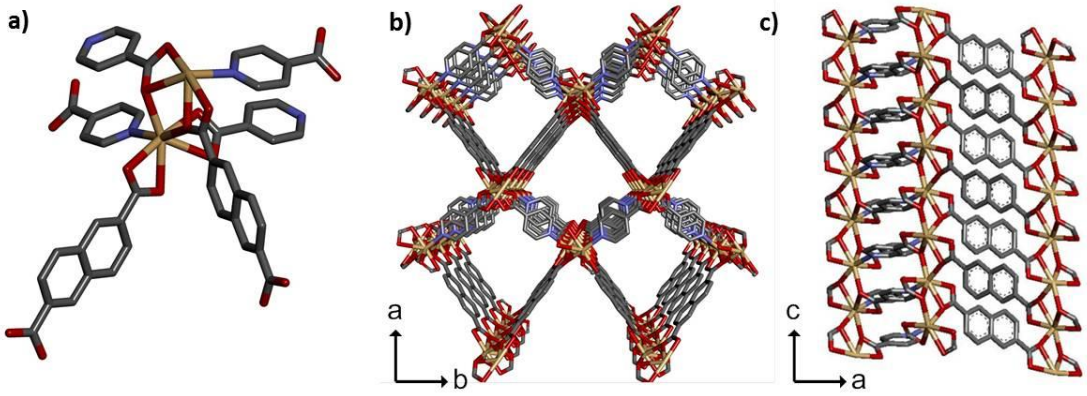

Figure 2.1: (a) Coordination environment around Cd(II) center, (b) 3D porous framework of compound **1** with 1D channels along the *c* axis, (c) 1D channel lined with naphthalene moieties along the *b* axis. Guest molecules and hydrogen atoms are removed for clarity. Gray, red, blue, yellow atoms represent Carbon, Oxygen, Nitrogen and Cadmium(II) respectively.

2.3.2 Phase Purity and Stability of 1:

Powder X-ray diffraction (PXRD) patterns of the bulk phase of compound **1** and simulated pattern matched indicating the phase purity, which was also supported by SC-XRD analysis of randomly selected crystals (Figure **2.2a**). The thermogravimetric analysis (TGA) curve indicates that the compound is stable up to 300 °C (Figure **2.2b**), which was also confirmed by variable temperature PXRD (Figure **2.2c**). The activated compound **1'** was obtained by exchanging occluded DEF molecules with low boiling MeCN. The MeCN was then removed at 120 °C under vacuum to avoid any partial damage to the framework. The overlapping PXRD pattern of activated and assynthesized confirmed the

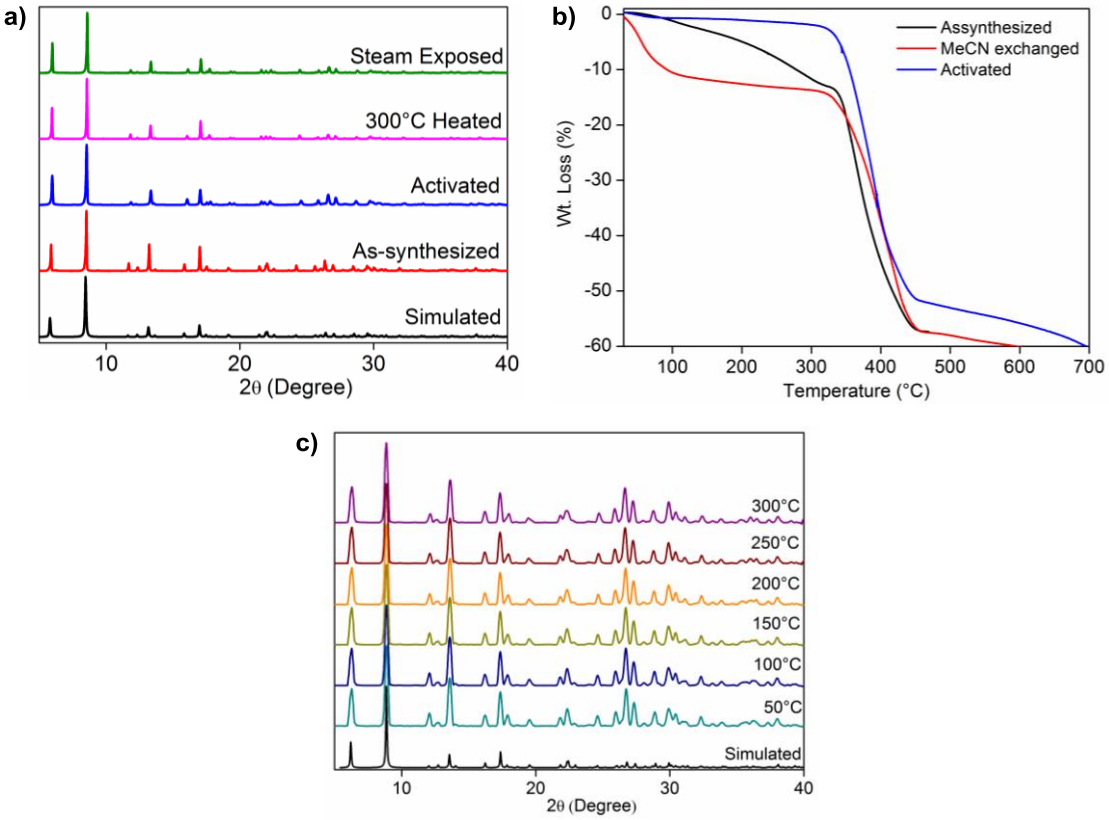

Figure 2.2: (a) PXRD patterns of as-synthesized, acetonitrile exchanged, activated MOF **1**. (b) Thermogravimetric analysis of as-synthesized, acetonitrile exchanged, activated MOF **1**. (c) Variable temperature PXRD pattern of **1**.

stability of the MOF upon guest removal (Figure **2.2a**). The activated compound was found stable even upon exposure to steam.

The porosity of activated compound **1'** was determined using gas adsorption analysis measured volumetrically. Adsorption isotherms for different gases were measured

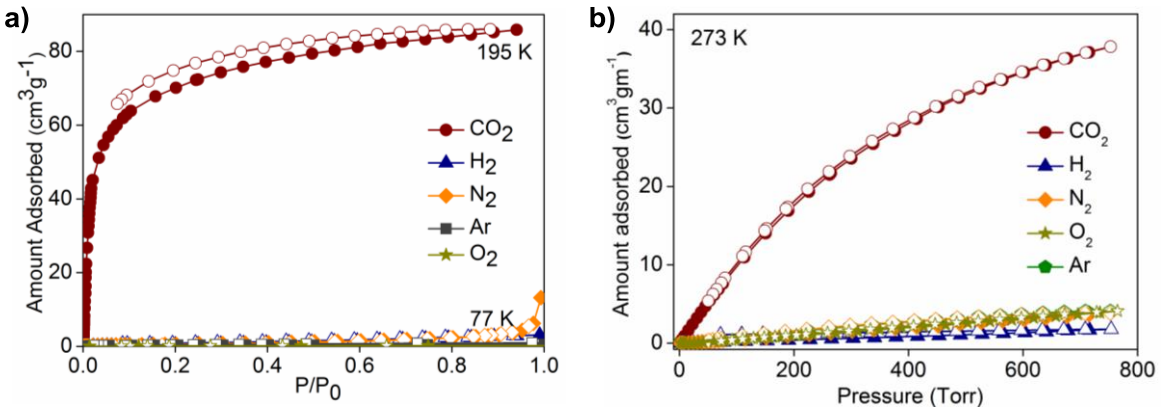

Figure 2.3: (a) Gas adsorption isotherms for **1'** at 77K (for CO_2 195K). (b) Gas adsorption isotherms for **1'** at 273 K. (filled symbols, adsorption; open symbols, desorption).

at 77K (195 K for CO_2) and 273 K. Surprisingly, the adsorption isotherms of Ar (kinetic diameter = 3.5 Å), H_2 (2.8 Å), and N_2 (3.6 Å) at 77 K and 273 K reveal no inclusion of guest molecules, although this rigid framework has much bigger pore size than the kinetic diameter of above gases (9.5 × 7.8 $Å^2$) (Figure **2.3**).

2.3.3 Photophysical Studies:

The photoluminescence spectrum of **1'** dispersed in MeCN exhibits strong emission at 384 nm when excited at 340 nm (Figure **2.4a**). To explore the ability of **1'** to sense a trace quantity of nitro explosives, fluorescence quenching titrations were performed with incremental addition of nitro analytes to **1'** dispersed in MeCN. Fast and high fluorescence quenching was observed upon incremental addition of TNP solution (1 mM). The visible bright blue emission of **1'** under UV light vanished upon the addition of the TNP solution and quenched nearly 78% of the initial fluorescence intensity (Figure **2.4b**). The fluorescence quenching by TNP could be easily discerned at low concentration of 0.9 ppm. Fluorescence quenching titrations were also performed with nitro aromatics such as TNT, 2,4-DNT, 2,6-dinitrotoluene (2,6-DNT), 1,3-dinitrobenzene (DNB), nitrobenzene (NB), and nitro aliphatic compounds such as 2,3-dimethyl-2,3-dinitrobutane (DMNB), nitromethane (NM), and 1,3,5-trinitro-1,3,5-triazacyclohexane (nitro amine RDX). All other nitro compounds showed little effect on the fluorescence intensity (Figures **2.4b**, and **2.A1-2.A8**). These results demonstrate that compound **1'** has high selectivity for TNP compared to other nitro compounds.

The PXRD patterns of compound **1'** showed that the compound remains stable, even after fluorescence titrations with different analytes (Figure **2.5a**). Further, the

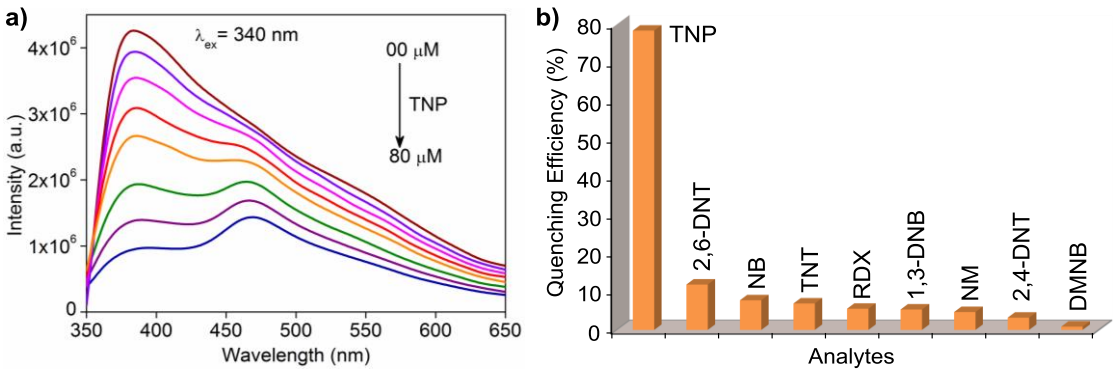

Figure 2.4: (a) Effect on the emission spectra of **1'** dispersed in MeCN upon incremental addition of a TNP solution. (b) Percentage of fluorescence quenching obtained for different analytes at room temperature.

fluorescence quenching efficiency was analysed using the Stern-Volmer (SV) equation, $(I_0/I)=K_{sv}$ [A] + 1, where I_0 is the initial fluorescence intensity before the addition of analyte, I is the fluorescence intensity in the presence of analyte, [A] is the molar concentration of analyte and K_{sv} is the quenching constant (M^{-1}). The SV plot for TNP was nearly linear at low concentrations which subsequently deviated from linearity, bending upwards at higher concentrations (Figure **2.5b**). The nonlinear nature of the SV plot of TNP can be ascribed to self-absorption or energy transfer process.[1a,20] All the other nitro compounds showed linear SV plots (Figure **2.5b**). The quenching constant for TNP was found to be 3.5×10^{-4} M^{-1}, which is comparable to known organic polymers.[21] The quenching constant for TNP is ~30 times greater than for TNT and RDX, which is the highest value known for MOF-based sensors indicating an excellent quenching efficiency towards luminescent **1'**.

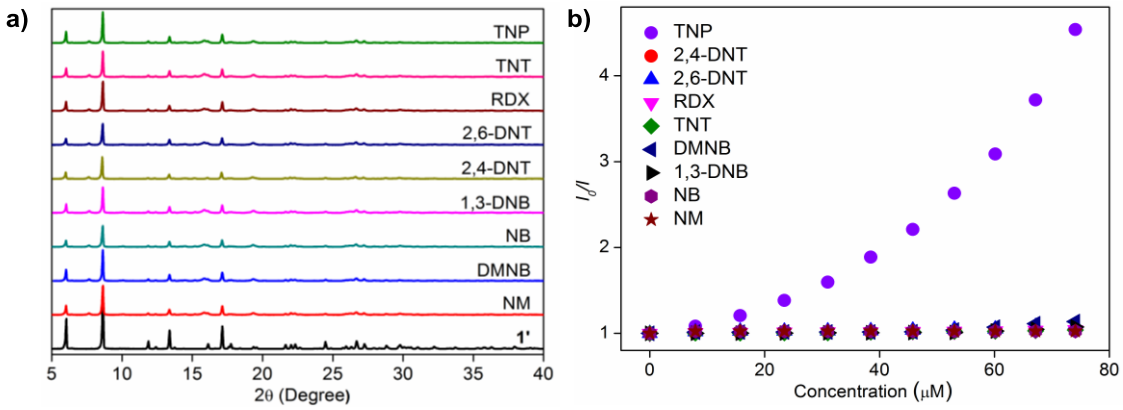

Figure 2.5: (a) PXRD patterns of **1'** after treatment with different nitro analytes. (b) Stern-Volmer plots of nitro analytes.

The selective detection of TNP in an aquatic system is highly desirable for practical applications. To study the selective detection of TNP from aqueous samples, the fluorescence response of **1'** (in MeCN) upon addition of water was initially monitored. The water showed a negligible effect on fluorescence intensity and the spectrum remains unaffected even after 1 h (Figure **2.6a**). The PXRD patterns before and after the addition of water demonstrates the stability of **1'** towards water (Figure **2.A9**). Interestingly the addition of an aqueous solution of TNP (1 mM) to **1'** (in MeCN) also resulted in a fast and high (78%) fluorescence quenching response (Figure **2.6b**)

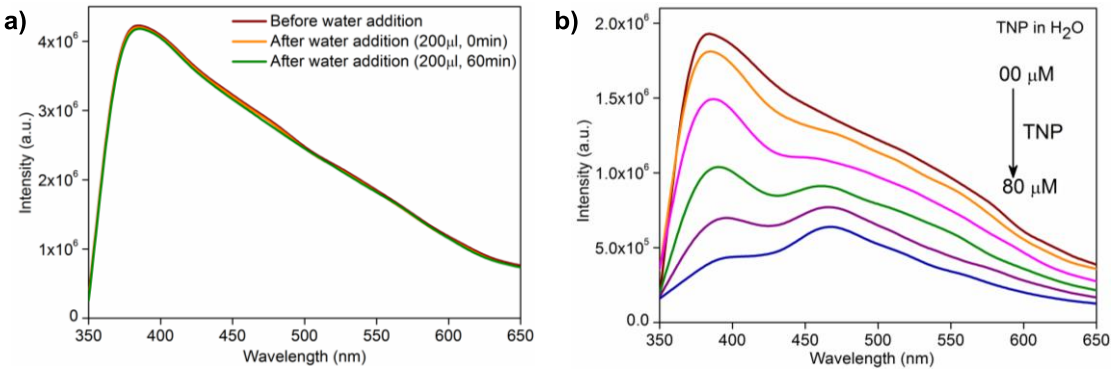

Figure 2.6: (a) Effect of water addition on fluorescence spectrum of **1'** dispersed in MeCN. (b) Effect on the emission spectra of **1'** dispersed in MeCN upon incremental addition of aqueous TNP solution (1mM).

Motivated by these results, we thought to check the selectivity for TNP in the presence of other nitro compounds. In a specially designed experiment, the fluorescence spectrum for **1'** dispersed in MeCN was recorded, to this was added a saturated aqueous solution of TNT (1 mM) followed by TNP (1 mM) and the corresponding emission spectra were monitored. The TNT was added initially, so that high affinity binding sites will be accessible to TNT, but the addition of TNT showed very little effect on fluorescence intensity. On the other hand, the addition of an aqueous solution of TNP to a TNT containing solution, gave significant fluorescence quenching. The quenching efficiency of TNP remaining unaffected, even in next addition sequences (Figure **2.7a**). The addition of aqueous solutions of competing nitro analytes also showed negligible effect on the fluorescence intensity, whereas aqueous TNP quenched the fluorescence effectively (Figure **2.A10-A17**). Similar results were obtained upon addition of MeCN

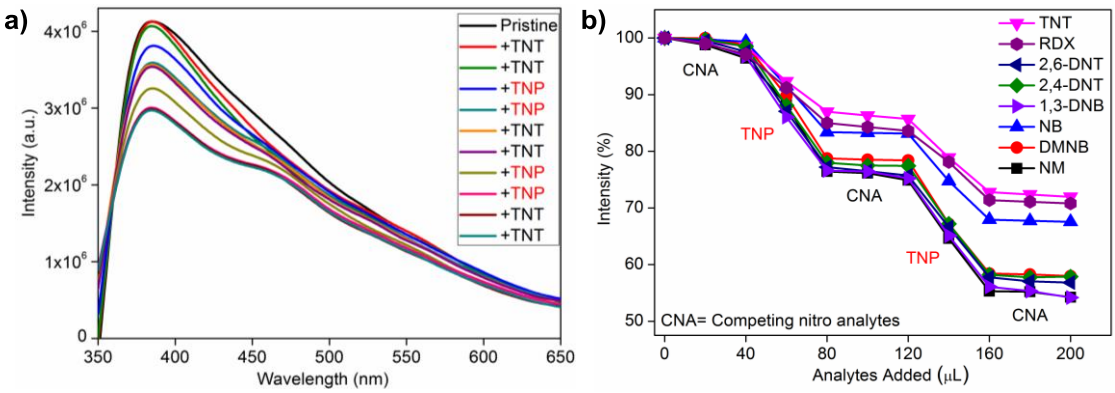

Figure 2.7: (a) Emission spectrum of **1'** upon addition of aqueous solution of TNT followed by TNP (20µl addition each time). (b) Decrease in percentage of fluorescence intensity of **1'** upon the addition of aqueous solutions of competing nitro analytes (CNA) followed by TNP.

solutions of nitro compounds followed by TNP to **1'** in MeCN (Figure **2.A18-A25**). The results can be easily visualized by plotting the percentage fluorescence intensity versus volume of analyte added (Figure **2.7b**). The stepwise decrease in fluorescence intensity clearly demonstrates the unprecedented selectivity of **1'** for TNP, even in the presence of a higher concentration of other nitro compounds. Species **1'** outperforms previously reported TNP chemo sensors, which are highly sensitive, but suffer interference from other electron deficient compounds. The highly selective detection in an aqueous sample in the presence of other nitro compounds makes **1'** a reliable sensor for TNP.[7]

2.3.4 Investigation of Quenching Mechanism:

To understand the origin of the high selectivity of **1'** towards TNP, the mechanism of quenching was investigated. The MOFs, especially with d^{10} metal ions, can be regarded as giant "molecules" and their valence and conduction bands can be treated in a fashion similar to molecular orbitals (MOs).[12b] Generally, the conduction band of a MOF lies at higher energies than the LUMOs of nitro analytes and thus maintains a better driving force for electron transfer to electron deficient analytes, in trurn resulting in fluorescence quenching. Figure **2.8a** shows the HOMO and LUMO orbital energies of electron deficient nitro compounds, as calculated by density functional theory at the B3LYP/6-31G* level (Table **2.A2**). These LUMO energy levels, which are arranged in descending energy order, are expected to represent how easily an electron can be transferred to the electron deficient analyte in the fluorescence quenching process.[2,21b] The LUMO energies were in good agreement with the maximum quenching observed for TNP, but the order of observed quenching efficiency is not fully in accordance with the LUMO energies of other nitro compounds. This indicates that the photoinduced electron transfer is not the only mechanism for quenching.

The non-linear S-V plot for TNP suggests energy transfer mechanism. The resonance energy transfer can occur from fluorophore to non-emissive analyte, if the fluorophore and analyte are close to each other and the absorption band of the analyte has an effective overlap with the emission band of the fluorophore. Resonance energy transfer can dramatically enhance fluorescence quenching efficiency and also improves sensitivity.[22] The probability of resonance energy transfer depends upon the extent of spectral overlap between the absorption band of the analyte and the emission band of the fluorophore. Figure **2.8b** shows that the absorption spectrum of TNP has a large overlap

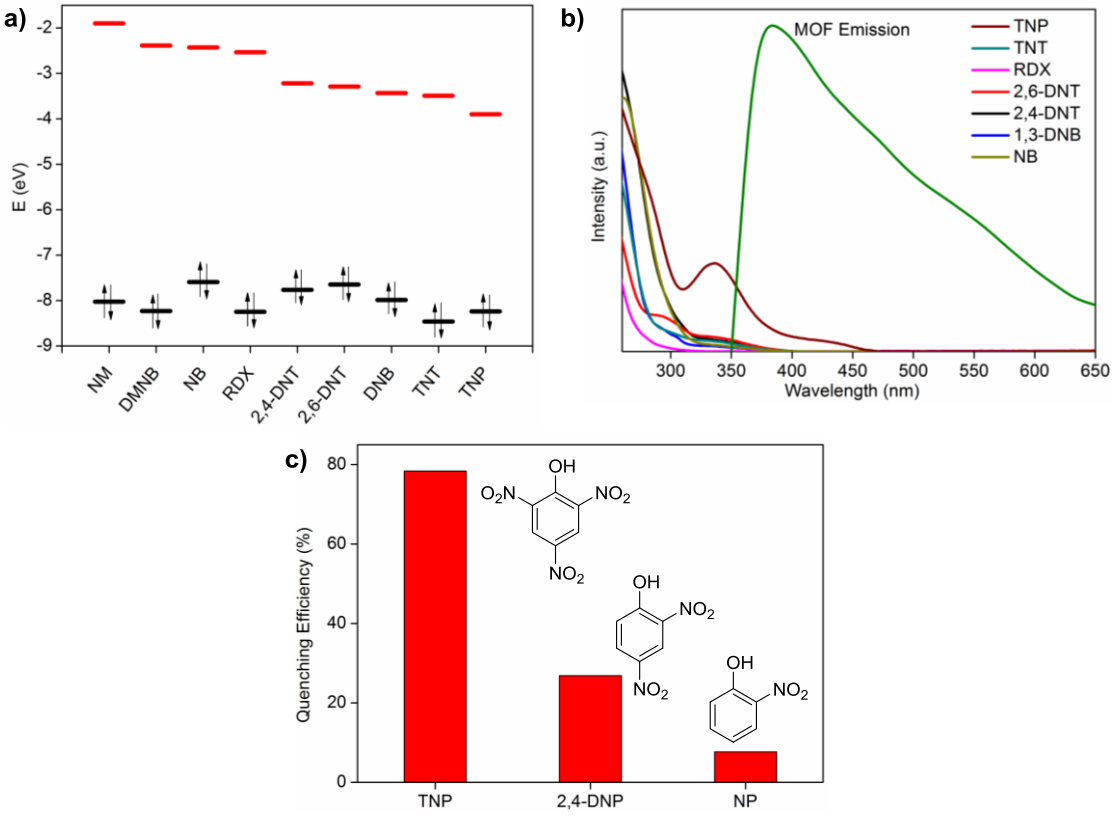

Figure 2.8: (a) HOMO and LUMO energies for nitro analytes arranged in descending order of LUMO energies. (b) Spectral overlap between the absorption spectra of nitro analytes and the emission spectrum of **1'** in MeCN. (c) Comparison of percentage fluorescence quenching obtained for NP, 2,4-DNP, TNP.

with the emission spectrum of **1'**, whereas almost no overlap was observed for RDX, DMNB, NM, or other nitro aromatics, suggesting presence of energy transfer in case of TNP.[23]

The presence of energy transfer can also be supported by the preferential quenching of the 384 nm peak over 470 nm in Figures **2.4a** and **2.6b**. The peak at 384 nm has a spectral overlap with the absorption spectrum of TNP, so the efficient quenching of this peak occurs by an energy transfer mechanism, which leads to a higher quenching response. On the other hand, the peak at 470 nm has no overlap with the absorption spectrum of TNP (Figure **2.8b**), so the quenching occurs by only an electron transfer mechanism and thus a small quenching response towards TNP is observed. The above results suggest that both energy transfer and electron transfer mechanisms are present, and that the energy transfer mechanism is predominant over the electron transfer mechanism in fluorescence quenching by TNP. For other nitro compounds, the quenching occurs only by

electron transfer. The energy transfer is a long-range process, thus emission quenching by TNP is carried over the surrounding fluorophores, thus amplifying the quenching response of **1'**. On the other hand, electron transfer is a short-range process, so the emission quenching by other nitro compounds is limited to the fluorophores that have direct interaction with the analyte. However, to get more insights and understand the exact quenching mechanism, detailed time resolved and advanced experiments are needed.

Species **1'** has an unsaturated Lewis basic pyridine nitrogens on the surface so, to trace presence of electrostatic interactions that can lead to the special selectivity of **1'** for TNP, fluorescence quenching titrations were performed with 4-nitrophenol (NP) and 2,4-dinitrophenol (2,4-DNP; Figure **A26, A27**). The order of the quenching efficiency was found to be TNP >> 2,4-DNP > NP, which is in complete agreement with the order of acidity of these analytes (TNP >> 2,4-DNP > NP; Figure **2.8c**). This may explain the unprecedented selectivity for TNP, as other nitro compounds do not have a hydroxy group they cannot interact strongly with the free Lewis basic sites of the fluorophore (pyridine nitrogen on the surface) in turn resulting in a very low quenching effect. On the other hand, hydroxy group containing analytes such as TNP, 2,4-DNP, NP can interact with the basic sites of **1'** and do so in the order of their acidity. TNP, with its highly acidic hydroxy group interact strongly with the fluorophore and the quenching effect is carried over long range owing to the presence of energy transfer mechanism, thus leading to an amplified response. So, compared to other nitro compounds, species **1'** exhibits a much higher fluorescence quenching response towards TNP, credited to favourable electron and energy transfer mechanisms, as well as electrostatic interactions. Thus, the presence of free Lewis basic sites in MOFs can be a useful tool to achieve the selective detection of TNP over other nitro compounds.

2.4 Summary and Conclusions:

In present chapter, a 3D fluorescent MOF **1'** for the highly selective detection of the nitro explosive TNP has been reported. The compound exhibited selective detection of TNP, even in the presence of other nitro compounds in both aqueous and organic solutions. The selectivity is ascribed to electron and energy transfer mechanisms, as well as electrostatic interactions between TNP and the fluorophore. Our results demonstrate a promising approach to achieve highly selective TNP sensing in MOFs. Thus, the luminescent porous MOFs with high water stability, large spectral overlap and

electrostatic interactions with TNP, could be promising candidates for practical TNP sensing.[17c] Finally, the present study provides a new insight into the design of MOF based explosive sensors, which are likely to be useful under more realistic conditions in the near future.

2.5 References:

(1) (a) Salinas, Y.; Martinez-Manez, R.; Marcos, M. D.; Sancenon, F.; Castero, A. M.; Parra, M.; Gil, S. *Chem. Soc. Rev.* **2012,** *41,* 1261-1296. (b) Thomas III, S.W. ; Joly, G. D.; Swager, T. M. *Chem. Soc. Rev.* **2007,** *36,* 1339-1386.

(2) Germain, M. E.; Knapp, M. J. *Chem. Soc. Rev.* **2009,** *38,* 2543-2555.

(3) Sohn, H.; Sailor, M. J.; Magde, D.; Trogler, W. C. *J. Am. Chem. Soc.* **2003,** *125,* 3821-3830.

(4) (a) Germain, M. E.; Knapp, M. J. *J. Am. Chem. Soc.* **2008,** *130,* 5422-5423. (b) Che, Y.; Gross, D. E.; Huang, H.; Yang, D.; Yang, X.; Discekici, E.; Xue, Z.; Zhao, H.; Moore, J. S.; Zang, L. *J. Am. Chem. Soc.* **2012,** *134,* 4978-4982. (c) Kartha, K. K.; Babu, S. S.; Srinivasan, S.; Ajayaghosh, A. *J. Am. Chem. Soc.* **2012,** *134,* 4834-4841. (d) Li, R.; Yuan, Y.-P.; Qui, L.-G.; Zhang, W.; Zhu, J.-F. s*mall* **2012,** *8,* 225-230. (e) Wang, Y.; La, A.; Ding, Y.; Liu, Y.; Lei, Y. *Adv. Funct. Mater* **2012,** *22,* 3547-3555.

(5) Xu, B.; Wu, X.; Li, H. Tong, H.; Wang, L. *Macromolecules* **2011,** *44,* 5089-5092.

(6) Venkatramaiah, N.; Kumar, S.; Patil, S. *Chem. Commun.* **2012,** *48,* 5007-5009.

(7) He, G.; Peng, H.; Liu, T.; Yang, M.; Zhang, Y.; Fang, Y. *J. Mater. Chem.* **2009,** *19,* 7347-7353.

(8) (a) Thorne, P. G.; Jenkins, T. F. *Field Anal. Chem. Technol.* **1997,** *1,* 165-170. (b) Wollin, K. M.; Dieter, H.H. *Arch. Environ. Contam. Toxicol.* **2005,** *49,* 18-26.

(9) (a) Kitaura, R.; Noro, S.; Kitagawa, S. *Angew. Chem. Int. Ed.* **2004,** *43,* 2334-2375. (b) Vittal, J. J. *Coord. Chem. Rev.* **2007,** *251,* 1781-1795. (c) Ferey, G.; Serre, C. *Chem. Soc. Rev.* **2009,** *38,* 1380-1399. (d) Cheng, X. N.; Zhang, W. X.; Lin, Y.-Y.; Zheng, Y. Z.; Chen, X.-M. *Adv. Mater.* **2007,** *19,* 1494-1498. (e) An, J.; Geib, S. J.; Rosi, N. L. *J. Am. Chem. Soc.* **2009,** *131,* 8376-8377. (f) Zheng, B.; Bai, J.; Duan, J.; Wojtas, L.; Zawototko, M. J. *J. Am. Chem. Soc.* **2011,** *133,* 748-751. (g) Zheng, S. T.; Bu, J. T.; Li, Y.; Wu, T.; Zuo, F.; Feng, P.; Bu, X. *J. Am. Chem. Soc.* **2010,** *132,* 17062-17064. (h) Banerjee, M.; Das, S.; Yoon, M.; Choi,

H. J.; Hyun, M. H.; Park, S. M.; Seo, G.; Kim, K. *J. Am. Chem. Soc.* **2009,** *131,* 7524-7525. (i) Cheetham, A. K.; Rao, C. N. R. *Science* **2007,** *318,* 58-59. (j) Zhou, H.-C.; Long, J. R.; Yaghi, O. M. *Chem. Rev.* **2012,** *112,* 673-74. (k) Allendorf, M. D.; Bauer, C. A.; Bhakta, R. K.; Houk, J. T. *Chem. Soc. Rev.* **2009,** *38,* 1330-1352. (l) Senkovska, I.; Hoffman, F.; Froba, M.; Getzschmann, J.; Bohlmann, W.; Kaskel, S. *Microporous Mesoporous Mater.* **2009,** *122,* 93-98.

(10) Stylianou, K. C.; Heck, R.; Chong, S. Y.; Bacsa, J.; Jones, J. T. A.; Khimyak, Y. Z.; Bradshaw, D.; Rosseinsky, M. J. *J. Am. Chem. Soc.* **2010,** *132,* 4119-4130.

(11) Kreno, L. E.; Leong, K.; Farah, O. K.; Allendorf, M.; Van Duyne, R. P.; Hupp, J. T. *Chem. Rev.* **2012,** *112,* 1105-1125.

(12) (a) Lan, A.; Li, K.; Wu, H.; Olson, D. H.; Emge, T. J.; Ki, W.; Hong, M.; Li, J. *Angew. Chem. Int. Ed.* **2009,** *48,* 2334-2338. (b) Pramanik, S.; Zheng, C.; Zhang, X.; Emge, T. J.; Li, J. *J. Am. Chem. Soc.* **2011,** *133,* 4153-4155. (c) Jiang, H. L.; Tatsu, Y.; Lu, Z. H.; Xu, Q. *J. Am. Chem. Soc.* **2010,** *132,* 5586-5587. (d) Das, S.; Bharadwaj, P. K. *Inorg. Chem.* **2006,** *45,* 5257-5259. (e) Zhang, Z.; Xiang, S.; Rao, X.; Zheng, Q.; Fronczek, F. R.; Qian, G.; Chen, B. *Chem. Commun.* **2010,** *46,* 7205-7207. (f) Xu, H.; Liu, F.; Cui, Y.; Chen, B.; Qian, G. *Chem. Commun.* **2011,** *47,* 3153-3155. (g) Zhang, C.; Che, Y.; Zhang, Z.; Yang, X.; Zang, L. *Chem. Commun.* **2011,** *47,* 2336-2338. (h) Gole, B.; Bar, A. K.; Mukherjee, P. S. *Chem. Commun.* **2011,** *47,* 12137-12139. (i) Wang, C.; Lin, W. *J. Am. Chem. Soc.* **2011,** *133,* 4232-4235.

(13) (a) Peng, Y.; Zhang, A. J.; Dong, M.; Wang, Y. W. *Chem. Commun.* **2011,** *47,* 4505-4507. (b) Zhang, Y.; Guo, Y.; Joo, Y. H.; Parrish, D. A.; Shreeve, J. M. *Chem. Eur. J.* **2010,** *16,* 10778-10784.

(14) SAINT Plus (Version 7.03); Bruker AXS Inc.: Madison, WI, **2004**.

(15) Sheldrick, G. M. SHELXTL Reference Manual, version 5.1; Bruker AXS: Madison, WI, **1997**.

(16) Sheldrick, G. M. *Acta Crystallogr., Sect. A: Found. Crystallogr.* **2008,** 112-122.

(17) Farrugia, L. J. WINGX version 1.80.05; University of Glasgow: Glasgow, **2009**.

(18) Spek, A. L. PLATON, A Multipurpose Crystallographic Tool; Utrecht University: Utrecht, The Netherlands, **2005**.

(19) Nagarkar, S. S.; Chaudhari, A. K.; Ghosh, S. K. *Inorg. Chem.* **2012,** *51,* 572-576.

(20) (a) Zhao, D.; Swager, T. M. *Macromolecules* **2005,** *38,* 9377-9384. (b) Wu, W.; Ye, S.; Yu, G.; Liu, Y.; Qin, J.; Li, Z. *Macromol. Rapid Commun.* **2012,** *33,* 164-171.

(21) (a) Saxena, A.; Fujiki, M.; Rai, R.; Kwak, G. *Chem. Mater.* **2005,** *17,* 2181-2185. (b) Sanchez, J. C.; DiPasquale, A. G.; Rheingold, A. L.; Trogler, W. C. *Chem. Mater*. **2007,** *19,* 6459-6470.

(22) Ramachandra, S.; Popovic, Z.D.; Schuermann, K. S.; Cucinotta, F.; Calzaferri, G.; Cola, L. D. *small* **2011,** *7,* 1488-1494.

(23) (a) Lakowicz, J. R. Principles of Florescence spectroscopy, 3rd ed., Springer, Singapore, **2010,** 443-472. (b) He, L.; Lin, W.; Xua, Q.; Weia, H. *Chem. Commun.* **2015,** DOI: 10.1039/c4cc08522a. (c) Li, D.; Liu, J.; Kwok, R. T. K.; Liang, Z.; Tang, B. Z.; Yu, J. *Chem. Commun.* **2012,** *48,* 7167-7169. (d) Wang, J.; Mei, J.; Yuan, W.; Lu, P.; Qin, A.; Sun, J.; Ma, Y.; Tang,B. Z. *J. Mater. Chem.* **2011,** *21,* 4056-4059. (e) Wei, W.; Huang, X.; Chen, K.; Tao, Y.; Tang, X. *RSC Adv.* **2012,** *2,* 3765-3771. (f) Dinda, D.; Gupta, A.; Shaw, B. K.; Sadhu, S.; Saha, S. K. *ACS Appl. Mater. Interfaces* **2014,** *6,* 10722-10728. (g) Zhang, S.-R.; Du, D.-Y.; Qin, J.-S.; Bao, S.-J.; Li, S.-L.; He, W.-W.; Lan, Y.-Q.; Shen, P.; Su, Z.-M. *Chem. Eur. J.* **2014,** *20,* 3589-3594.

Chapter 3

Aqueous Phase Selective Nitro Explosive TNP Sensing by Fluorescent Metal-Organic Framework with Guest Accessible Secondary Functional Groups

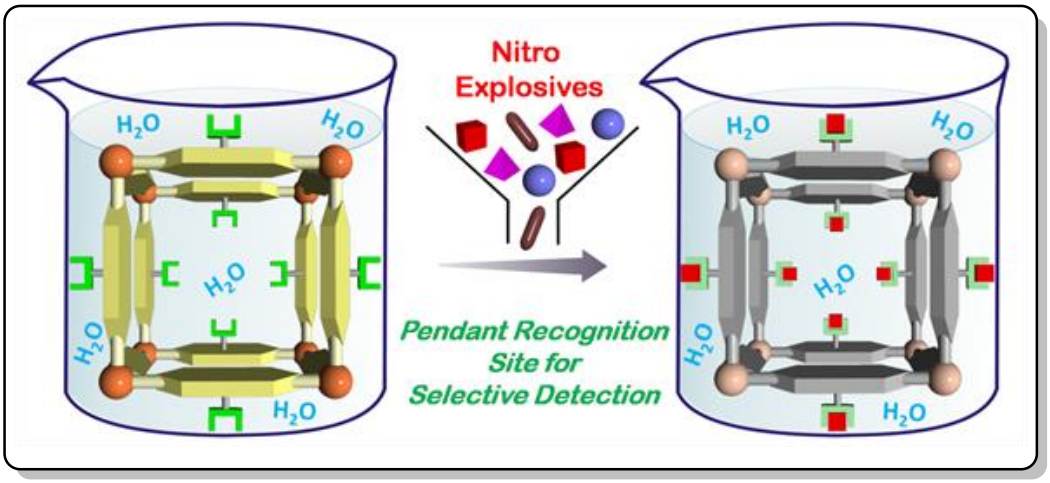

Chapter 3

Section A

Fluorescent MOF with Guest Accessible Pyridyl Moieties for Selective Sensing of Nitro Explosive TNP in an Aqueous Phase

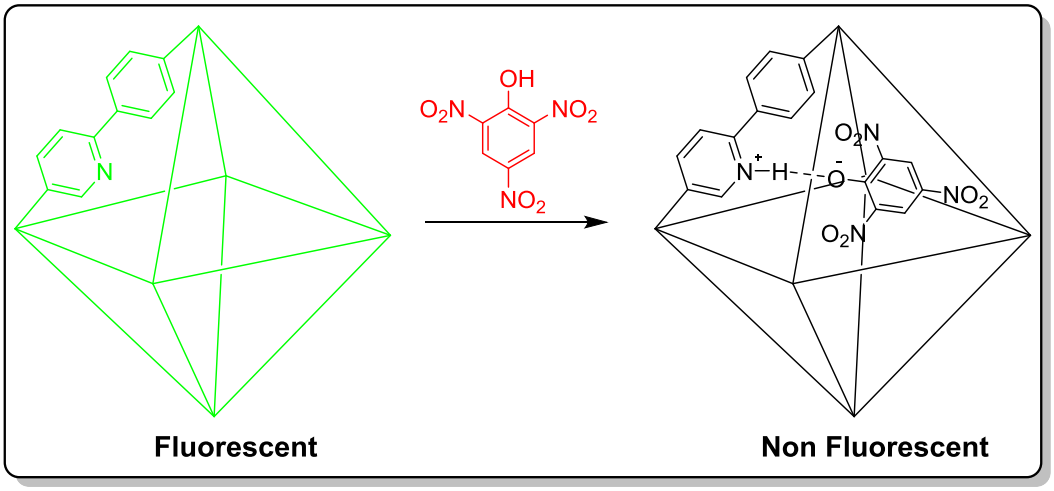

3A.1 Introduction:

Selective and sensitive detection of highly explosive and explosive like substances has become a serious issue concerning national security and environmental protection.[1] Nitro explosives such as 2,4,6-trinitrotoluene (TNT), 2,4-dinitrotoluene (2,4-DNT), 2,4,6-trinitrophenol (TNP), and nitrobenzene (NB) are the main constituents of numerous unexploded land mines used during World War II, and even in today's land mines.[1c] Amongst these nitro explosives, TNP has higher explosive power than TNT and is commonly used in dyes, fireworks, matches, glass and leather industries.[2] In addition to explosive nature, TNP has also been recognized as a toxic pollutant. TNP and its mammalian metabolite, picramic acid, are known for their mutagenic properties.[3] TNP is released into the environment during commercial production and use, leading to the contamination of soil and aquatic systems. Thus the selective and sensitive detection of TNP present in soil and ground water is very important for tracing buried explosives and environmental monitoring near industrial areas. However, selective and sensitive detection of TNP in the presence of other nitro compounds in water is a challenge due to their strong electron affinities, leading to false responses.[4]

Although current explosive detection methods, including trained canines and modern analytical techniques, are selective and accurate, they suffer from disadvantages like high operational cost and portability issues during in-field use.[5] Fluorescence based detection methods have attracted great attention recently by virtue of their high sensitivity, portability, short response time and applicability in both the solid and solution phase.[6] Variety of materials including conjugated organic molecules, nanoparticles and metal complexes have been employed for fluorescence based explosive detection.[7] Despite this fact, their widespread use is limited due to stability, toxicity, multi-step processing and lack of control over molecular organization.[8]

Metal-organic frameworks (MOFs) have been extensively used for gas storage/separation, catalysis, sensing, optoelectronics, clean energy and biomedical applications owing to their high surface areas, designable architectures and host-guest interactions.[9] In particular, as luminescent sensors MOFs provide several advantages over conventional fluorophores.[10a,b] Their designable architectures allow improved host-guest interactions and act as pre-concentrators for target analytes. Additionally,

the immobilization of organic struts in MOFs gives rise to strong emissions due to reduced non-radiative relaxation. The infinite number of choices of organic linkers and/or metal centers allows the fine tuning of the electronic properties of MOFs. Furthermore, the introduction of secondary functional groups endorses preferred binding of the chosen analyte giving rise to better selectivity.

For in-field selective detection of nitro explosives present in soil and ground water, probe working in aqueous media is highly desirable. Although MOFs have been employed for liquid phase explosive detection, to the best of our knowledge there is no report of MOF based probe which can selectively detect nitro explosives in aqueous media till this time.[10] In previous chapter, we reported the fluorescent MOF **1'**, which exhibit highly selective response towards TNP even in the presence of competing nitro analytes due to free Lewis basic sites.[11] However, like most MOFs its poor water stability limits its application to organic solvents. Moreover, the toxic nature of Cd(II) hinders its routine use in environmental applications. In our efforts to develop fluorescent MOFs that work in aqueous media for the selective detection of nitro explosives, we became interested in 2-phenylpyridine-5,4'-dicarboxylic acid ($H_2\mathbf{L_3}$) and the Zr(IV) based MOF $Zr_6O_4(OH)_4(\mathbf{L_3})_6$ (**2**, UiO-67@N).[12] The MOF is composed of non-toxic Zr(IV) metal centers and remains highly stable in water. We envisioned that the sizes of the pore windows (11.5 Å and 23 Å), which are larger than the size of the analytes, could permit easy diffusion of analytes inside the MOF, keeping the electron rich MOF and electron deficient nitro analytes in close proximity (Scheme **3A.1**). Additionally, the guest accessible free Lewis basic sites (pyridyl groups) protruding toward pore may allow selective interaction between TNP and the MOF, giving rise to an efficient response.

3A.2 Experimental Section:

Caution!: TNT, RDX and TNP are highly explosive and should be handled carefully and in small amounts. TNP (Common name Picric acid) forms shock-sensitive compounds with heavy metals.

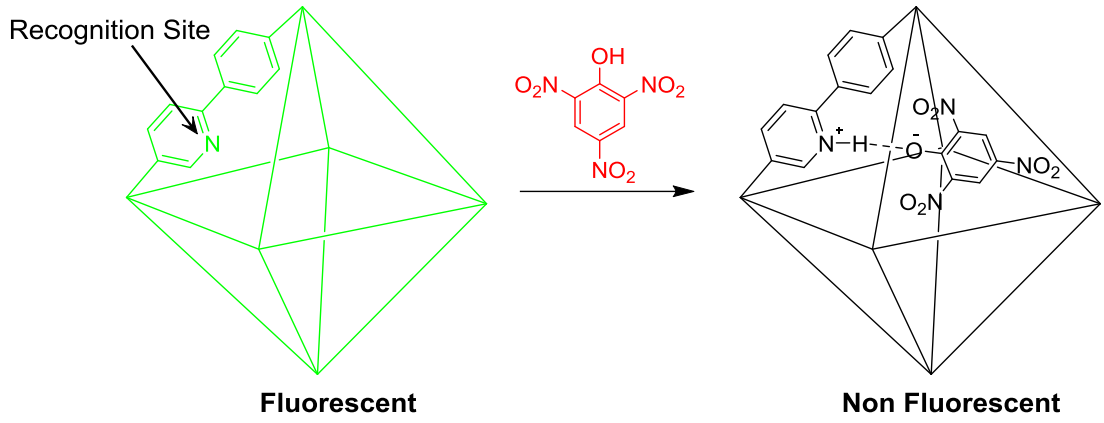

Scheme 3A.1: Schematic representation of selective detection of TNP by luminescent MOF **2'** with guest accessible pyridyl groups.

3A.2.1 Material and Methods:

TNT and RDX were obtained from HEMRL Pune (India) and used without further purification. All the other reagents and solvents were commercially available and used as received. Powder X-ray diffraction patterns (PXRD) were measured on Bruker D8 Advanced X-Ray diffractometer using Cu K_α radiation (λ= 1.5406 Å) with a tube voltage of 40 kV and current of 40 mA in 5 to 40° 2θ range. Thermogravimetric analyses were recorded on Perkin-Elmer STA 6000 TGA analyzer under N_2 atmosphere with a heating rate of 10 °C min^{-1}. Fluorescence measurements were done using Horiba FluoroMax 4 with stirring attachment. ^{1}H NMR was recorded in 400 MHz Jeol ECS-400 Instrument. The UV-Vis measurements were performed using Chemito SPECTRASCAN UV-2600.

3A.2.2 Synthesis of $Zr_6O_4(OH)_4(L_3)_6 \cdot Gx$ (2):

The ligand 2-phenylpyridine-5,4'-dicarboxylic acid (H_2**L_3**) was synthesized using procedure previously reported and characterized by ^{1}H-NMR (Figure **3A.A1**).[13] For synthesis of **2,** $ZrCl_4$ (0.06 g), H_2**L_3** (0.06 g) were dissolved in N,N-dimethylformamide (DMF, 4 mL) in a Teflon lined stainless steel vessel (17 mL). The vessel was sealed and placed in oven and heated at 120 °C for 24 h. After cooling to room temperature, the white crystalline product was isolated by filtration the solid was washed with DMF.

3A.2.3 Activation of Compound 2 (2'):

The occluded solvent present in pores of **2** was then exchanged with MeOH by dipping it in MeOH for 3 days and replacing it with fresh MeOH every 24 h. The guest free porous MOF (**2'**) was obtained by heating the MeOH exchanged MOF at 130 °C under vacuum for 24 h which was then used for fluorescence measurements.

3A.2.4 Photophysical Measurements:

In typical experimental setup, 1 mg of **2'** is weighed and added to cuvette containing 2 mL of water under stirring. The fluorescence response in 330-630 nm range upon excitation at 320 nm was measured *in-situ* after incremental addition of freshly prepared aqueous analyte solutions (1 mM or saturated) and corresponding fluorescence intensity was monitored at 438 nm. The solution was stirred at constant rate in fluorescence instrument with stirring attachment during experiment to maintain homogeneity of solution.

3A.3 Results and Discussion:

3A.3.1 Synthesis and X-ray Structure of 2:

Compound **2** is composed of $Zr_6O_4(OH)_4(CO_2)_{12}$ secondary building unit (SBU). In hexameric SBU each zirconium atom is eight-coordinated with square-antiprismatic coordination environment. One square face is formed by oxygen atoms supplied by μ_3-O and μ_3-OH groups, while the second square face is formed by oxygen atoms coming from carboxylate groups of ligand $\mathbf{L_3}$. The linear dicarboxylate ligand connects the SBU through carboxylate groups giving rise to cubic porous structure (Figure **3A.1**). There are two types of pore windows having dimensions of 11.5 Å and 23 Å and the pores are decorated with free pyridyl functionality protruding towards the pore. Owing to larger pore window and high symmetry the free pyridyl functionality are easily accessible to incoming guest molecules.

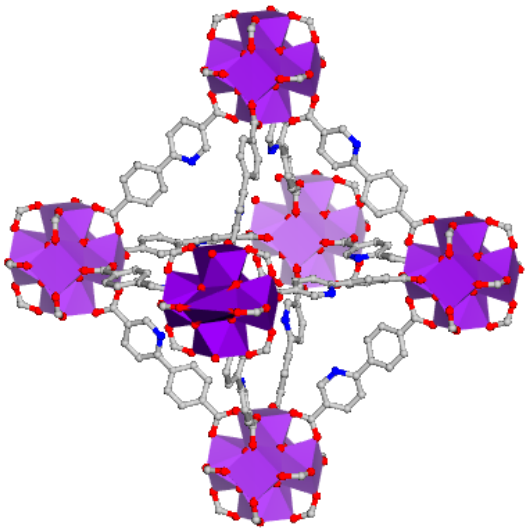

Figure 3A.1: Proposed crystal structure of **2**. Purple octahedra represent the $[Zr_6O_4(OH)4(CO_2)_{12}]^{12+}$ cluster; grey, red and blue spheres represent carbon, oxygen and nitrogen atoms, respectively. Hydrogen atoms are omitted for clarity.

3A.3.2 Phase Purity and Stability of 2:

The PXRD patterns of as-synthesized compound **2** and simulated patterns showed good overlap confirming the successful formation of **2** (Figure **3A.2a**). The compound was found to be stable up to 400 °C with ~20 % weight loss below 100 °C (Figure **3A.2b**). The guest molecules present in pores of **2** were removed by exchanging it with low boiling solvent MeOH for three days. The structure of compound **2** was maintained upon MeOH exchange as seen from PXRD patterns (Figure **3A.2a**). The activated or guest free porous form **2'** was obtained by heating MeOH exchanged sample under reduced pressure. The observed data is in good

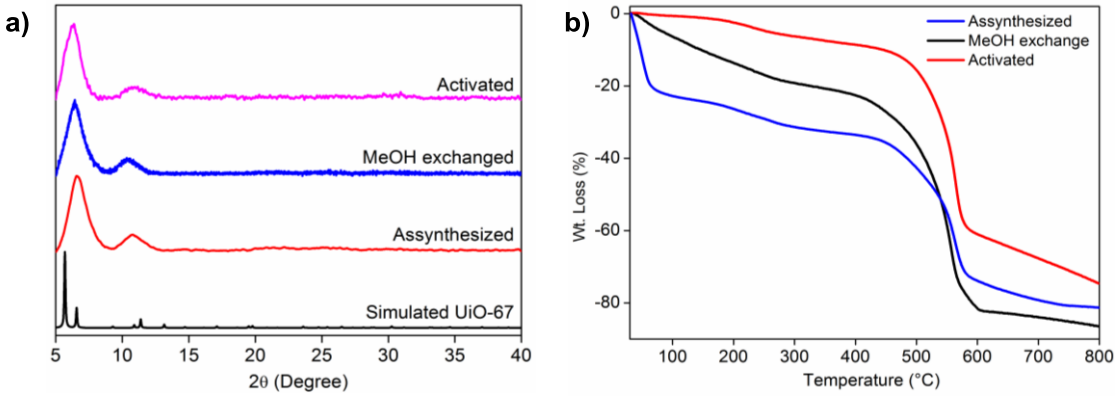

Figure 3A.2: (a) PXRD patterns of as-synthesized, MeOH exchanged and activated MOF **2'**. (b) Thermogravimetric analysis of as-synthesized, MeOH exchanged and activated MOF **2'**.

agreement with the literature. The broad peaks are ascribed to smaller crystallite size.[9e]

3A.3.3 Photophysical Studies:

The guest free MOF **2'** when dispersed in water exhibited strong fluorescence upon excitation at 320 nm (Figure **3A.3a**). To trace the explosive sensing ability of **2'**, changes in the fluorescence intensity of **2'** dispersed in water towards different nitro aromatic compounds like TNP, TNT, 2,4-DNT, 2,6-dinitrotoluene (2,6-DNT), 1,3-dinitrobenzene (DNB), NB and 1,3,5-trinitro-1,3,5-triazacyclohexane (nitro-amine RDX), and nitro-aliphatic compounds such as 2,3-dimethyl-2,3-dinitrobutane (DMNB) and nitromethane (NM), in aqueous solutions were investigated (Figure **3A.3** and Figure **3A.A2-A9**). Figure **3A.3a** shows the changes in the fluorescence spectra of **2'** with increasing amounts of TNP in water. As expected the incremental addition of TNP to **2'** resulted in fast and high fluorescence quenching (73%). Fluorescence quenching can be clearly observed for TNP concentrations of as low as 0.6 ppm. In contrast, all of the other nitro analytes had minor effects on the fluorescence intensity of **2'** (Figure **3A.3b**). This clearly demonstrates the high selectivity of **2'** towards TNP over other nitro analytes.

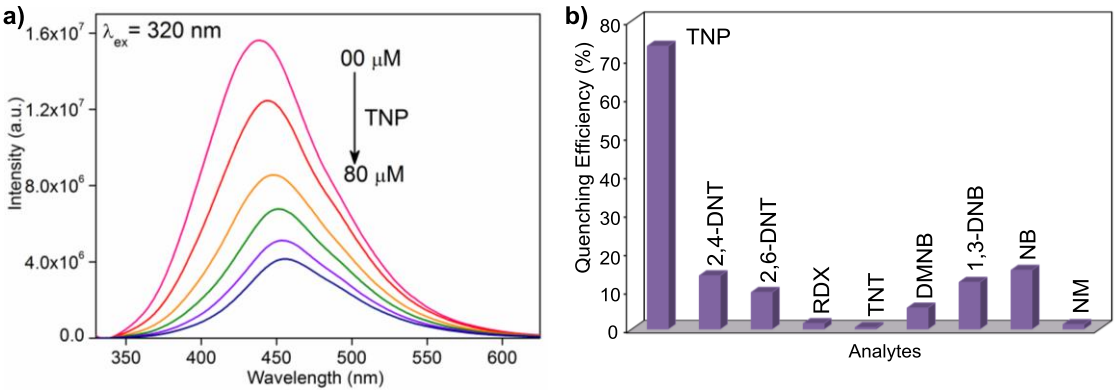

Figure 3A.3: (a) Effect on the emission spectra of **2'** dispersed in water upon incremental addition of an aqueous TNP solution. (b) Percentage of fluorescence quenching obtained for **2'** upon addition of different nitro analytes at room temperature.

Using Stern-Volmer (SV) plots in water, we were able to calculate the quenching constants and analyse the quenching efficiency of the analytes. Using the SV equation $(I_0/I) = K_{sv}[A] + 1$, where I_0 and I are the fluorescence intensities before and after the addition of the respective analyte, [A] is the molar concentration of the analyte and K_{sv} is the quenching constant (M^{-1}). At low TNP concentrations a linear

increase in the SV plot was observed, which upon further increasing the concentration diverged from linearity and began to bend upwards, while other nitro analytes showed linear increases in the SV plots (Figure **3A.4**). This non-linear nature of the SV plot of TNP suggests presence of self-absorption, a combination of static and dynamic quenching or an energy transfer process between TNP and the MOF.[15] The fitting of the SV plot for TNP gave a quenching constant of 2.9×10^4 M^{-1}, which is amongst the highest values known for MOFs. Notably, the quenching constant for TNP was found to be comparable to organic polymers and is much higher than those of TNT, RDX or other nitro analytes, demonstrating the super-quenching ability of TNP towards **2'**.[14]

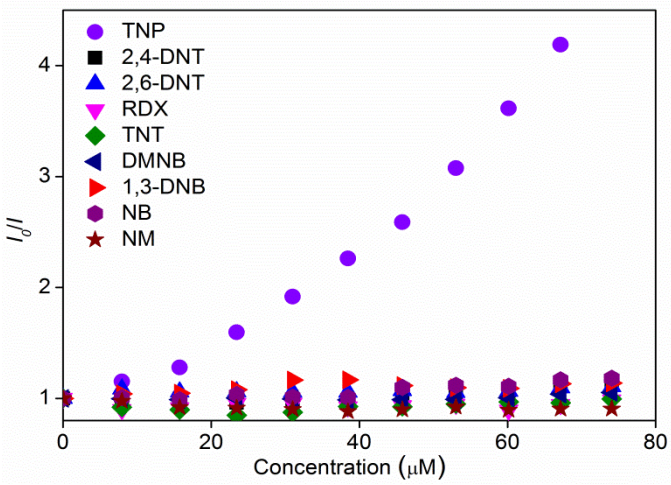

Figure 3A.4: Stern-Volmer (SV) plots for various nitro analytes added to **2'** in water.

Encouraged by these results, the selectivity of **2'** towards TNP in the presence of other nitro analytes in water was investigated. The initial fluorescence spectrum of **2'** dispersed in water was recorded. To this, aqueous TNT solution (40 μL in two equal portions) was added so that high affinity basic sites were accessible to TNT. Negligible fluorescence quenching was observed upon TNT addition. To this, an equal amount of aqueous TNP (40 μL) was added which resulted in significant quenching (Figure **3A.5**). The trend was also repeated in the subsequent addition cycles and the quenching ability of TNP remained unaffected. Similar results were observed when other competing nitro analytes (CNA) were used instead of TNT. This ascertains the exceptional selectivity of **2'** towards TNP even in the presence of competing nitro analytes in water. The high selectivity and sensitivity of **2'** towards TNP in water makes **2'** a reliable and efficient in-field sensor for TNP that works in aqueous media.

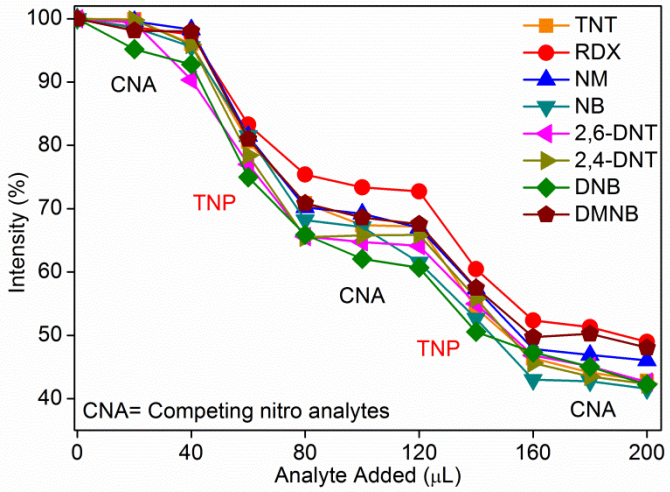

Figure 3A.5: Decrease in percentage of fluorescence intensity of **2'** upon the addition of aqueous solutions of competing nitro analytes (CNA) followed by TNP.

3A.3.4 Investigation of Quenching Mechanism:

Usually, the conduction band (CB) of the electron rich MOF lies higher than the LUMO energies of the nitro analytes and upon excitation the excited electron from the CB transfers to the LUMO orbitals of the nitro analytes, thus quenching the fluorescence intensity.[15] The efficient fluorescence quenching observed for TNP is in accordance with the low LUMO energy of TNP compared to the other nitro analytes (Figure **3A.6a**). However, the correlation between the quenching efficiency and corresponding LUMO energies of the nitro analytes suggests that the electron transfer is not the only mechanism contributing to fluorescence quenching.

As mentioned previously the non-linear trend of the SV plot for TNP indicates the presence of resonance energy transfer mechanism. The greater the spectral overlap between the absorbance spectrum of the analyte and the emission spectrum of the MOF, the higher the probability of energy transfer and hence fluorescence quenching. Figure **3A.6b** shows that the greatest spectral overlap is between TNP and **2'** while all of the other nitro analytes showed negligible spectral overlap with the emission spectrum of **2'**. Additionally, the confinement of analytes in the MOF pores, keeps the analytes and MOF in close proximity, improving the probability of energy transfer process. Thus we believe that similar to probe **1'** reported in chapter 2, TNP can efficiently quench the fluorescence of **2'** via both electron and long range energy transfer processes, as against for other nitro analytes which quench fluorescence by an electron transfer process only. Additionally, the increasing quenching efficiency with

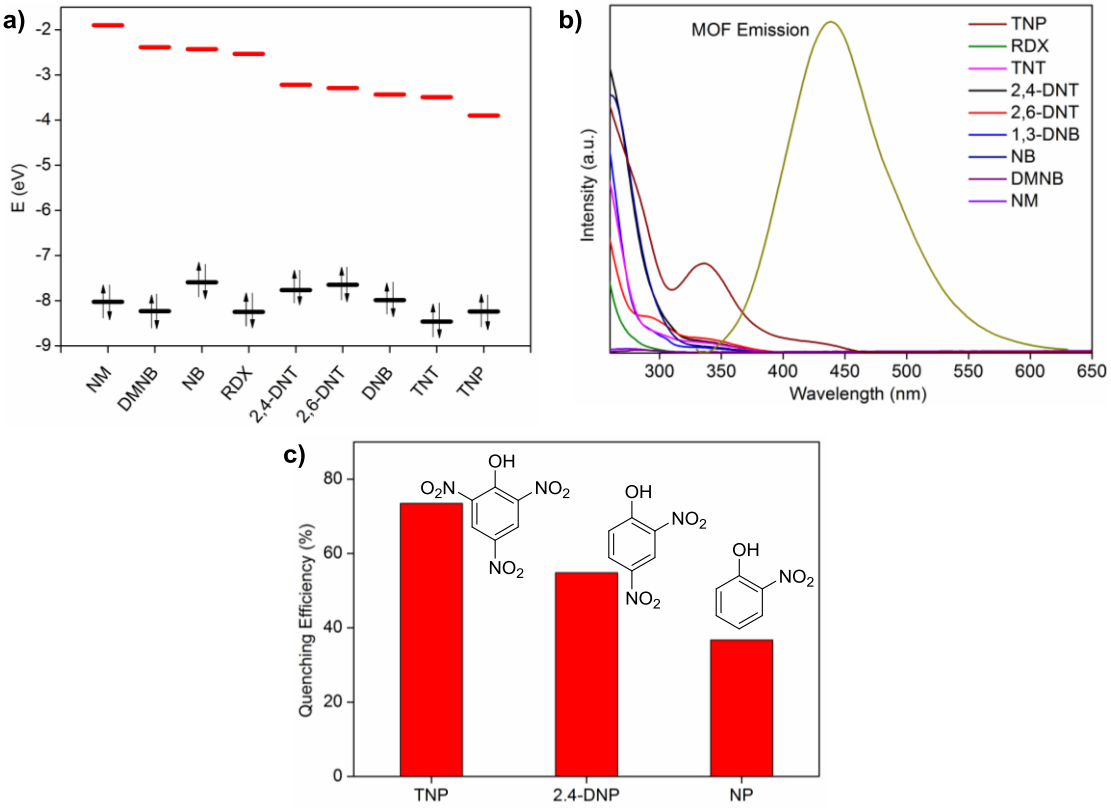

Figure 3A.6: (a) HOMO and LUMO energies for explosive analytes arranged in descending order of LUMO energies. (b) Spectral overlap between the absorption spectra of analytes and the emission spectrum of **2'** in water. (c) Comparison of percentage fluorescence quenching obtained for NP, 2,4-DNP, TNP.

increasing acidity of the phenolic analytes and a red shift in the emission maxima upon the addition of TNP. This may be due to the complex formation between TNP and the MOF (Figure **3A.3a**, **3A.6c, 3A.A10-A11**).[2b] Thus, due to the occurrence of electron transfer and energy transfer processes in addition to electrostatic interaction, TNP shows highly selective and sensitive fluorescence quenching responses over other nitro analytes in water.

3A.4 Summary and Conclusions:

In present section (A), a fluorescent porous MOF **2'** with guest accessible Lewis basic pyridyl functionality demonstrates highly selective and sensitive detection of TNP in aqueous media even in the presence of competing nitro analytes. **2'** respond to TNP in few seconds and the detection limit was calculated to be 0.6 ppm. The occurrence of both electron and energy transfer processes, in addition to electrostatic interaction between the **2'** and TNP, contribute to the unprecedented selective

fluorescence quenching. The present work for the first-time demonstrates the potential of a fluorescent MOF for real-time aqueous phase selective and sensitive explosive detection for environmental application.

3A.5 References:

(1) (a) Salinas, Y.; Martinez-Manez, R.; Marcos, M. D.; Sancenon, F.; Castero, A. M.; Parra, M.; Gil, S. *Chem. Soc. Rev.* **2012,** *41,* 1261-1296. (b) Thomas III, S. W.; Joly, G. D.; Swager, T. M. *Chem. Soc. Rev.* **2007,** *36,* 1339-1386. (c) Germain, M. E.; Knapp, M. J. *Chem. Soc. Rev.* **2009,** *38,* 2543-2555.

(2) (a) He, G.; Peng, H.; Liu, T.; Yang, M.; Zhang, Y.; Fang, Y. *J. Mater. Chem.* **2009,** *19,* 7347-7353. (b) Dong, M.; Wang, Y.-W.; Zhang, A.-J.; Peng, Y. *Chem. Asian J.* **2013,** *8,* 1321-1330.

(3) (a) Thorne, P. G.; Jenkins, T. F. *Field Anal. Chem. Technol.* **1997,** *1,* 165-170. (b) Wollin, K. M.; Dieter, H. H. *Arch. Environ. Contam. Toxicol.* **2005,** *49,* 18-26.

(4) Xu, B.; Wu, X.; Li, H.; Tong, H.; Wang, L. *Macromolecules* **2011,** *44,* 5089-5092.

(5) Sohn, H.; Sailor, M. J.; Magde, D.; Trogler, W. C. *J. Am. Chem. Soc.* **2003,** *125,* 3821-3830.

(6) Xin, Y.; Wang, Q.; Liu, T.; Wang, L.; Li, J.; Fang, Y. *Lab Chip* **2012,** *12,* 4821-4828.

(7) (a) Richardson, S.; Barcena, H. S.; Turnbull, G. A.; Burn, P. L.; Samuel, I. D. W. *Appl. Phys. Lett.* **2009,** *95,* 063305-063308. (b) Li, D.; Liu, J.; Kwok, R. T.K.; Liang, Z.; Tang, B. Z.; Yu, J. *Chem. Commun.* **2012,** *48,* 7167-7169. (c) Meaney, M. S.; McGuffin, V. L. *Anal. Bioanal. Chem.* **2008,** *391,* 2557-2576. (d) Snow, E. S.; Perkins, F. K.; Houser, E. J.; Badescu, S. C.; Reinecke, T. L. *Science* **2005,** *307,* 1942-1945. (e) Gole, B.; Shanmugaraju, S.; Bar, A. K.; Mukherjee, P. S. *Chem. Commun.* **2011,** *47,* 10046-10048. (f) Shanmugaraju, S.; Joshi, S. A.; Mukherjee, P. S. *Inorg. Chem.* **2011,** *50,* 11736-11745. (g) Kartha, K. K.; Babu, S. S.; Srinivasan, S.; Ajayaghosh, A. *J. Am. Chem. Soc.* **2012,** *134,* 4834-4841.

(8) Zhang, S.-R.; Du, D.-Y.; Qin, J.-S.; Bao, S.-J.; Li, S.-L.; He, W.-W.; Lan, Y.-Q.; Shen, P.; Su, Z.-M. *Chem. Eur. J.* **2014,** *20,* 3589-3594.

(9) (a) Furukawa, H.; Cordova, K. E.; Okeeffe, M.; M. Yaghi, O. M. *Science* **2013,** *341,* 1230444. (b) Nagarkar, S. S.; Desai, A. V.; Ghosh, S. K. *Chem. Asian J.* **2014,** *9,* 2358-2376. (c) Kreno, L. E.; Leong, K.; Farha, O. K.; Allendorf, M.; Duyne, R. P. V.; Hupp, J. T. *Chem. Rev.* **2012,** *112,* 1105-1125. (d) Horcajada, P.; Gref, R.; Baati, T.; Allan, P. K.; Maurine, G.; Couvreur, P.; Ferey, G.; Morris, R.; Serre, C. *Chem. Rev.* **2012,** *112,* 1232-1268. (e) Schaate, A.; Roy, P.; Godt, A.; Lippke, J.; Waltz, F.; Wiebcke, M.; Behrens, P. *Chem. Eur. J.* **2011,** *17,* 6643- 6651.

(10) (a) Hu, Z.; Deibert, B. J.; Li, J. *Chem. Soc. Rev.* **2014,** *43,* 5815-5840. (b) Cui, Y.; Yue, Y.; Qian, G.; Chen, B. *Chem. Rev.* **2012,** *112,* 1126-1162. (c) Lan, A.; Li, K.; Wu, H.; Olson, D. H.; Emge, T. J.; Ki, W.; Hong, M.; Li, J. *Angew. Chem., Int. Ed.* **2009,** 48, 2334-2338. (d) Das, S.; Bharadwaj, P. K. *Inorg. Chem.* **2006,** *45,* 5257-5259. (e) Wang, C.; Lin, W. *J. Am. Chem. Soc.* **2011,** *133,* 4232-4235. (f) Zhang, C.; Che, Y.; Zhang, Z.; Yang, X.; Zang, L. *Chem. Commun.* **2011,** *47,* 2336-2338. (g) Zhang, Z.; Xiang, S.; Rao, X.; Zheng, Q.; Fronczek, F. R.; Qian, G.; Chen, B. *Chem. Commun.* **2010,** *46,* 7205-7207. (h) Jiang, H. L.; Tatsu, Y.; Lu, Z. H.; Xu, Q. *J. Am. Chem. Soc.* **2010,** *132,* 5586-5587. (i) Xu, H.; Liu, F.; Cui, Y.; Chen, B.; Qian, G. *Chem. Commun.* **2011,** *47,* 3153-3155. (j) Gole, B.; Bar, a. K.; Mukherjee, P. S. *Chem. Eur. J.* **2014,** *20,* 2276-2291. (k) Wang, G.-Y.; Song, C.; Kong, D.-M.; Ruan, W.-J.; Chang, Z.; Li, Y. *J. Mater. Chem. A* **2014,** *2,* 2213-2220.

(11) Nagarkar, S. S.; Joarder, B.; Chaudhari, A. K.; Mukherjee, S.; Ghosh, S. K. *Angew. Chem., Int. Ed.* **2013,** *52,* 2881-2885.

(12) Dau, P. V.; Min, M.; Cohen, S. M. *Chem. Sci.* **2013,** *4,* 601-605.

(13) Dau, P. V.; Kim, M.; Garibay, S. J.; Munch, F. H. L.; Moore, C. E.; Cohen, S. M. *Inorg. Chem.* **2012,** *51,* 5671-5676.

(14) Sanchez, J. C.; DiPasquale, A.; Rheingold, A. L.; Trogler, W. C. *Chem. Mater.* **2007,** *19,* 6459-6470.

(15) (a) Wu, W.; Ye, S.; Yu, G.; Liu, Y.; Qin, J.; Li, Z. *Macromol. Rapid Commun.* **2012,** *33,* 164-171. (b) Zhao, D.; Swager, T. M. *Macromolecules* **2005,** *38,* 9377-9384. (c) Acharya, K.; Mukherjee, P. S. *Chem. Commun.* **2014,** *50,* 15788-15789.

(16) Toal, S. J.; Trogler, W. C. *J. Mater. Chem.* **2006,** *16,* 2871-2883.

Chapter 3

Section B

Fluorescent MOF with Guest Accessible Amine Moieties for Selective Sensing of Nitro Explosive TNP in an Aqueous Phase

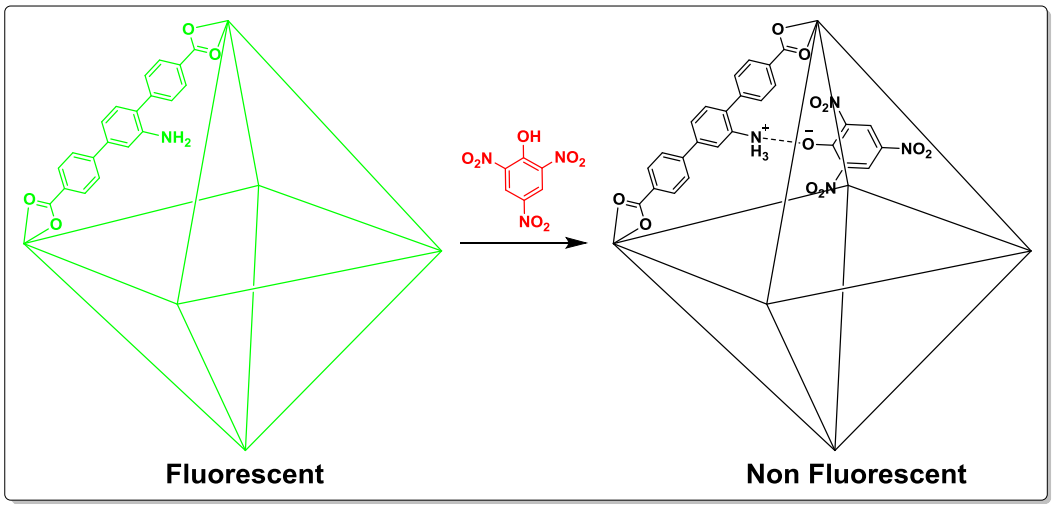

3B.1 Introduction:

The selective and sensitive detection of lethal explosives material is decisive for homeland security, anti-terrorist operations and civilian safety.[1] The most commonly used explosive ingredients are nitroaromatics like 2,4,6-trinitrotoluene (TNT), 2,4-dinitrotoluene (2,4-DNT), 2,6-dinitrotoluene (2,6-DNT), 2,4,6-trinitrophenol (TNP), nitro aliphatic compounds like 1,3,5-trinitro-1,3,5-triazacyclohexane (RDX), explosive tag like 2,3-Dimethyl-2,3-dinitrobutane (DMNB). Among these, TNP has higher explosive power in similar class of explosive compounds.[2] Apart from explosive nature TNP causes skin/eye irritation, headache, anaemia, liver injury, male infertility.[3] Despite this fact TNP is widely used in fireworks, leather, dyes industries.[4] Because of high water solubility TNP can easily lead to contamination of nearby soil and aquatic system, posing serious health hazards. Furthermore owing to highly electron deficient nature, biodegradation of TNP is very difficult. Curiously, less efforts have been devoted for selective TNP detection, thus the development of efficient sensor material for TNP detection and constant monitoring of soil and aquatic system is highly demanded. However, the selective detection of TNP in presence of competing nitro analytes is very difficult.[5] Fluorescence based chemosensors have attracted great attention for in-field use over current sophisticated detection systems, owing to sensitivity, portability, short response time, low cost and compatibility in both solid as well as solution state.[6] Numerous luminescent materials have been studied as fluorescence based explosives sensors till date, but their multi-step processing, toxicity and lack of control over molecular organization limits their wide use.[1a]

Metal-organic frameworks (MOFs), have emerged as promising material for gas storage/separation, chemical sensing, heterogeneous catalysis, biomedicine, magnetism, clean energy and optoelectronics in recent times.[7] Especially as fluorescence based chemical sensor, MOF offer great promise by virtue of its crystalline nature, permanent porosity, designable/modifiable pores, systematically tunable band gaps and electronic structures.[8] The fluorescence sensing performance of MOF is determined by interactions between target analyte and MOF backbone. The porosity allows pre-concentration of analyte in MOF matrix while the designable pore size/shape renders molecular sieving effect. The pendant recognition sites allow selective interaction with adsorbate via open metal sites, hydrogen bonding, Mulliken-

type interactions, Lewis acidic/basic sites, etc. Additionally immobilization of organic ligands in rigid MOF framework leads to stronger emissions. Most importantly the limitless combinations of organic ligands and metal centers allow tuning of valance and/or conduction band and in turn the band gap of MOF, crucial for sensing applications. Owing to above advantages, variety of MOFs have been designed and studied for detection of cations, anions, small molecules, explosives and biomolecules.[9]

Despite recent advances, the reports of fluorescent MOF for selective and sensitive TNP detection in presence of other nitro analytes are rare and that exhibit unprecedented selectivity in aqueous system are rarer still.[9,10] The Zirconium based UiO series MOFs are chemically stable and porous.[11] In previous section we have utilized Zr(IV) based stable fluorescent MOF **2'** for aqueous phase selective TNP detection.[10b] We deployed Lewis basic pyridyl functionality in 3D (three dimensional) MOF matrix to achieve highly selective TNP detection in aqueous phase. We reasoned that, similarly Lewis basic amine functionality can also be promising recognition site for selective TNP detection owing to its possible ionic and hydrogen bonding interactions with TNP.[12] Thus on similar line, we chose Zirconium based chemically stable porous MOF $Zr_6O_4(OH)_4(\mathbf{L_4})_6$ (**3**, UiO-68@NH_2, $H_2\mathbf{L_4}$ = 2'-amino-[1,1':4',1"-terphenyl]-4,4"-dicarboxylic acid) with pendant amine functionality for aqueous phase selective TNP sensing (Scheme **3B.1**).[13] The porous MOF has large pores of 11 and 25 Å,[13a] which are expected to allow easy diffusion and concentration of analytes and

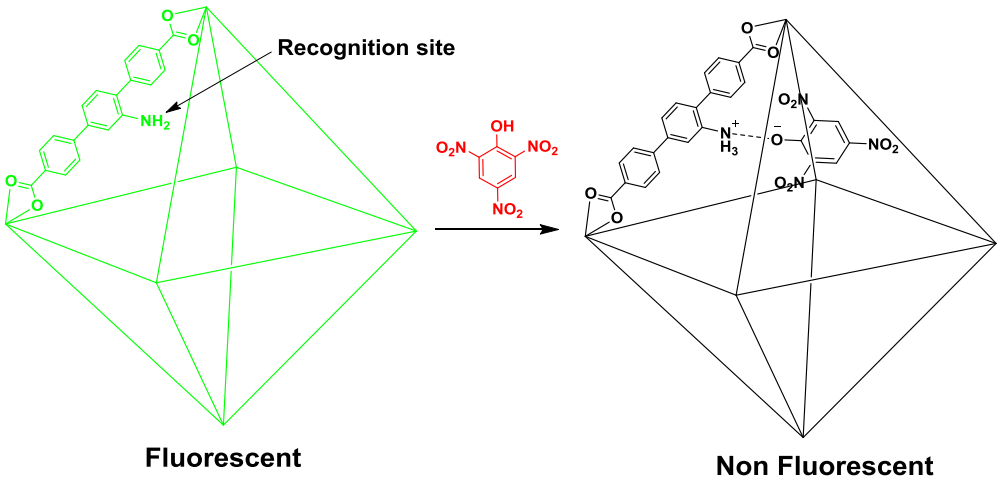

Scheme 3B.1: Schematic representation of selective detection of TNP by luminescent MOF **3'** with guest accessible amine groups.

facile host-guest interactions. The guest accessible Lewis basic amine functionalities will act as recognition sites for TNP via ionic and hydrogen bonding interactions. Also excitation and emission wavelengths of MOF **3**, are in visible region making it an ideal material to study TNP sensing performance.

3B.2 Experimental Section:

Caution! TNT, RDX and TNP are highly explosive and should be handled carefully and in small amounts. The explosives were handled as dilute solutions and with safety measures to avoid explosion.

3B.2.1 Material and Methods:

TNT and RDX were provided by HEMRL Pune (India). TNP, 2,4-DNT, 2,6-DNT, DMNB were purchased from Aldrich, while 1,3-DNB, NB purchased from local company. All the chemicals were used as received. Dry solvents were used during complete analysis and were obtained locally. ^{1}H NMR was recorded in 400 MHz Jeol ECS-400 Instrument. Thermogravimetric analyses were recorded on Perkin-Elmer STA 6000 TGA analyzer under N_2 atmosphere with a heating rate of 10 °C min^{-1}. Powder X-ray diffraction patterns (PXRD) were measured on Bruker D8 Advanced X-Ray diffractometer using Cu K_α radiation (λ= 1.5406 Å) with a tube voltage of 40 kV and current of 40 mA in 5 to 40° 2θ range. Fluorescence measurements were done using Horiba FluoroMax 4 with stirring attachment. The UV-Vis measurements were performed using Chemito SPECTRASCAN UV-2600.

3B.2.2 Synthesis of $Zr_6O_4(OH)_4(L_4)_6 \cdot G_x$ (3):

The Ligand 2'-amino-[1,1':4',1''-terphenyl]-4,4''-dicarboxylic acid (H_2**L$_4$**) was synthesized using procedure previously reported (Figure **3B.A1**).[13a] For synthesis of **3** $ZrCl_4$ (0.024 g), H_2**L$_4$** (0.056 g) were dissolved in N,N-dimethylformamide (DMF, 3 mL) in a Teflon lined stainless steel vessel (17 mL). The vessel was sealed and placed in oven and heated at 120 °C for 16 h. After cooling to room temperature, the crystalline product was isolated by filtration the solid was washed with DMF.

3B.2.3 Activation of Compound 3 (3'):

The occluded solvent and starting material in MOF was then exchanged with MeOH by dipping it in MeOH for 3 days. Over 3 days the MeOH was replaced with

fresh MeOH every 24 h. The guest free porous MOF (**3'**) was obtained by heating the MeOH exchanged MOF at 130 °C under vacuum for 24 h which was then used for fluorescence measurements.

3B.2.4 Photophysical Measurements:

In typical experimental setup, 1 mg of **3'** is weighed and added to cuvette containing 2 mL of water and stirred. Upon excitation at 395 nm, fluorescence response of **3'** was measured *in-situ* in 410-780 nm range and corresponding fluorescence intensity was monitored at 500 nm. For fluorescence titration, emission was recorded upon incremental addition of freshly prepared analyte solutions (1 mM or saturated). To maintain homogeneity solution was stirred at constant rate during experiment.

3B.3 Results and Discussion:

3B.3.1 Synthesis and X-ray Structure of 3:

The MOF **3** was synthesized by reaction between $ZrCl_4$ and $H_2\mathbf{L_4}$ in DMF at 120 °C solvothermally. The MOF composed of hexameric Zr(IV) node $Zr_6O_4(OH)_4(CO_2)_{12}$. Each zirconium atom is eight-coordinated with square-antiprismatic coordination environment, where one square face is formed by oxygen atoms supplied by μ_3-O and μ_3-OH groups, while the second square face is formed by oxygen atoms coming from carboxylate groups of ligand $\mathbf{L_4}$ (Figure **3B.1**). The hexameric Zr(IV) node $Zr_6O_4(OH)_4(CO_2)_{12}$ are connected by ligand $\mathbf{L_4}$ forming 3D porous structure of **3**. The larger pore window has size of 25 Å while the smaller pore has size of 11 Å expected to allow pre-concentration of analytes. The pores are decorated with the guest accessible Lewis basic amine moieties which can act as recognition site for TNP giving rise to efficient quenching response.

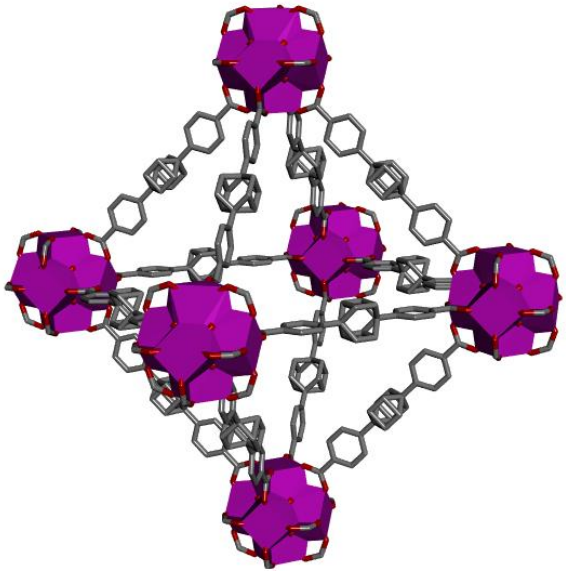

Figure 3B.1: Single crystal X-ray structure of **3** (amine groups are disordered and removed for clarity).[13a] Purple octahedra represent the $[Zr_6O_4(OH)_4]^{12+}$ cluster; grey, red and blue spheres represent carbon, oxygen and nitrogen atoms, respectively. Hydrogen atoms are omitted for clarity.

3B.3.2 Phase Purity and Stability of 3:

Overlapping PXRD patterns of as-synthesized sample and simulated pattern confirmed the successful formation and bulk phase purity of **3** (Figure **3B.2a**). The Thermogravimetric analysis of **3** showed ~45 % weight loss below 100 °C assigned to loss of occluded DMF molecules and the compound was found to be stable up to 400 °C (Figure **3B.2b**). The porous guest-free form **3'** was obtained by solvent exchange method. The occluded guest molecules in pores of **3** were exchanged with MeOH for

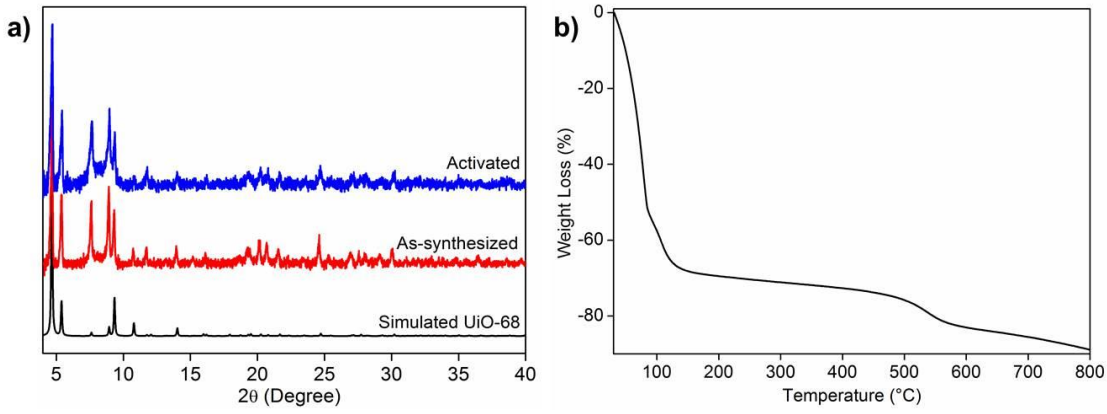

Figure 3B.2: (a) Comparison between PXRD patterns of simulated, as-synthesized, and activated MOF **3**. (b) Thermogravimetric analysis of as-synthesized MOF **3**.

three days, where the MeOH was replaced by fresh MeOH every 24 h. The MeOH exchanged **3** was then filtered and evacuated under reduced pressure to get activated or guest free porous form **3'**. The observed data is in good agreement with the previous report.

3B.3.3 Photophysical Studies:

The photoluminescence spectra of **3'** in water exhibit strong emission peak at 500 nm upon excitation at 395 nm at room temperature (Figure **3B.3a**). To explore the potential application of **3'** to detect TNP in aqueous medium, fluorescence quenching titration was performed by gradual addition of aqueous TNP solution. As anticipated the incremental addition of TNP resulted in fast and efficient fluorescence quenching of 86 % (Figure **3B.3**). **3'** can recognize TNP at as low as 0.4 ppm concentration, which is comparable to or better than previous MOF reports.[10a] We also checked the quenching ability of other competing nitro analytes like TNT, RDX, 2,4-DNT, 2,6-DNT, DNB, NB, DMNB in water (Figure **3B.3** and **3B.A2–3B.A8**). Compared to TNP, the competing nitro analytes showed petite effect on emission intensity of **3'** (Figure **3B.3b**). This clearly demonstrates the selectivity of **3'** towards TNP compared to potentially interfering nitro analytes.

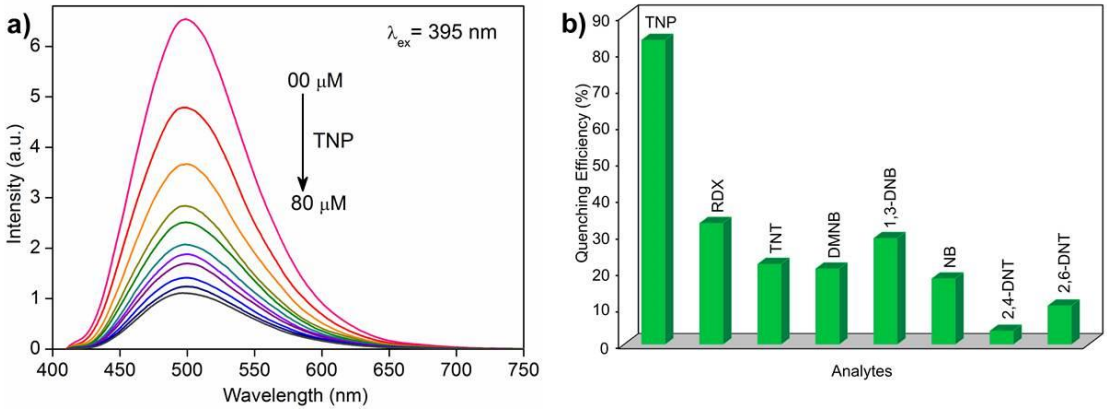

Figure 3B.3: (a) Effect on the emission spectra of **3'** dispersed in water upon incremental addition of a TNP solution. (b) Percentage of fluorescence quenching obtained for **3'** upon addition of different nitro analytes at room temperature.

To further quantify the quenching efficiency, Stern-Volmer (SV) plots of relative luminescent intensities (I_0/I) of all the nitro analytes were compared where, I_0

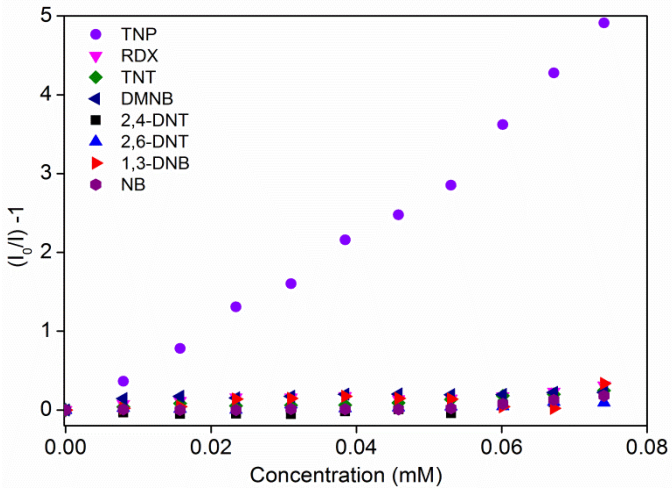

Figure 3B.4: Stern-Volmer (SV) plots for various nitro analytes added to **3'** in water.

and *I* are the intensities in absence and in presence of respective nitro analytes. All the nitro analytes except TNP showed linear SV plots (Figure **3B.4**). Interestingly, at low concentration TNP showed linear SV plot, which upon further increase in TNP concentration preceded in slightly non-linear fashion. This non-linear SV plot suggests presence of consolidation of both dynamic as well as static quenching and/or presence of energy transfer phenomenon between **3'** and TNP.[14] Using SV plot the quenching constant for TNP was calculated to be $5.8 \times 10^4\ M^{-1}$. The observed quenching constant for TNP is equivalent to organic polymer based probes and is ~23 times higher than its aromatic (TNT) and aliphatic (RDX) tri-nitro analogue respectively, demonstrating the superior performance.[15]

In real scenario, the selective detection of TNP in presence of other competing nitro analytes in aqueous system is highly desirable. To assess the selectivity of **3'** towards TNP in presence of competing nitro analytes we designed a competitive fluorescence quenching assay. Initially, the fluorescence spectrum of **3'** dispersed in water was recorded. To above solution aqueous TNT solution was added in two equal portions (total 40 μL) to allow effective access to pendant free Lewis basic amine sites and the fluorescence response was recorded. No significant fluorescence quenching was observed upon addition of aqueous TNT solution (Figure **3B.5**). However when same quantity of aqueous TNP solution (40 μL in two equal portions) was added to above solution significant fluorescence quenching was observed. The trend repeated even in next TNT and TNP addition cycles. Similar phenomenon was observed in

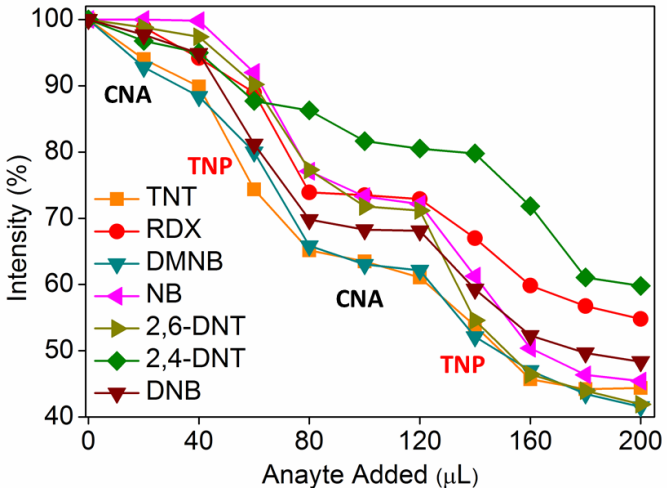

Figure 3B.5: Decrease in percentage of fluorescence intensity of **3'** upon the addition of aqueous solutions of competing nitro analytes (CNA) followed by TNP.

competitive assay for competing nitro analytes (CNA) demonstrating unprecedented selectivity of **3'** towards TNP in presence of competing nitro analytes.

For in-field aqueous phase detection, paper strips method comes handy. We prepared MOF coated black paper strips for in-field aqueous phase TNP detection. The pristine strip under UV illumination showed good fluorescence, the individual strips were then partially dipped in aqueous nitro analytes solutions (Figure **3B.6a**). The strip dipped in TNP solution showed significant fluorescence quenching when visualized under UV light (Figure **3B.6b**, strip A) while the unexposed part of same strip still showed good fluorescence. All the other strips dipped in competing nitro analytes showed negligible fluorescence quenching response (Figure **3B.6b**, strip B-H). Thus

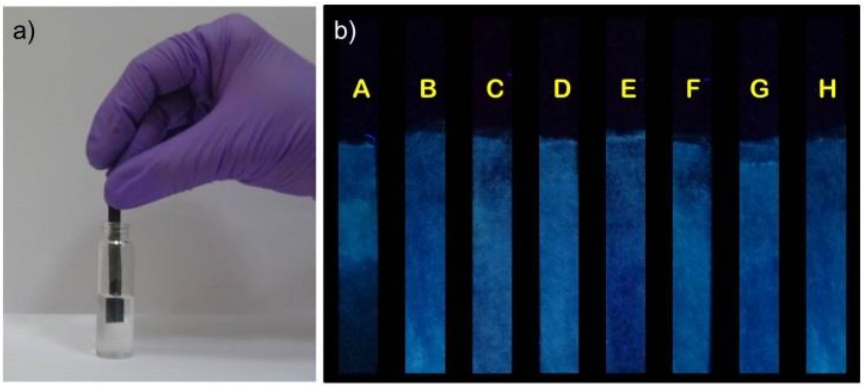

Figure 3B.6: (a) MOF coated paper strip for aqueous phase explosive detection, (b) Response of MOF coated paper strips towards various nitro analytes under UV light (A = TNP, B = TNT, C = RDX, D = 2,4-DNT, E = DNB, F = 2,6-DNT, G = NB, H = DMNB).

the MOF **3'** coated paper strip provides an efficient way to trace the presence of TNP in aqueous system and demonstrates the potential of **3'** towards real-time in-field sensing application.

3B.3.4 Investigation of Quenching Mechanism:

To gain more insight in to the superior sensing ability of **3'** we sought to examine the electronic properties of both MOF and nitro analytes. The fluorescence quenching by electron transfer from conduction band (CB) of MOF to LUMO orbitals of electron deficient nitro analyte is well established quenching mechanism.[16] Lower the LUMO energy higher is the electron accepting ability of nitro analyte and thus the efficiency of fluorescence quenching. The effective fluorescence quenching by TNP is in good agreement with its lowest LUMO energy compared to other nitro analytes (Figure **3B.7a**). However, the fluorescence quenching performance of other nitro analytes does not follow the LUMO energy trend indicating simultaneous presence of

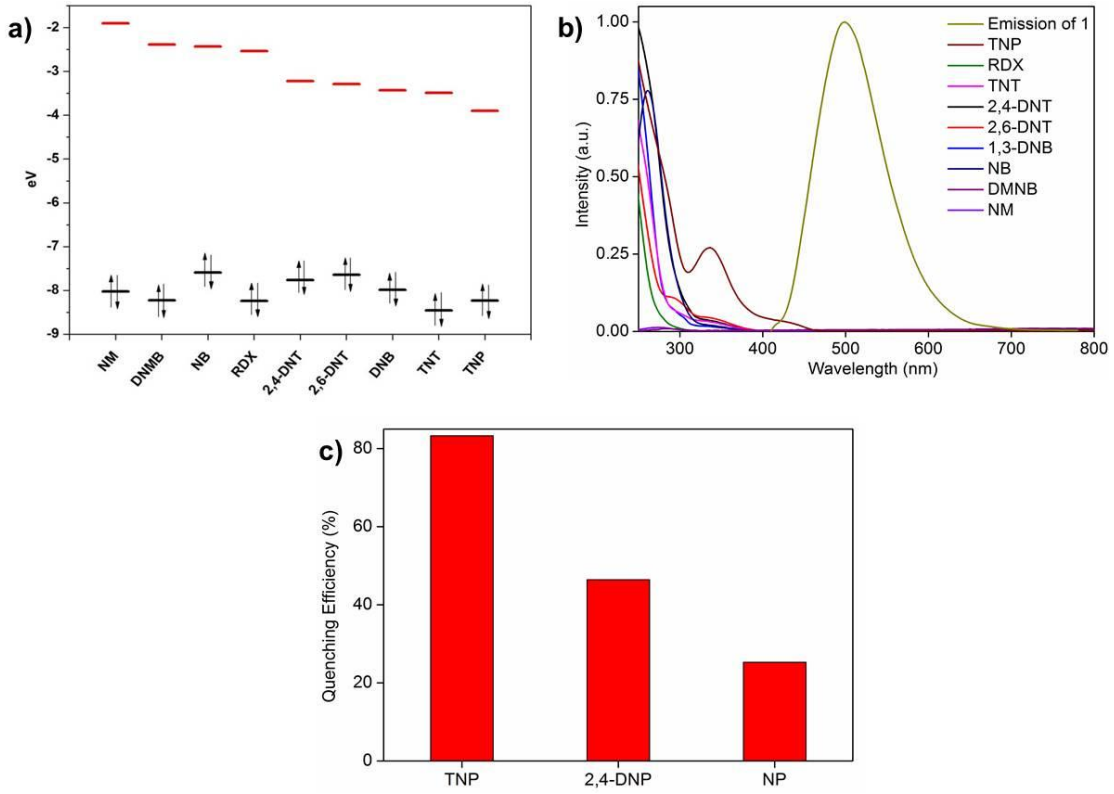

Figure 3B.7: (a) HOMO and LUMO energies for nitro explosive analytes arranged in descending order of LUMO energies. (b) Spectral overlap between the absorption spectra of nitro analytes and the emission spectrum of **3'** in water. (c) Comparison of percentage fluorescence quenching obtained for TNP, 2,4-DNP, NP.

other quenching mechanism in addition to electron transfer. The resonance energy transfer is another effective fluorescence quenching mechanism. The non-linear SV plot advocates the presence of long range resonance energy transfer. The effectiveness of energy transfer heavily depends on extent of spectral overlap between emission of fluorophore and absorption spectrum of analyte. The absorption spectrum of TNP shows higher extent of overlap with emission of **3'** as against other competing nitro analytes (Figure **3B.7b**). This observation is in good agreement with observed higher quenching efficiency obtained for TNP compared to other nitro analytes. Thus it is apparent that in the case of TNP both electron and energy transfer mechanism are operational while for other nitro analytes only electron transfer mechanism operates, as explained in chapter 2.

Nitro explosive TNP is known to interact with Lewis basic sites owing to acidic phenolic proton. To probe the role of pendant Lewis basic free amine towards the observed selectivity, fluorescence quenching titrations were performed with 2,4-DNP and NP. The fluorescence quenching performance of phenolic analytes is in accordance with acidity of phenolic protons TNP>2,4-DNP>NP. This indicates the presence of electrostatic interaction between TNP and amine functionality, similar to pyridyl functionalized MOF reported in earlier section (Figure **3B.7c and 3B.A9-A10**).[12] This supports the observed selectivity of **3'** for TNP. The highly acidic TNP selectively and strongly interacts with Lewis basic amine group via ionic and hydrogen bonding interactions leading to amplified quenching response. While in case of other nitro analytes such interactions are absent and so result in low quenching effect. Thus the Lewis basic amine functionality act as recognition site for TNP and combination of electron transfer, energy transfer quenching mechanism gives rise to unprecedented selectivity for TNP in aqueous phase.

3B.4 Summary and Conclusions:

In present section (B), we have reported a chemically stable porous fluorescent MOF **3'** with Lewis basic free amine functionality as pendant recognition sites for selective and sensitive detection of TNP in aqueous phase. Both the excitation and emission wavelengths of **3'** are in visible region. **3'** can detect TNP at as low as 0.4 ppm concentration in few seconds and importantly the high selectivity is observed even in presence of competing nitro analytes. The combination of electron and energy

transfer mechanism along with Lewis basic recognition sites is credited to high selectivity of **3'** towards TNP. The MOF based paper strip provides an effective and efficient way for in-field aqueous phase TNP detection for security and environmental monitoring applications.

3B.5 References:

(1) (a) Salinas, Y.; Martinez-Manez, R.; Marcos, M. D.; Sancenon, F.; Castero, A. M.; Parra, M.; Gil, S. *Chem. Soc. Rev.* **2012,** *41*, 1261-1296. (b) Germain, M. E.; Knapp, M. J. *Chem. Soc. Rev.* **2009,** *38*, 2543-2555. (c) Thomas III, S. W.; Joly, G. D.; Swager, T. M. *Chem. Soc. Rev.* **2007,** *36*, 1339-1386.

(2) Venkatramaiah, N.; Kumar, S.; Patil, S. *Chem. Commun.* **2010,** *48*, 5007-5009.

(3) Wyman, J. F.; Serve, M. P.; Honson, D. W.; Lee, L. H.; Uddin, D. E. *J. Toxicol. Environ. Health* **1992,** *37*, 313-327.

(4) Akhavan, J. The Chemistry of Explosives, Royal Society of Chemistry, Cambridge, **2004,** p. 4.

(5) Xu, B.; Wu, X.; Li, H.; Tong, H.; Wang, L. *Macromolecules* **2011,** *44*, 5089-5092.

(6) (a) Xin, Y.; Wang, Q.; Liu, T.; Wang, L.; Li, J.; Fang, Y. *Lab Chip* **2012,** *12*, 4821-4828. (b) Basabe-Desmonts, L.; Reinhoudt, D. N.; Crego-Calama, M. *Chem. Soc. Rev.* **2007,** *36*, 993-1017.

(7) (a) Furukawa, H.; Cordova, K. E.; Okeeffe, M.; M. Yaghi, O. M. *Science* **2013,** *341*, 1230444. (b) Horike, S.; Shimomura, S.; Kitagawa, S. *Nat. Chem.* **2009,** *1*, 695-704. (c) Kuppler, R. J.; Timmons, D. J.; Fang, Q-R.; Li, J.-R.; Makal, T. A.; Young, M. D.; Yuan, D.; Zhao, D.; Zhuang, W.; Zhou, H.-C. *Coord. Chem. Rev.* **2009,** *253*, 3042-3066. (d) Aijaz, A.; Lama, P.; Bharadwaj, P. K. *Inorg. Chem.* **2010,** *49*, 5883-5889. (e) Nagarkar, S. S.; Unni, S. M.; Sharma, A.; Kurungot, S.; Ghosh, S. K. *Angew. Chem. Int. Ed.* **2014,** *53*, 2638-2642.

(8) Cui, Y.; Yue, Y.; Qian, G.; Chen, B. *Chem. Rev.* **2012,** *112*, 1126-1162.

(9) (a) Kreno, L. E.; Leong, K.; Farha, O. K.; Allendorf, M.; Duyne, R. P. V.; Hupp, J. T. *Chem. Rev.* **2012,** *112*, 1105-1125. (b) Nagarkar, S. S.; Joarder, B.; Chaudhari, A. K.; Mukherjee, S.; Ghosh, S. K. *Angew. Chem., Int. Ed.* **2013,** *52*, 2881-2885. (c) Joarder, B.; Desai, A. V.; Samanta, P.; Mukherjee, S.; Ghosh, S. K. *Chem. Eur. J.* **2014**, DOI: 10.1002/chem.201405167. (d) Singh,

D. K.; Bhattacharya, S.; Majee, P.; Mondal, S. K.; Kumar, M.; Mahata, P. *J. Mater. Chem. A* **2014,** *2*, 20908-20915. (e) Ye, J.; Zhao, L.; Bogale, R. F.; Gao, Y.; Wang, X.; Qian, X.; Guo, S.; Zhao, J.; Ning, G. *Chem. Eur. J.* DOI: 10.1002/chem.201405267.

(10) (a) Hu, Z.; Deibert, B. J.; Li, J. *Chem. Soc. Rev.* **2014,** *43*, 5815-5840. (b) Nagarkar, S. S.; Desai, A. V.; Ghosh, S. K. *Chem. Commun.* **2014,** *50*, 8915-8918. (c) Song, X. Z.; Song, S. Y.; Zhao, S. N.; Hao, Z. M.; Zhu, M.; Meng, X.; Wu, L. L.; Zhang, H. J. *Adv. Funct. Mater.* **2014,** *24*, 4034-4041.

(11) (a) Cavka, J. H.; Jakobsen, S.; Olsbye, U.; Guillou, N.; Lamberti, C.; Bordiga, S.; Lillerud, K. P. *J. Am. Chem. Soc.* **2008,** *130*, 13850-13851. (b) Kandiah, M.; Nilsen, M. H.; Usseglio, S.; Jakobsen, S.; Olsbye, U.; Tilset, M.; Larabi, C.; Quadrelli, E. A.; Bonino, F.; Lillerud, K. P. *Chem. Mater.* **2010,** *22*, 6632-6640. (c) Horcajada, P.; Gref, R.; Baati, T.; Allan, P. K.; Maurine, G.; Couvreur, P.; Ferey, G.; Morris, R.; Serre, C. *Chem. Rev.* **2012,** *112*, 1232-1268.

(12) He, G.; Peng, H.; Liu, T.; Yang, M.; Zhang, Y.; Fang, Y. *J. Mater. Chem.* **2009,** *19*, 7347-7353.

(13) (a) Schaate, A.; Roy, P.; Godt, A.; Lippke, J.; Waltz, F.; Wiebcke, M.; Behrens, P. *Chem. Eur. J.* **2011,** *17*, 6643-6651. (b) Jiang, H.-L.; Feng, D.; Liu, T.-F.; Li, J.-R.; Zhou, H.-C. *J. Am. Chem. Soc.* **2012,** *134*, 14690-14693.

(14) (a) Wu, W.; Ye, S.; Yu, G.; Liu, Y.; Qin, J.; Li, Z. *Macromol. Rapid Commun.* **2012,** *33*, 164-171. (b) Zhao, D.; Swager, T. M. *Macromolecules* **2005,** *38*, 9377-9384. (c) Acharya, K.; Mukherjee, P. S. *Chem. Commun.* **2014,** *50*, 15788-15789.

(15) (a) Saxena, A.; Fujiki, M.; Rai, R.; Kwak, G. *Chem. Mater.* **2005,** *17*, 2181-2185. (b) Sanchez, J. C.; DiPasquale, A.; Rheingold, A. L.; Trogler, W. C. *Chem. Mater.* **2007,** *19*, 6459-6470.

(16) (a) Pramanik, S.; Zheng, C.; Zhang, X.; Emge, T. J.; Li, J. *J. Am. Chem. Soc.* **2011,** *133*, 4153-4155. (b) Toal, S. J.; Trogler, W. C. *J. Mater. Chem.* **2006,** *16*, 2871-2883.

Chapter 4

Metal-Organic Framework as Reaction based Fluorescence Turn-on Probe for H_2S Sensing

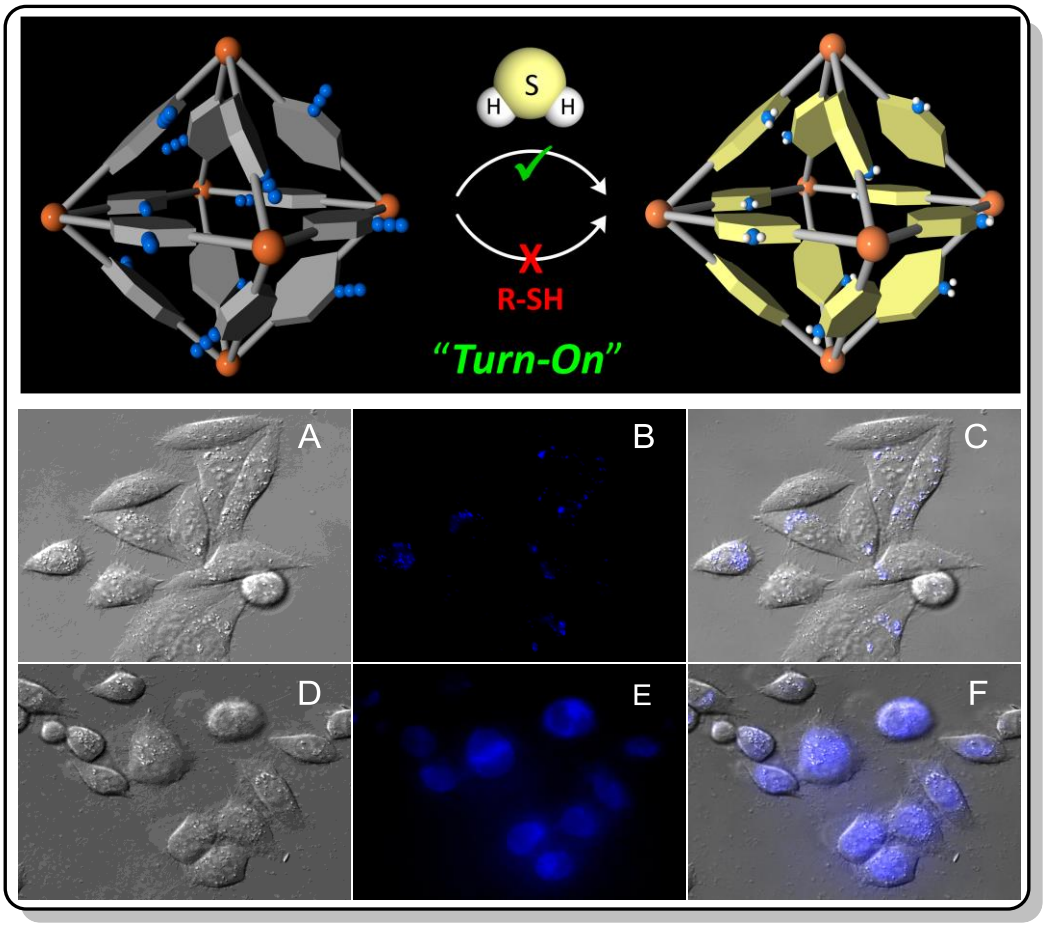

Chapter 4

Section A

Azide (-N_3) Functionalized Metal-Organic Framework as a Reaction based Fluorescence Turn-on Probe for H_2S Sensing

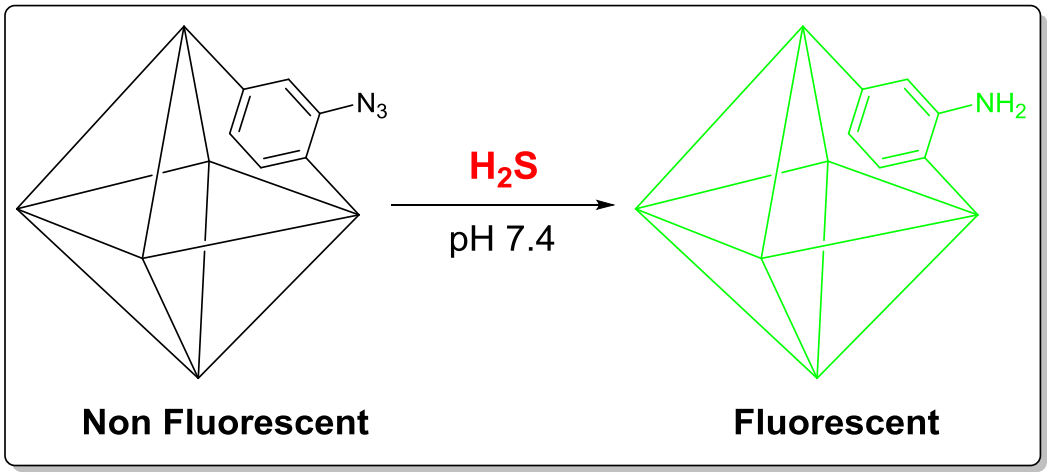

4A.1 Introduction:

Hydrogen sulfide (H_2S), a colorless flammable gas, released from geothermal, anthropogenic and biological sources is well-known for its lethal effects upon overexposure.[1] However, this traditionally considered toxic chemical species has recently emerged as a third gasotransmitter gas (biological signaling molecule) after Nitric Oxide (NO) and Carbon Monoxide (CO).[2] Organisms ranging from bacteria to mammals use H_2S for signal transduction, immune response and energy production.[3] H_2S therapy can also be used as a treatment to create hypothermia/hypometabolic state in surgical situations, to benefit conditions like trauma, reperfusion injury, and pyrexia.[4] The abnormal levels of H_2S in cells known to be related to Alzheimer's disease,[5] diabetes,[6] Down's syndrome,[7] and cancer.[8] This makes H_2S a potential target in the diagnostics and treatments of above diseases. Despite all recent progresses, efforts elucidating the molecular mechanism of H_2S in physiological and pathological processes are still on-going.

Considering the complex biological functions of H_2S selective and real-time detection of endogenous H_2S is necessary to expand our knowledge about its exact physiological and pathological role. But due to its volatile and reactive nature, the accurate detection of H_2S heavily depends on sample preparation and detection methods.[9] In this regard, the fluorescence based methods are preferred because of their high sensitivity, simplicity, short response time, non-invasive nature, real-time monitoring and precludes other sample processing.[10] An efficient fluorescent probe should show significant change in fluorescence in response to H_2S, high selectivity for H_2S over other interfering biological species, react fast enough (within minutes or even seconds) with H_2S and should be cell permeable.[9] In particular, fluorescence turn-on probes are preferred to avoid false response and improved signal to noise ratio as the detection occurs relative to dark background. Combining all the properties in one probe is a challenge, thus the development of fluorescent probe for H_2S is an active area of the current research.

Metal-organic frameworks (MOFs) composed of metal centers and organic struts have shown great potential in storage/separation, selective sensing, biomedical applications, etc.[11] Especially, the luminescent MOFs have been utilized for detection of range of organic molecules and ions.[12] The designable architecture and choice of luminescent building units allows the fine tuning of luminescence properties of MOFs. Also, the molecular size exclusion (molecular sieving effect) can be used as a tool to nullify interference from potentially competing molecules and can act as pre-

concentrator.[13] Tunable pore size also allows control over MOF analyte interactions improving sensitivity and molecular diffusion to modulate the response time. Finally, the high chemical stability and pre/post-synthetic modifications provides ample opportunities for MOF functionalization.[14] Owing to these advantages, MOF based fluorescence turn-on probe for H_2S can be a promising material for visualizing and real-time monitoring of H_2S. But MOFs exhibiting fluorescence turn-on in response to analyte are rare; in addition MOFs which show high selectivity along with turn-on response are still rare.[15]

Although, very recently MOFs have been used for selective adsorption and delivery of H_2S, their utilization as selective turn-on probe of H_2S has rarely been reported.[11d,16] H_2S detection in a living system relies on selective interactions, bioorthogonal to native cellular processes. The H_2S mediated reduction of azide to amine is a well-known bioorthogonal reaction which works under physiological conditions.[17] The amine functionalized MOF UiO-66@NH_2 (**4**) composed of non-toxic and poorly absorbed zirconium metal attracted our attention.[18] Compound **4** is luminescent and chemically stable, which may allow the post synthetic modification of amine functionality to azide UiO-66@N_3 (**5**). In addition to this, the UiO-66 analogues remain highly stable in physiological pH conditions for hours. Thus we sought to utilize **5** as switch to probe H_2S under physiological pH conditions (Scheme **4A.1**).

In this section (A), we report, metal-organic framework **5** as fluorescence turn-on probe for H_2S detection. Compound **5** shows fast and selective turn-on response towards H_2S even in presence of potentially competing biomolecules under physiological conditions. Also the live cell imaging studies demonstrated that probe can sense the H_2S in live cells. The high selectivity and sensitivity along with low toxicity make **5** a promising material for monitoring H_2S chemistry in biological system. To our knowledge this is the first example of MOF that exhibit fast and highly selective fluorescence turn-on response towards H_2S under physiological conditions.

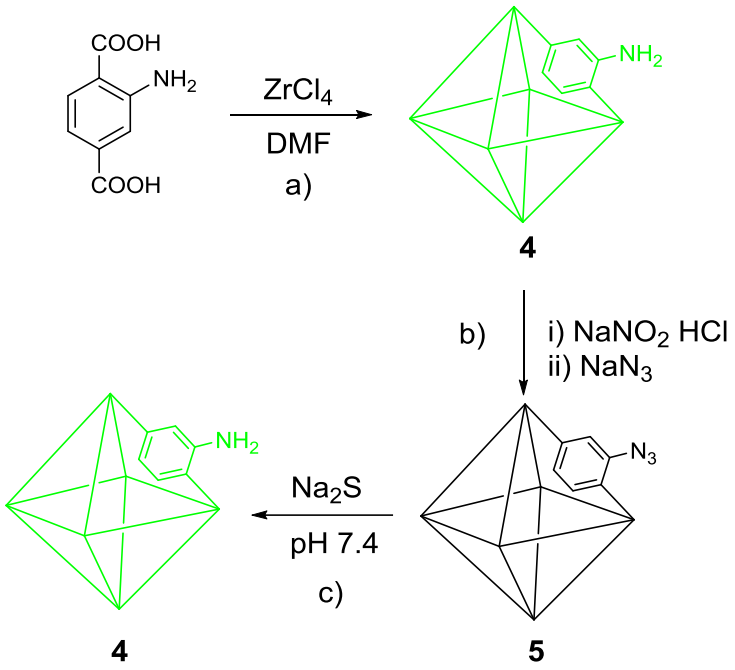

Scheme 4A.1: (a) Synthetic scheme for Zr(IV) based amine functionalized fluorescent MOF **4**. (b) Postsynthetic modification of **4** via diazotization route giving rise to turn-off state **5**. (c) H_2S mediated reduction of -N_3 in **5** to -NH_2 (**4**) upon addition of Na_2S at physiological pH giving rise to fluorescence turn-on response.

4A.2 Experimental Section:

4A.2.1 Material and Methods:

All the reagents and solvents were commercially available and used without further purification. Powder X-Ray diffraction patterns (PXRD) were measured on BrukerD8 Advanced X-Ray diffractometer using Cu K_α radiation (λ = 1.5406 Å) in 5 to 40° 2Θ range. The IR spectra were recorded on NICOLET 6700 FT-IR spectrophotometer using KBr pellet in 400-4000 cm^{-1} range. Gas adsorption analysis was performed using BelSorp-max instrument from Bel Japan. Fluorescence measurements were done using Horiba FluoroLog instrument. ^{1}H-NMR analysis was performed using JeolECS-400 400 MHz instrument. The fluorescence images of cells were taken using Olympus Inverted IX81 equipped with Hamamatsu Orca R2 microscope.

Note: Direct synthesis of **5** using of 2-azido-benzene-1,4-dicarboxylic acid (H_2**L$_6$**) did not yield desired product, thus **5** was synthesized via postsynthetic modification (PSM) route starting from **4**.

4A.2.2 Synthesis of $Zr_6O_4(OH)_4(L_5)_6 \cdot G_x$(4):

Compound **4** was synthesized by slight modification of previously reported procedure.[18] 2-amino-benzene-1,4-dicarboxylic acid ($H_2\mathbf{L_5}$, 0.760 g) was dissolved in 14 mL DMF and anhydrous $ZrCl_4$ (0.326 g) was dissolved in 42 mL DMF. Both the solutions were then mixed and sonicated for 10 min. The mixture then distributed in 7 Teflon lined autoclave vessels and heated at 120 °C for 24 h. After cooling overnight, the yellowish microcrystalline material was isolated by centrifugation. The material was then rinsed three times with DMF followed by three additional washings with methanol and then dried overnight in a vacuum oven at 70 °C.

4A.2.3 Activation of Compound 4 (4'):

The unreacted starting material and occluded solvent molecules were removed by exchanging it with MeOH over 5 days and the volatile MeOH was removed under vacuum at 120 °C. Activated compound **4'** was then used for synthesis of **5** using post synthetic modification method.

4A.2.4 Low Pressure Gas Sorption Measurements:

Low pressure gas sorption measurements were performed using BelSorpmax (Bel Japan). N_2 gas used was of 99.999% purity. Prior to adsorption measurement, the guest-free sample **4'** was pretreated at 120 °C under vacuum for 12 h using BelPrepvacII. The adsorption isotherm for the N_2 gas was measured at 77 K.

4A.2.5 Synthesis of $Zr_6O_4(OH)_4(L_6)_6 \cdot G_x$ (5):

Solution of $NaNO_2$ (0.066 g) in H_2O (2 mL) was drop wise added to the suspension of activated MOF **4'** in H_2O-HCl (1:1, 4 mL) at 0 °C. After stirring for 30 min, the suspension was then added drop wise to ice cold solution of NaN_3 (0.150 g) in H_2O (2 mL). Upon complete addition, solution was warmed to room temperature and stirred overnight. The suspension was then vacuum filtered and three times washed with cold water and dried under reduced pressure.

4A.2.6 Activation of Compound 5 (5'):

The post synthetically modified compound **5** was activated by exchanging it with H_2O at RT for 2 days followed by thermal treatment at 120 °C under vacuum to yield guest free **5'**.

4A.2.7 Preparation of HEPES Buffer:

Deionized water was used throughout all experiments. HEPES (4-(2-hydroxyethyl)piperazine-1-ethanesulfonic acid) buffer was prepared by dissolving solid HEPES (2.383 g) in deionized water (1 L) followed by adjustment of pH by NaOH solution 0.5 (N).

4A.2.8 Photophysical Measurements:

In typical experimental setup, 0.5 mg of **5'** was weighed and added to cuvette containing 2 mL of HEPES buffer (10 mM, pH 7.4) under constant stirring. The fluorescence spectra were recorded in range 350-650 nm by exciting **5'** at 334 nm. To determine the fluorescence turn-on response of **5'** towards H_2S, 10 equivalents of solid Na_2S (H_2S source) was added to the cuvette and the fluorescence spectra were recorded at regular time intervals (every 60 seconds) till saturation. Similar experiment was also performed by replacing Na_2S by analyte of interest (Glutathione, Cysteine, Alanine, Serine, NaCl, NaBr, NaI, $NaNO_2$, $NaNO_3$).

4A.2.9 NMR Analysis:

~10 mg respective MOFs was digested with DMSO-d_6 (600 μL) and 48% HF (30 μL) by sonication. Upon complete dissolution of the functionalized MOF, the clear solution was analyzed by ^{1}H-NMR.

4A.2.10 MTT Cell Viability Assay:

Cells were dispersed in a 96-well microtiter plate at density of 10^4 cells per 100 mL an incubated at 37 °C in a 5% CO_2 for 16 hours. **5'** was added to each well in different concentration and incubated for another 6 hrs. DMEM solution of **5'** in each well was replaced by 110 μL of MTT-DMEM mixture (0.5 mg MTT/mL of DMEM) and incubated for 4 h in identical condition. After 4 h remaining MTT solution was removed and 100 μL of DMSO was added in each well to dissolve the formazan crystals. The absorbance was recorded in a microplate reader (Varioskan Flash) at the wavelength of 570 nm. All experiments were performed in quadruplicate, and the relative cell viability (%) was expressed as a percentage relative to the untreated control cells.

4A.2.11 Cell Imaging Experiment:

The HeLa cells were purchased from National Centre for Cell Science, Pune (India). HeLa cells were grown in DMEM supplemented with 10% heat inactivated fetal bovine serum (FBS), 100 IU/mL penicillin, 100 mg/mL streptomycin and 2 mM L-glutamine. Cultures were maintained in a humidified atmosphere with 5% CO_2 at 37 °C. The cultured cells were subcultured twice in each week, seeding at a density of about 15 × 10^4 cells/mL. Typan blue dye exclusion method was used to determine Cell viability. The fluorescence images were taken using Olympus Inverted IX81 equipped with Hamamatsu Orca R2 microscope by using DAPI filter. The 0.5 mg of **5'** was added to 2 mL water and sonicated for 10 minutes. The suspension was then passed through 0.2 μM filter and used for imaging study. The HeLa cells were incubated with above dispersion (50 μL) of **5'** in DMEM at pH 7.4, 37 °C for 6 h. After washing with PBS the fluorescence images were acquired. In this case no significant fluorescence was observed. Same set of HeLa cells were treated with Na_2S (8 mM) at 37 °C for 30 min. After washing with PBS the fluorescence images showed blue fluorescence.

4A.3 Results and Discussion:

4A.3.1 Synthesis and X-ray Structure of 4:

Probe **5** was synthesized using **4** as precursor, as the azide functionalized ligand did not yield desired product. Compound **4** was synthesized solvothermally using 2-amino-1,4-benzenedicarboxylic acid ($H_2\mathbf{L_5}$) and $ZrCl_4$ in DMF as light yellow powder (Scheme **4A.2**).[19] Compound **4** has same structure as that of UiO-66 analogue except free -NH_2 group is composed of $Zr_6O_4(OH)_4(CO_2)_{12}$ secondary building unit (SBU).[18] Each zirconium atom in hexameric SBU is eight-coordinated with square-antiprismatic coordination environment. One square face is formed by oxygen atoms supplied by μ_3-O and μ_3-OH groups, while the second square face is formed by oxygen atoms coming from carboxylate groups of ligand $\mathbf{L_5}$. The linear dicarboxylate ligand connects the SBU through carboxylate groups giving rise to cubic porous structure with free amine groups decorating the pore (Figure **4A.1**).

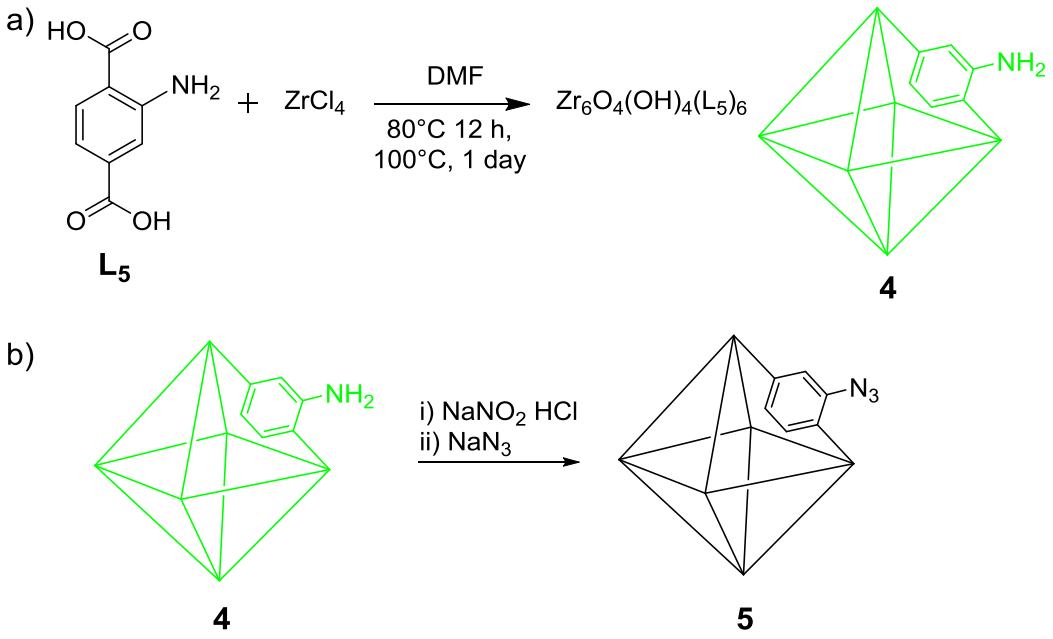

Scheme 4A.2: (a) Synthetic scheme for compound **4**. (b) Synthesis of probe **5** via postsynthetic modification route starting from **4**.

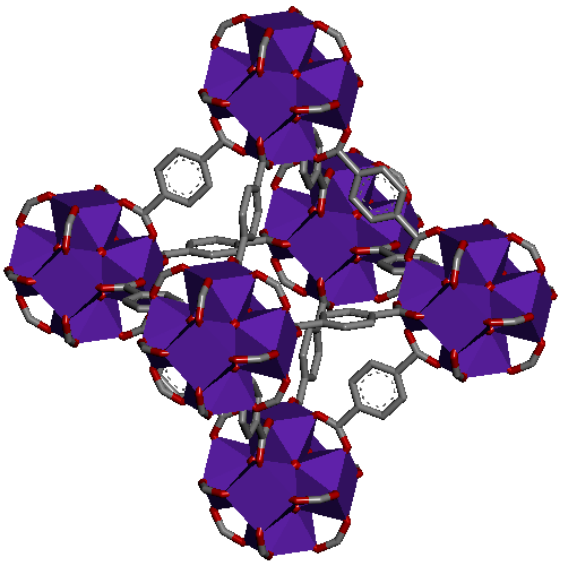

Figure 4A.1: Single crystal X-Ray structure of UiO-66.[18b] Purple octahedra represent the $[Zr_6O_4(OH)_4(CO_2)_{12}]^{12+}$ cluster; grey, red and blue spheres represent carbon, oxygen and nitrogen atoms, respectively. Hydrogen atoms are omitted for clarity.

4A.3.2 Phase Purity and Stability of 4:

The phase purity of bulk compound **4** was confirmed by matching powder X-ray diffraction (PXRD) patterns of simulated and as-synthesized bulk compound (Figure **4A.2a**). Thermogravimetric analysis revealed that **4** lost entrapped solvent molecules on

heating and remains stable up to 200 °C (Figure **4A.2b**). The occluded guest molecules in **4** were exchanged with low boiling MeOH over 5 days and the exchanged MeOH molecules were then removed by thermal treatment under reduced pressure to get guest free porous **4'**. The successful activation of **4'** was confirmed by N_2 adsorption isotherm at 77 K (Figure **4A.2c**).

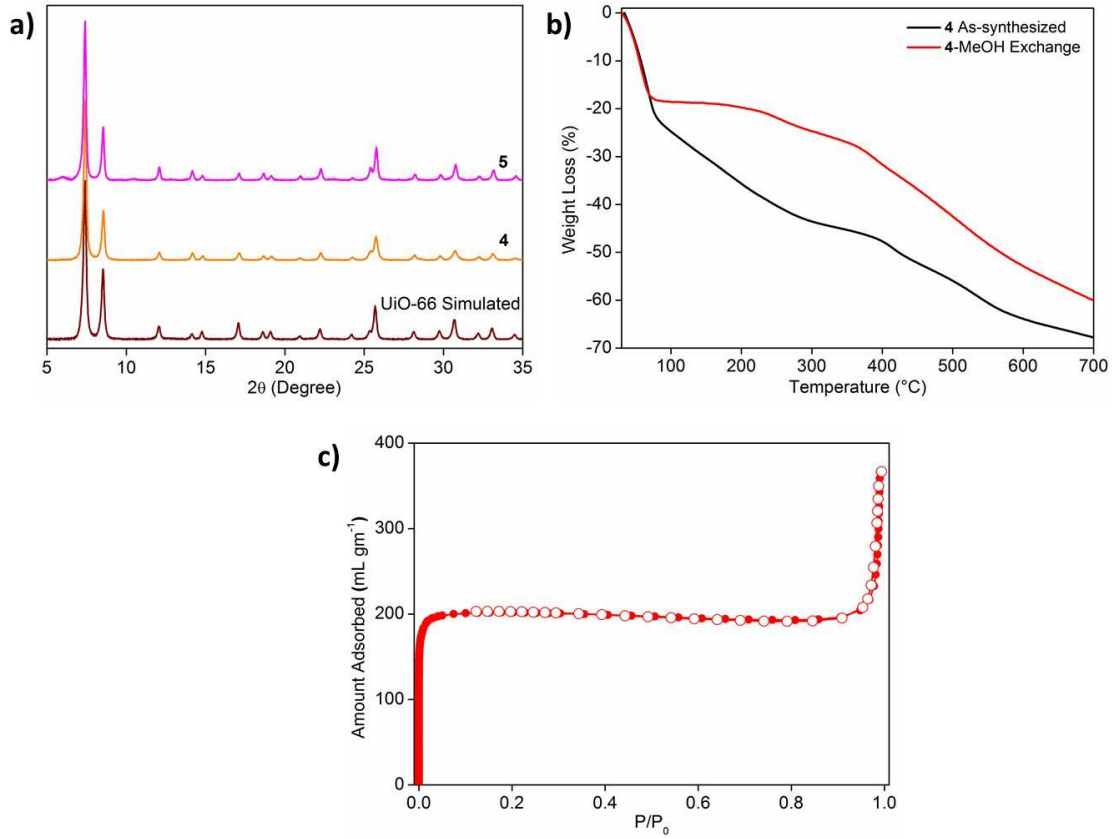

Figure 4A.2: (a) PXRD patterns of UiO-66 (simulated), as-synthesized MOF **4** and chemically modified MOF **5**. (b) Thermogravimetric analysis of **4**. (c) N_2 adsorption isotherm for **4'** at 77 K.

4A.3.3 Synthesis of 5:

The chemical modification of free -NH_2 in **4'** to -N_3 (**5**) was achieved by diazotization of free -NH_2 followed by NaN_3 treatment. **5** was then exchanged with H_2O for 2 days and then activated under reduced pressure to get **5'**. The structural integrity of **5'** upon post-synthetic modification was confirmed by PXRD patterns. The overlapping PXRD patterns of **4** and **5** confirmed the structural integrity of **5** (Figure **4A.2a**). The FT-IR spectrum **5'** showed appearance of new distinct peak at 2127 cm^{-1} corresponding to azide group which is absent in **4'** confirmed the transformation of -NH_2 to -N_3 (Figure **4A.3a**). The chemical transformation was further confirmed using ^{1}H-NMR. The **4'** and **5'**

were digested with DMSO-d_6 and HF to get clear solution which was then subjected to NMR analysis. ^{1}H-NMR of **4'** showed peak corresponding to ammonium protons, this peak was absent in **5'** which also confirmed the successful transformation of -NH_2 to -N_3 (Figure **4A.3b**).

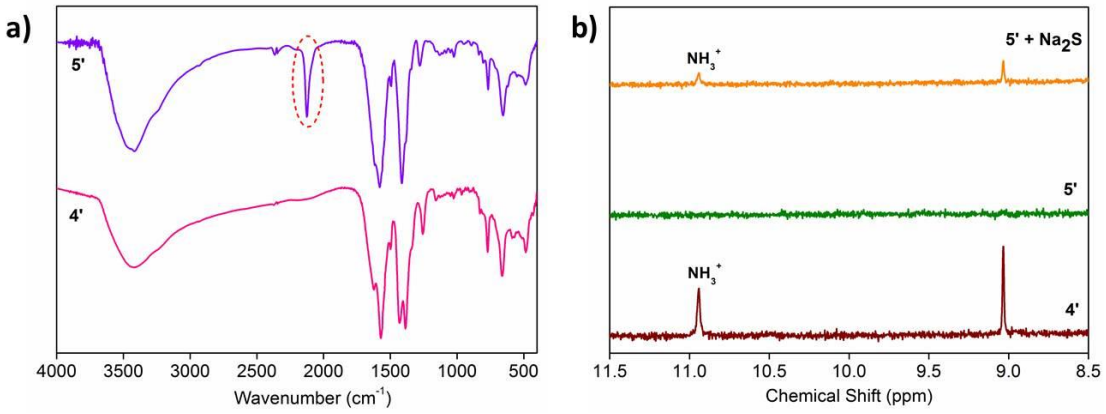

Figure 4A.3: (a) FT-IR spectra of MOFs **4'** and **5'**. (b) ^{1}H-NMR of acid digested MOFs **4'**, **5'** and **5'** upon Na_2S treatment.

4A.3.4 Photophysical Studies:

To probe the fluorescence turn-on response of **5'** towards H_2S, **5'** was excited at 334 nm and the fluorescence spectrum was recorded in 350-650 nm range (in HEPES buffer 10 mM, pH 7.4). As expected, **5'** showed very weak fluorescence response, owing to the electron withdrawing azido group and remained in turn-off state (Figure **4A.4a**). However, treatment of **5'** with Na_2S (H_2S source) resulted in remarkable increase in fluorescence intensity. To evaluate response time of **5'** towards H_2S, fluorescence spectra were acquired with time (Figure **4A.4a**). Almost 16 fold fluorescence enhancement was observed with $t_{1/2}$ = 13.6 s and the reaction completes within t_R = 180 s, which is comparable or better than known H_2S probes.[9a,16i] Considering fast metabolism and variable nature of endogenous H_2S in biological systems, the quick response shown by **5'** demonstrates the potential of **5'** in real-time intracellular H_2S imaging.

In complex biological systems highly selective response towards target analyte over potentially competing biological species is crucial for successful detection. Recently, malonitrile functionalized MOF has been employed for detection of H_2S by taking the advantage of reaction between malonitrile and thiol compounds with enhancement of photoluminescence. But the MOF is not selective to H_2S and thiol containing amino acid cysteine (Cys) also showed fluorescence turn-on response under identical conditions.[16i]

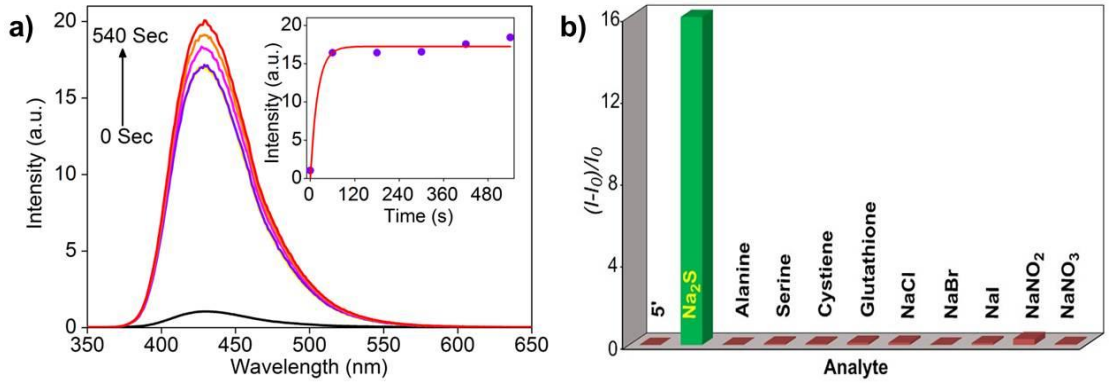

Figure 4A.4: (a) Fluorescence response of **5'** towards addition of Na_2S after 0, 60, 180, 300, 420 and 540 seconds. Inset: Time dependence of emission intensity at 436 nm. (b) Relative fluorescence response of **5'** towards various analytes after 540 seconds of analyte addition.

Therefore, we examined the fluorescence response of **5'** towards an array of potentially interfering biological species (Figure **4A.4b, 4A.A1-A9**). The reducing anions such as bromide, iodide did not show any effect on fluorescence intensity, despite the fact that the selective recognition of H_2S by **5'** is based on H_2S mediated reduction of azide to fluorescent amine. The biothiols like glutathione (GSH) and cysteine (Cys) are also known to reduce azide leading to off-target H_2S detection.[20] However, addition of GSH or Cys showed negligible effect on fluorescence intensity of **5'** (Figure **4A.4b**).

Encouraged from these results selectivity of **5'** towards H_2S in presence of these interfering analytes was also investigated. In a typical experiment, the solution containing **5'** and competing analyte was treated with Na_2S and the fluorescence response was

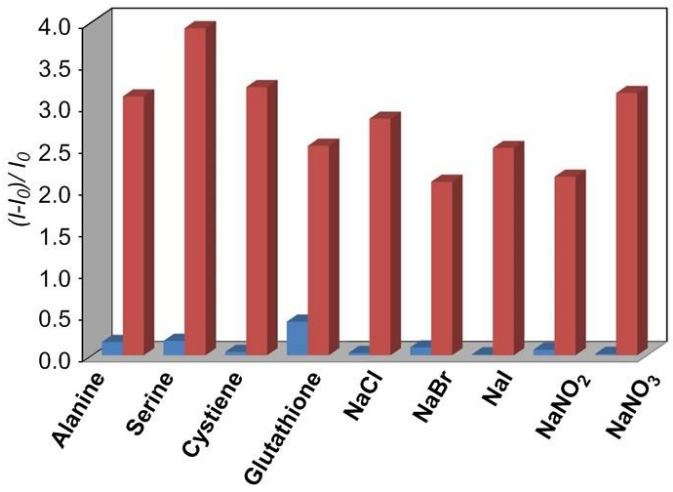

Figure 4A.5: Turn-on response of probe **5'** at 436 nm in presence of respective analyte (blue), followed by addition of Na_2S to same solution containing analyte (red) (in HEPES buffer).

recorded after 10 min (Figure **4A.5**). The MOF showed turn-on response towards H_2S even in presence of potentially competing analytes validating the high selectivity of **5'** towards H_2S. Presence of competing analytes showed negligible effect on the turn-on efficiency of the H_2S. Considering the complex biological system, **5'** can detect H_2S without any interference from competing biological species avoiding off-target reactivity and false response.

The quantitative response of probe **5'** towards H_2S was examined by fluorometric titration in HEPES buffer (10 mM, pH 7.4) (Figure **4A.6**). The incremental addition of Na_2S resulted in enhancement of characteristic fluorescence emission peak at 436 nm. The plot of fluorescence intensity at 436 nm against H_2S concentration exhibited excellent linear correlationship (R = 0.99315) (Figure **4A.6** Inset). The H_2S detection limit for **5'** was found to be 118 μM (signal to noise ratio, S/N = 3) which is in the range of H_2S concentration found in most of the biological systems.[3c-e]

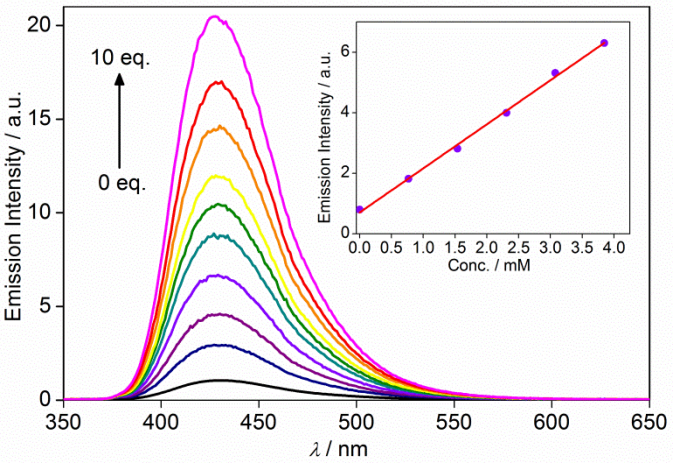

Figure 4A.6: Fluorescence response of **5'** with increasing concentrations of Na_2S. All the experiments carried in HEPES buffer (10 mM, pH 7.4).

To ascertain the structural integrity and the mechanism of turn-on response of **5'** towards H_2S, PXRD and ^{1}H-NMR experiments were carried out. The overlapping PXRD patterns of **5'** before and after treatment of H_2S demonstrated the stability of the probe under experimental conditions (Figure **4A.A10**). Most importantly the ^{1}H-NMR spectrum of **5'** did not show any peak corresponding to amine functionality but upon H_2S treatment the peak corresponding to amine appears (Figure **4A.3b**). This suggests that the fluorescence turn-on response of **5'** towards H_2S is due to the reduction of 'dark' azide group to emissive amino group.

4A.3.5 Cell Imaging:

To demonstrate the H_2S sensing ability of MOF **5'** in the biological system, cytotoxicity and live cell imaging studies were carried out using HeLa cell line. The cytotoxicity of **5'** was determined by MTT assay. Various concentrations of **5'** were used to determine toxicity level of **5'** towards HeLa cell. HeLa cells upon incubation with **5'** for 6 h showed low toxicity and about 97% cell viability was determined at 0.025 mg/mL (Figure **4A.7a**) with comparable fluorescence turn-on response (14 fold, Figure **4A.7b**) thus has chosen as working concentration for imaging studies.

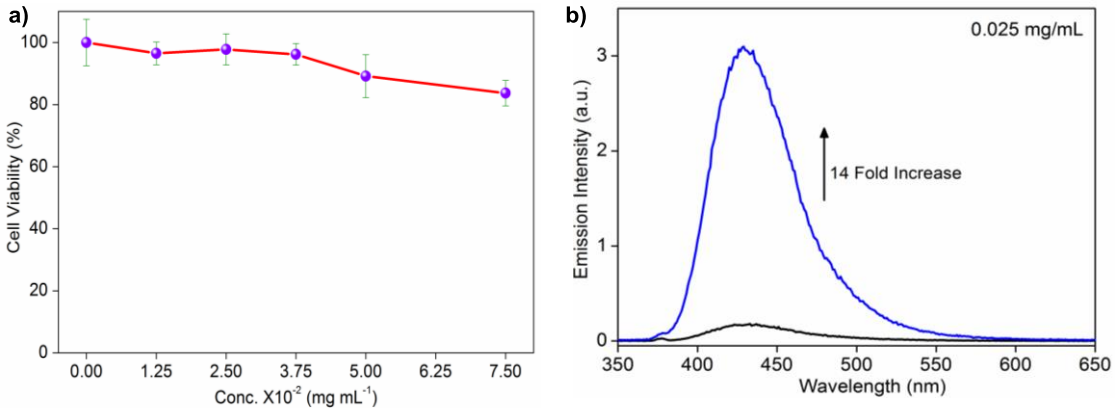

Figure 4A.7: (a) MTT cell viability assay for MOF **5'** using HeLa cells. (b) Fluorescence turn-on response of **5'** towards Na_2S at low concentration (0.025 mg/mL).

In cell imaging study, very low fluorescence was observed when HeLa cells were incubated with only **5'** at 37 °C for 6 h (Figure **4.8A-C**). However, when same cells were

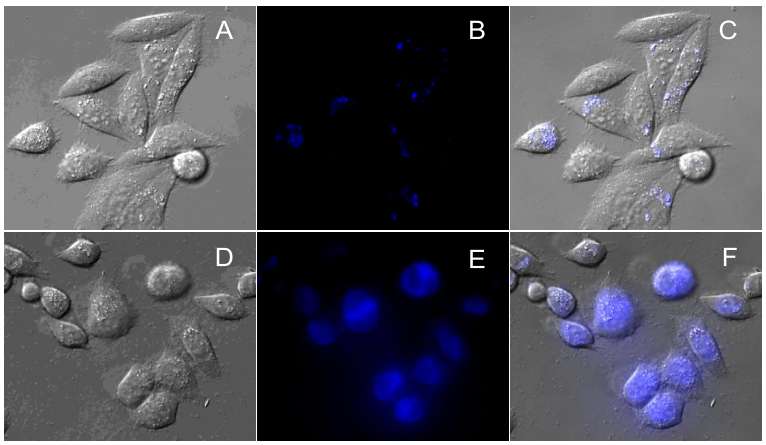

Figure 4A.8: Cell imaging study for **5'** (A) DIC images, (B) fluorescence, and (C) overlay image of HeLa cells incubated with **5'** for 6 h. (D-F) are respective DIC, fluorescence and overlay images of HeLa cells pre-incubated with **5'** followed by Na_2S for 30 min.

incubated with Na_2S at 37 °C for 30 min under identical conditions, strong fluorescence was observed inside the cells (Figure **4.8D-F**). The exact mechanism of cellular uptake is not known at present; however the HeLa cells are known to take up particles less than 200 nm via endocytosis pathway.[21] The experiments suggest that **5'** can be used to monitor intracellular H_2S and we believe that this is the first report of MOF based turn-on probe for H_2S employed in living cell.

4A.4 Summary and Conclusions:

In this section (A), we have reported an azide functionalized MOF **5'** as a fluorescence turn-on probe for selective sensing of H_2S. The **5'** shows highly selective and fast fluorescence turn-on response towards H_2S over potentially interfering chemical species including biothiols, amino acids and reducing anions. The low toxicity of **5'** and live cell imaging studies demonstrates the potential of **5'** in visualization and real-time monitoring of H_2S in biological systems. To the best of our knowledge **5'** is the first example of MOF based selective turn-on probes for H_2S. We anticipate that MOF based turn-on sensors for H_2S are still in infancy and there is much to explore for the improvement of the performance.

4A.5 References:

(1) (a) Reiffenstein, R. J.; Hulbert, W. C.; Roth, S. H. *Annu. Rev. Pharmacol. Toxicol.* **1992,** *32,* 109-134. (b) Iversen, K. J.; Spencer, M. J. S. *J. Phys. Chem. C* **2013,** *117,* 26106-26118.

(2) (a) Szabo, C. *Nat. Rev. Drug Discov.* **2007,** *6,* 917-935. (b) Boehning, D.; Synder, S. H. *Annu. Rev. Nurosci.* **2003,** *26,* 105-135. (c) Wang, R. *FASEB J.* **2002,** *16,* 1792-1798. (d) Bailey, T. S.; Pluth, M. D. *J. Am. Chem. Soc.* **2013,** *135,* 16697-16704.

(3) (a) Lin, V. S., Lippert, A. R.; Chang, C. J. *Proc. Natl. Acad. Sci. U.S.A.* **2013,** *110,* 7131-7135. (b) Yang, G.; Wu, L.; Jiang, B.; Yang, W.; Qi, J.; Cao, K.; Meng, Q.; Mustafa, A. K.; Mu, W.; Zhang, S.; Snyder, S. H.; Wang, R. *Science* **2008,** *322,* 587-590. (c) Li, L.; Rose, P.; Moore, P. K. *Annu. Rev. Pharmacol. Toxicol.* **2011,** *51,* 169-187. (d) Liu, J.; Sun, Y.-Q.; Zhang, J.; Yang, T.; Cao, J.; Zhang, L.; Guo, W. *Chem. Eur. J.* **2013,** *19,* 4717-4722. (e) Wu, P.; Zhang, J.; Wang, S.; Zhu, A.; Hou, X. *Chem. Eur. J.* **2014,** *20,* 952-956.

(4) Drew, K. L.; Rice, M. E.; Kuhn, T. B.; Smith, M. A. *Free Radical Biol. Med.* **2001,** *31,* 563-573.

(5) Eto, K.; Asada, T.; Arima, K.; Makifuchi, T.; Kimura, H. *Bio-Chem. Biophys. Res. Commun.* **2002,** *293,* 1485-1488.

(6) Kamoun, P.; Belardinelli, M.-C.; Chabli, A.; Lallouchi, K.; Chadefaux-Vekemans, B. *Am. J. Med. Genet.* **2003,** *116A,* 310-311.

(7) Yang, W.; Yang, G.; Jia, X.; Wu, L.; Wang, R. *J. Physiol.* **2005,** *569,* 519-531.

(8) Szabo, C.; Coletta, C.; Chao, C.; Modis, K.; Szczesny, B.; Papapetropoulos, A.; Hellmich, M. R. *Proc. Natl. Acad. Sci. U.S.A.* **2013,** *110,* 12474-12479.

(9) (a) Peng, H.; Chen, W.; Burroughs, S.; Wang, B. *Curr. Org. Chem.* **2013,** *17,* 641-653. (b) Mao, G.-J.; Wei, T.-T.; Wang, X.-X.; Huan, S.-Y.; Lu, D.-Q.; Zhang, J.; Zhang, X.-B.; Tan, W.; Shen, G.-L.; Yu, R.-Q. *Anal. Chem.* **2013,** *85,* 7875-7881.

(10) (a) Liu, C.; Pan, J.; Li, S.; Zhao, Y.; Wu, L. Y.; Berkman, C. E.; Whorton, A. R.; Xian, M. *Angew. Chem. Int. Ed.* **2011,** *50,* 10327-10329. (b) Chen, Y.; Zhu, C.; Yang, Z.; Chen, J.; He, Y.; Jiao, Y.; He, W.; Qiu, L.; Cen, J.; Guo, Z. *Angew. Chem. Int. Ed.* **2013,** *52,* 1688-1691.

(11) (a) Eddaoudi, M.; Kim, J.; Rosi, N.; Vodak, D.; Wachter, J.; Okeeffe, M.; Yaghi, O. M. *Science* **2002,** *295,* 469-472. (b) Takashima, Y.; Martinez, V. M.; Furukawa, S.; Konda, M.; Shimomura, S.; Uehara, H.; Nakahama, M.; Sugimoto, K.; Kitagawa, S. *Nat. Commun.* **2011,** 2:168 doi: 10.1038/ncomms1170. (c) Kreno, L. E.; Leong, K.; Farha, O. K.; Allendorf, M.; Duyne, R. P.; Hupp, J. T. *Chem. Rev.* **2012,** *112,* 1105-1125. (d) Horcajada, P.; Gref, R.; Baati, T.; Allan, P. K.; Maurine, G.; Couvreur, P.; Ferey, G.; Morris, R.; Serre, C. *Chem. Rev.* **2012,** *112,* 1232-1268. (e) Kupller. R. J.; Timmons, D. J.; Fang, Q.-R.; Li, J. R.; Makal, T. A.; Young, M. D.; Yuan, D.; Zhao, D.; Zhuang, W.; Zhou, H.-C. *Coord. Chem. Rev.* **2009,** *253,* 3042-3066. (f) Nagarkar, S. S.; Desai, A. V.; Ghosh, S. K. *Chem. Asian J.* **2014,** *9,* 2358-2376. (g) Diring, S.; Wang, D. O.; Kim, C.; Kondo, M.; Chen, Y.; Kitagawa, S.; Kamei, K.-i.; Furukawa, S. *Nat. Commun.* **2013,** 4:2684 doi: 10.1038/ncomms3684. (h) Yoon, M.; Suh, K.; Natarajan, S.; Kim, K. *Angew. Chem. Int. Ed.* **2013,** *52,* 2688-2700.

(12) (a) Allendorf, M. D.; Bauer, C. A.; Bhakta, R. K.; Houk, R. J. T. *Chem. Soc. Rev.* **2009,** *38,* 1330-1352. (b) Hu, Z.; Deibert, B. J.; Li, J. *Chem. Soc. Rev.* **2014,** *43,* 5815-5840. (c) Nagarkar, S. S.; Joarder, B.; Chaudhari, A. K.; Mukherjee, S.;

Ghosh, S. K. *Angew. Chem. Int. Ed.* **2013,** *52,* 2881-2885. (d) Foucault-Collet, A.; Gogick, K. A.; White, K. A.; Villette, S.; Pallier, A.; Collet, G.; Kieda, C.; Li, T.; Geib, S. J.; Rosi, N. L.; Petoud, S. *Proc. Natl. Acad. Sci. U.S.A.* **2013,** *110,* 17199-17204. (e) Wu, P.; Wang, J.; He, C.; Zhang, X.; Wang, Y.; Liu, T.; Duan, C. *Adv. Funct. Mater.* **2012,** *22,* 1698-1703. (f) Cui, Y.; Yue, Y.; Qian, G.; Chen, B. *Chem. Rev.* **2012,** *112,* 1126-1162. (g) Sen, S.; Nair, N. N.; Yamada, T.; Kitagawa, H.; Bharadwaj, P. K. *J. Am. Chem. Soc.* **2012,** *134,* 19432-19437.

(13) Xiong, R.; Odbadrakh, K.; Michalkova, A.; Luna, J. P.; Petrova, T.; Keffer, D. J.; Nicholson, D. M.; Fuentes-Cabrera, M. A.; Lewis, J. P.; Leszczynski, J. *Sens. and Actuators B* **2010,** *148,* 459-468.

(14) Wang, Z.; Cohen, S. M. *Chem. Soc. Rev.* **2009,** *38,* 1315-1329.

(15) Shustova, N. B.; Cozzolino, A. F.; Reineke, S.; Baldo, M.; Dinca, M. *J. Am. Chem. Soc.* **2013,** *135,* 13326-13329.

(16) (a) Hamon, L.; Serre, C.; Devic, T.; Loiseau, T.; Millange, F.; Férey, G.; Weireld, G. D. *J. Am. Chem. Soc.* **2009,** *131,* 8775-8777. (b) Petit, C.; Mendoza, B.; Bandosz, T. J. *ChemPhysChem* **2010,** *11,* 3678-3684. (c) Petit, C.; Bandosz, T. J. *Dalton Trans.* **2012,** *41,* 4027-4035. (d) Allan, P. K.; Wheatley, P. S.; Aldous, D.; Infas Mohideen, M.; Tang, C.; Hriljac, J. A.; Megson, I. L.; Chapman, K. W.; Weireld, G. D.; Vaesen, S.; Morris, R. E. *Dalton Trans.* **2012,** *41,* 4060-4066. (e) Gutierrez-Sevillano, J. J.; Martin-Calvo, A.; Dubbeldam, D.; Calero, S.; Hamad, S. *RSC Adv.* **2013,** *3,* 14737-14749. (f) Chavan, S.; Bonino, F.; Valenzano, L.; Civalleri, B.; Lamberti, C.; Acerbi, N,; Cavka, J. H.; Leistner, M.; Bordiga, S. *J. Phys. Chem. C* **2013,** *117,* 15615-15622. (g) Nickerl, G.; Leistner, M.; Helten, S.; Bon, V.; Senkovska, I.; Kaskel, S. *Inorg. Chem. Front.* **2014,** *1,* 325-330. (h) Liu, B.; Chen, Y. *Anal. Chem.* **2013,** *85,* 11020-11025. (i) Li, H.; Feng, X.; Guo, Y.; Chen, D.; Li, R.; Ren, X.; Jiang, X.; Dong, Y.; Wang, B. *Sci. Rep.* **2014,** 4,4366; doi:10.1038/srep04366. (j) Liu, J.; Yee, K.-K.; Lo, K. K.-W.; Zhang, K. Y.; To, W.-P.; Che, C.-M.; Xu, Z. *J. Am. Chem. Soc.* **2014,** *136,* 2818-2824.

(17) Lippert, A. R.; New, E. J.; Chang, C. J. *J. Am. Chem. Soc.* **2011,** *133,* 10078-10080.

(18) (a) Kandiah, M.; Nilsen. M. H.; Usseglio, S.; Jakobsen, S.; Olsbye, U.; Tilset, M.; Larabi, C.; Quadrelli, E. A.; Bonino, F.; Lillerud, K. P. *Chem. Mater.* **2010,** *22,*

6632-6640. (b) Cavka, J. H.; Jakobsen, S.; Olsbye, U.; Guillou, N.; Lamberti, C.; Bordiga, S.; Lillerud, K. P. *J. Am. Chem. Soc.* **2008,** *130,* 13850-13851.

(19) Morris, W.; Doonan, C. J.; Yaghi, O. M. *Inorg. Chem.* **2011,** *50,* 6853-6855.

(20) (a) Lippert, A. R. *J. Inorg. BioChem.* **2014,** *133,* 136-142. (b) Sasakura, K.; Hanaoka, K.; Shibuya, N.; Mikami, Y.; Kimura, Y.; Komatsu, T.; Ueno, T.; Terai, T.; Kimura, H.; Nagano, T. *J. Am. Chem. Soc.* **2011,** *133,* 18003-18005.

(21) (a) Vivero-Escoto, J. L.; Slowing, I. I.; Trewyn, B. G.; Lin, V. S. Y. *small* **2010,** *6,* 1952-1967. (b) Yin, L.; He, C.; Huang, C.; Zhu, W.; Wang, X.; Xu, Y.; Qian, X. *Chem. Commun.* **2012,** *18,* 4486-4488.

Chapter 4

Section B

Nitro (-NO_2) Functionalized Metal-Organic Framework as a Reaction based Fluorescence Turn-on Probe for H_2S Sensing

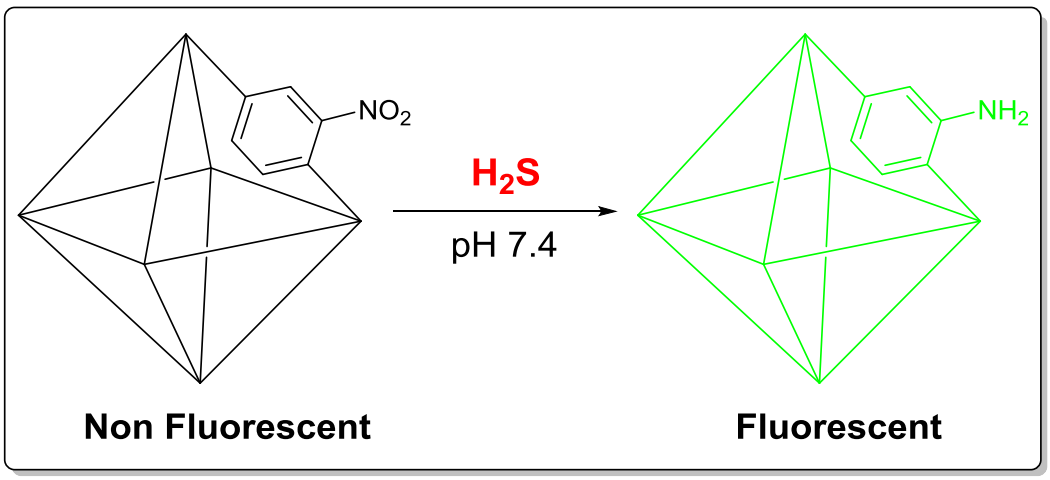

4B.1 Introduction:

Hydrogen sulfide (H_2S), a colorless gas with distinct rotten egg smell is released as byproduct from range of industries including petroleum refining, waste management, natural gas production, etc.[1] The H_2S is flammable gas and its high lipid solubility allows it to pass through cellular membrane in body and prevent cellular respiration.[1] The exposure to H_2S causes olfactory paralysis, unconsciousness and even death in case of prolong exposures.[2] However, this toxic gas has emerged as one of the third endogenous signaling molecule (gasotransmitter) in biological systems, apart from Nitric Oxide (NO) and Carbon Monoxide (CO).[3] H_2S is utilized by variety organism ranging from bacteria to mammals for signal transduction, immune response and energy production.[4] The H_2S is known for modulation of blood pressure, neurotransmission and anti-inflammatory activity.[5] Recently the abnormal levels of H_2S are identified to be related to Alzheimer's disease,[6] diabetes,[7] Down's syndrome,[8] cancer[9] making it a potential target to diagnostics and treatment of these diseases. Thus the investigation of mode of production and action of H_2S to better understand H_2S related physiological and pathological process in biological systems is very crucial.

In pursuit of understanding the role of H_2S and its mechanism in different physiological and pathological processes, selective and real-time detection is important. Owing to highly volatile and reactive nature the precise detection of H_2S profoundly depends on sample preparation and detection method.[10] The fluorescence based detection methods are getting increasing attention in this regard because of their high sensitivity, simplicity, short response time, non-invasive nature, real-time monitoring and easy sample preparation.[11] An ideal fluorescence probe should display noteworthy change in fluorescence intensity, should be selective even in presence interfering biomolecules, most importantly should interact fast and should be cell permeable.[12] In general, fluorescence turn-on probes are favored for better signal to noise ratio and avoid false response as detection occurs relative to dark background.

Metal-organic frameworks (MOFs), crystalline porous solid have emerged as novel functional material with applications ranging from gas storage/separation, sensing, biomedical and clean energy applications, etc.[13] MOF as sensing material provide several advantages like designable architecture allows fine-tuning of electronic properties, molecular sieving effect improves selectivity and pre-concentrates the analyte in MOF matrix for effective host-guest interactions.[14] By virtue of chemical

stability and possibility of post-synthetic modification, MOFs can be tailored to append the appropriate functionality in the coordination spaces and construct probes for detection of the targeted analyte. MOFs have been utilized for storage and delivery of H_2S gas, however they rarely been utilized as reaction based selective fluorescence turn-on probe.[15] In previous section (A) we reported azide ($-N_3$) functionalized MOF as fluorescence turn-on probe for highly selective detection of H_2S under physiological conditions.[16] The 'dark' azide groups in MOF undergo H_2S mediated reduction to 'emissive' amine counterpart under physiological conditions and thus giving rise to turn-on response. Similar to azide group 'dark' nitro ($-NO_2$) group also undergo H_2S mediated reduction to emissive amine in bioorthogonal manner.[17] We reasoned that, if we synthesize nitro functionalized biocompatible stable porous MOF, it should undergo H_2S mediated reduction of nitro group to corresponding amine group giving rise to fluorescence turn-on response (Scheme **4B.1**).

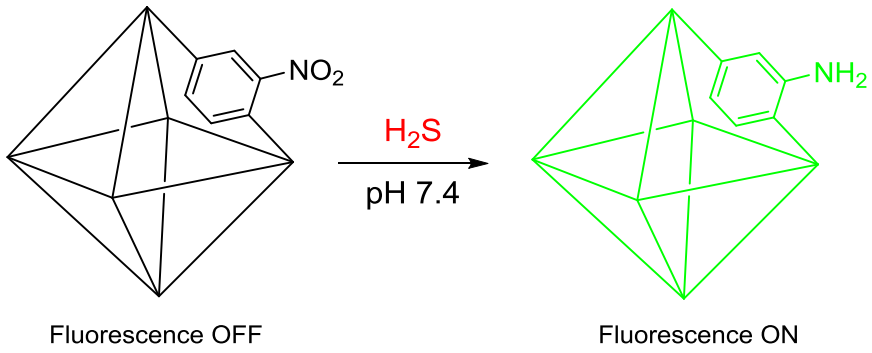

Scheme 4B.1: H_2S mediated reduction of $-NO_2$ in MOF to $-NH_2$ upon addition of Na_2S at physiological pH giving rise to fluorescence turn-on response.

Nitro functionalized UiO-66@NO_2 (**6**) is composed of low absorbing non-toxic Zr(IV) metal also it stable under physiological conditions for hours.[18] Also **6** can be prepared in good yield and in single step as against azide MOF which needs two steps. In addition, we have reported in previous section that the UiO-66 analogues are less toxic to cells.[16] Thus we envisioned that **6** can potentially be used as reaction probe for H_2S under physiological conditions. In present section (B) we report, fast and selective fluorescence turn-on response of nitro functionalized probe **6** towards H_2S under physiology mimicking conditions. The selectivity was consistent even in presence of potentially competing biomolecules. Compound **6** can detect H_2S at as low as 188 μM concentration under physiological conditions with response time of 460 s.

4B.2 Experimental Section:

4B.2.1 Material and Methods:

All the reagents and solvents were commercially available and used without further purification. Powder X-Ray diffraction patterns (PXRD) were measured on BrukerD8 Advanced X-Ray diffractometer using Cu K_α radiation (λ = 1.5406 Å) in 5 to 40° 2Θ range. The IR spectra were recorded on NICOLET 6700 FT-IR spectrophotometer using KBr pellet in 400-4000 cm^{-1} range. Gas adsorption analysis was performed using BelSorp-max instrument from Bel Japan. Fluorescence measurements were done using Horiba FluoroLog instrument.

4B.2.2 Synthesis of $Zr_6O_4(OH)_4(L_7)_6 \cdot G_x$ (6):

Compound **6** was synthesized by slight modification of previously reported procedure.[19] 2-nitro-benzene-1,4-dicarboxylic acid ($H_2\mathbf{L_7}$, 0.074 g), anhydrous $ZrCl_4$ (0.082 g) and 4 mL DMF were added to Teflon lined vessel. Teflon lined autoclave vessel was then heated at 120 °C for 24 h. After cooling overnight, the white microcrystalline material was isolated by centrifugation. The material was then rinsed three times with DMF followed by three additional washings with methanol and then dried overnight in a vacuum at 70 °C.

4B.2.3 Activation of Compound 6 (6'):

The unreacted starting material and occluded solvent molecules were removed by exchanging it with MeOH over 5 days. The MeOH exchanged sample was then heated at 120 °C under reduced pressure for overnight to remove volatile MeOH solvent and get activated compound **6'**.

4B.2.4 Low Pressure Gas Sorption Measurements:

Low pressure gas sorption measurements were performed using BelSorpmax (Bel Japan). CO_2 gas used was of 99.999% purity. Prior to adsorption measurement, the guest-free sample **6'** was pretreated at 120 °C under vacuum for 12 h using BelPrepvacII. The adsorption isotherm for the CO_2 gas was measured at 195 K.

4B.2.5 Preparation of HEPES Buffer:

Deionized water was used throughout all experiments. HEPES (4-(2-hydroxyethyl)piperazine-1-ethanesulfonic acid) buffer was prepared by dissolving

solid HEPES (2.383 g) in deionized water (1 L) followed by adjustment of pH by NaOH solution 0.5 (N).

4B.2.6 Photophysical Measurements:

In typical experimental setup, 0.5 mg of **6'** was weighed and added to cuvette containing 2 mL of HEPES buffer (10 mM, pH 7.4) under constant stirring. The fluorescence spectra were recorded in range 360-650 nm by exciting **6'** at 334 nm. To determine the fluorescence turn-on response of **6'** towards H_2S, 10 equivalents of solid Na_2S (H_2S source) was added to the cuvette and the fluorescence spectra were recorded at regular time intervals (every 60 seconds) till saturation. Similar experiment was also performed by replacing Na_2S by analyte of interest (Glutathione, Cysteine, Alanine, Serine, NaCl, NaBr, NaI, $NaNO_2$, $NaNO_3$).

4B.3 Results and Discussion:

4B.3.1 Synthesis and X-ray Structure of 6:

Probe **6** was synthesized as white crystalline powder upon reaction between $ZrCl_4$ and 2-nitro-benzene-1,4-dicarboxylic acid ($H_2\mathbf{L}_7$) in DMF under solvothermal conditions. Compound **6** has same structure as that of UiO-66 analogues except guest accessible free nitro ($-NO_2$) group (Figure **4B.1**).[18] **6** is composed of

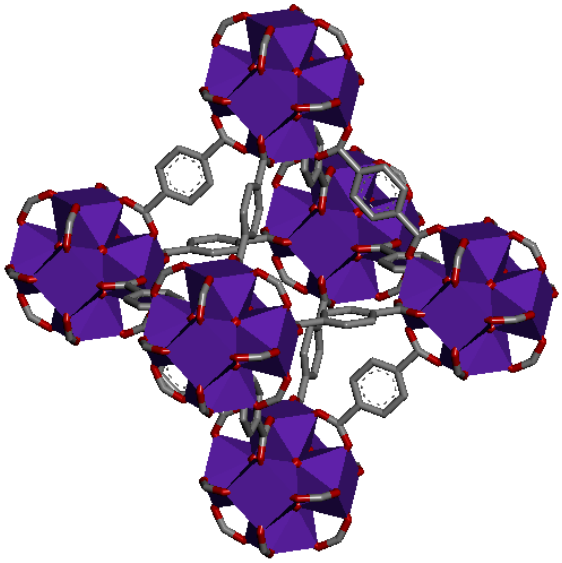

Figure 4B.1: Single crystal X-Ray structure of UiO-66.[18b] Purple octahedra represent the $[Zr_6O_4(OH)_4]^{12+}$ cluster; grey, red and blue spheres represent carbon, oxygen and nitrogen atoms, respectively. Hydrogen atoms are omitted for clarity.

$Zr_6O_4(OH)_4(CO_2)_{12}$ secondary building unit (SBU) with each zirconium atom in hexameric SBU is eight-coordinated with square-antiprismatic coordination environment, where one square face is formed by oxygen atoms supplied by μ_3-O and μ_3-OH groups, while the second square face is formed by oxygen atoms coming from carboxylate groups of ligand **L**$_7$. The linear dicarboxylate ligand connects the SBU through carboxylate groups giving rise to cubic porous structure with free nitro groups decorating the pore.

4B.3.2 Phase Purity and Stability of 6:

The PXRD pattern of as-synthesized MOF **6** matches well with the simulated PXRD pattern confirming the phase purity of bulk crystalline sample (Figure **4B.2a**). The MOF loses guest solvent molecules upon heating remains stable up to ~300 °C as evident from thermogravimetric analysis (Figure **4B.2b**). To get porous guest free form, guest molecules in matrix of **6** were exchanged with methanol over 5 days followed by heating at 120 °C overnight under reduced pressure. The porosity of guest

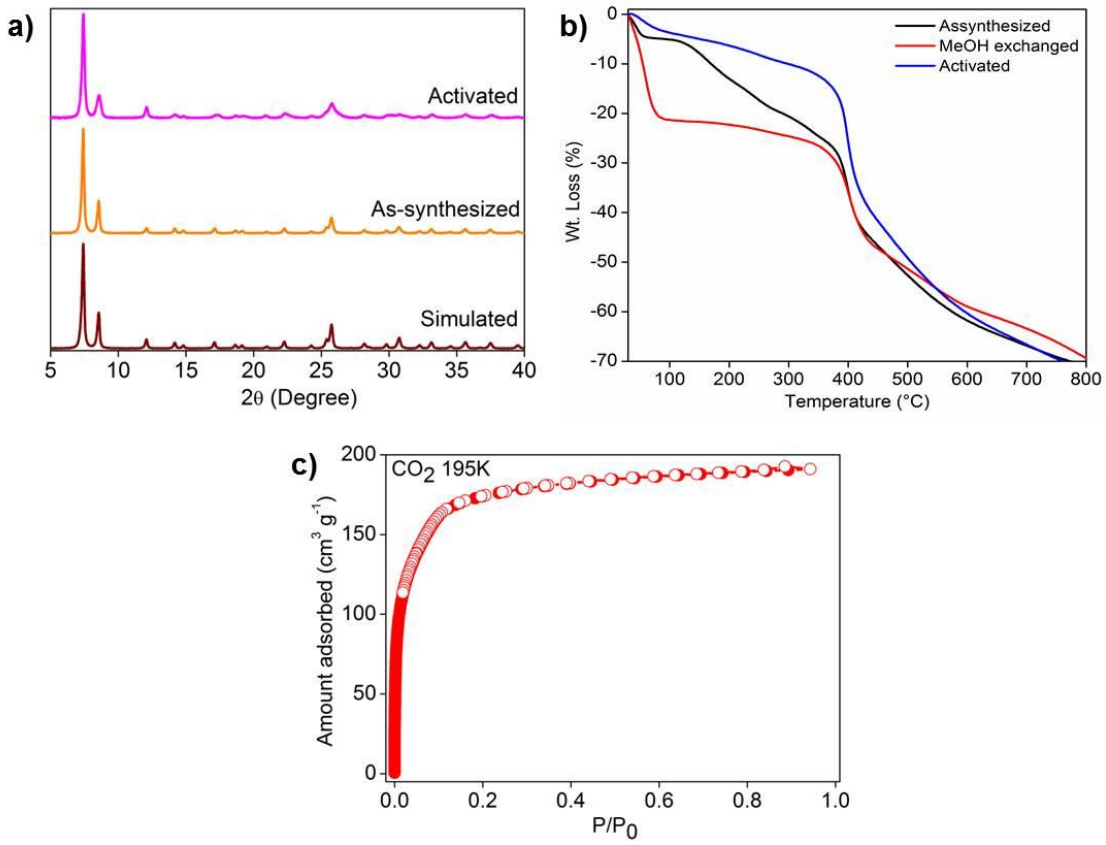

Figure 4B.2: (a) PXRD patterns of UiO66 (simulated), as-synthesized MOF **6** and activated MOF **6'**. (b) Thermogravimetric analysis of **6**. (c) CO_2 adsorption isotherm for **6'** at 195 K.

free form of **6'** was investigated by gas adsorption analysis. The CO_2 sorption analysis of **6'** at 195 K confirmed the successful activation of MOF (Figure **4B.2c**).

4B.3.3 Photophysical Studies:

Fluorescence spectrum of **6'** was recorded in 360-650 nm range in HEPES (10 mM, 7.4 pH) upon excitation at 334 nm. **6'** exhibited very weak fluorescence and remained in turn-off state, owing to presence of electron withdrawing nitro group (Figure **4B.3a**). To probe the fluorescence turn-on response of **6'** towards H_2S, **6'** in HEPES was treated with Na_2S (H_2S source). The treatment of Na_2S resulted in remarkable increase in fluorescence intensity. Fluorescence spectra were recorded at regular time interval and the increase in fluorescence intensity was monitored at 436 nm to calculate response time of **6'**. Addition of Na_2S resulted in 6 fold fluorescence increase with $t_{1/2}$ = 36.3 s and the reaction almost completes in t_R = ~ 460 s. The longer reaction time compared to azide probe ($t_{1/2}$ = 180 s) is expected owing to sluggish nature of nitro to amine reduction reaction compared to corresponding azide analogue.

Considering complex biological system, high selectivity towards target analyte to avoid false response is very vital. We inspected the effect of potentially interfering biomolecules on fluorescence response of **6'** (Figure **4B.3b**, **4B.A1-A9**). The amino acids like alanine and serine showed petite effect on fluorescence intensity of **6'**. The thiol containing amino acids like glutathione (GSH) and cysteine (Cys) are known for reducing character and thus the off-target response, also showed negligible fluorescence change in fluorescence intensity of **6'**. We also checked the effect of

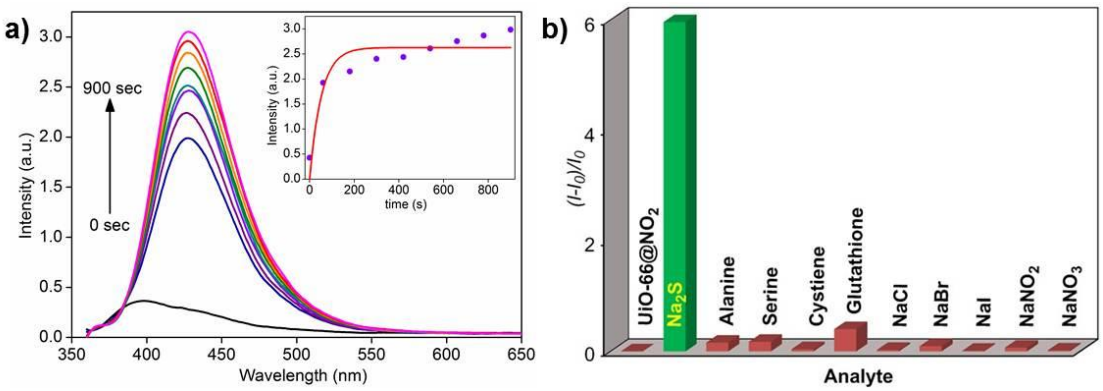

Figure 4B.3: (a) Fluorescence response of **6'** towards addition of Na_2S after 0, 60, 180, 300, 420 and 540 seconds. Inset: Time dependence of emission intensity at 436 nm. (b) Relative fluorescence response of **6'** towards various analytes after 540 seconds of analyte addition.

reducing anions like bromide, iodide and $NaNO_2$, $NaNO_3$, NaCl on fluorescence spectra of **6'**. Despite the fact that H_2S shows efficient turn-on response via H_2S mediated reduction of nitro to amine, these reducing biomolecules did not show any effect on fluorescence spectrum.

For real time application selective and efficient detection in presence of potentially interfering biomolecules is crucial. Likewise, the selective response of the probe in concurrent presence of competing biomolecules was examined. Initially the solution containing **6'** in HEPES was treated with competing analyte and fluorescence response was recorded. To above analyte containing solution, Na_2S was added and fluorescence turn-on response in presence of competing analyte was recorded (Figure **4B.4**). The H_2S showed significant fluorescence turn-on response even in presence of competing biomolecules. This demonstrates potential of **6'** towards selective H_2S detection in complex biological system avoiding off-target reactivity and false response.

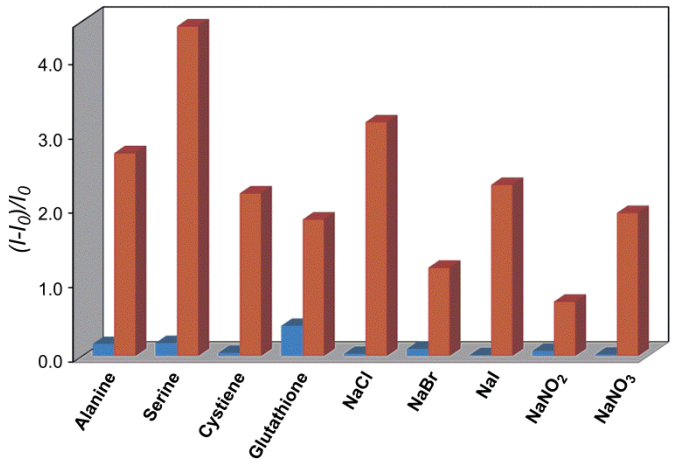

Figure 4B.4: Turn-on response of probe **6'** at 436 nm in presence of respective analytes (blue), followed by addition of Na_2S in solution containing analyte (red).

Performing fluorometric titration, quantitative fluorescence response of **6'** towards H_2S in HEPES buffer was determined. With increasing Na_2S (H_2S) concentration the fluorescence intensity of **6'** was found to be increasing (Figure **4B.5**). The Inset shows plot of fluorescence intensity of **6'** at 436 nm versus concentration of H_2S added, which shows excellent linear correlation (R = 0.9930).

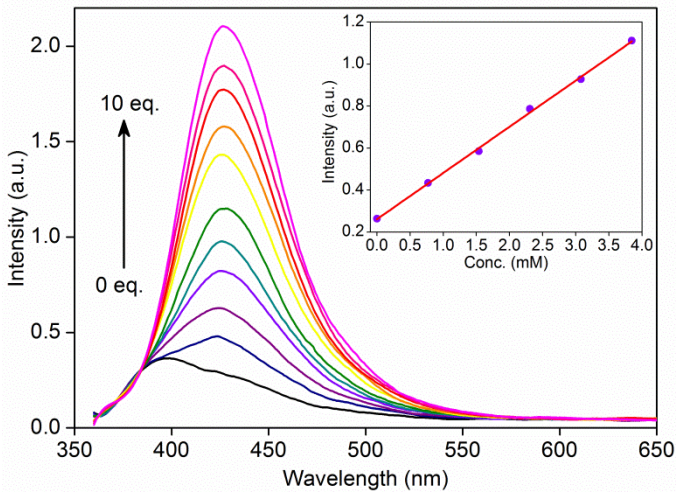

Figure 4B.5: Fluorescence response of **6'** with increasing concentrations of Na_2S. All the experiments carried in HEPES buffer (10 mM, pH 7.4).

The detection limit of **6'** towards H_2S was calculated to be 188 μM, keeping signal to noise ratio (S/N) = 3. The detection limit is higher than corresponding azide analogue but it is in the range of H_2S concentration found in biological systems.[20]

4B.4 Summary and Conclusions:

In present section (B), we have utilized nitro (-NO_2) functionalized MOF **6'** as a fluorescence turn-on probe for selective H_2S detection. Selective and fast fluorescence turn-on response of **6'** towards H_2S was observed even in presence of potentially interfering chemical species including biothiols, amino acids and reducing anions. We anticipate that there is further scope for the improvement of the MOF performance in terms of fold increase, shorter response time, detection limit, etc. by opting novel strategies. We expect that the present chapter will stimulate the research in the field of MOF based sensors for H_2S and other biologically important molecules to probe their physiological and pathological roles.

4B.5 References:

(1) (a) Reiffenstein, R. J.; Hulbert, W. C.; Roth, S. H. *Annu. Rev. Pharmacol. Toxicol.* **1992,** *32,* 109-134. (b) Hendrickson, R. G.; Chang, A.; Hamilton, R. J. Co-worker Fatalities from Hydrogen Sulfide. *Am. J. Ind. Med.* **2004,** *45,* 346-S350.

(2) Iversen, K. J.; Spencer, M. J. S. *J Phys. Chem. C* **2013,** *117,* 26106-26118.

(3) (a) Wang, R. *FASEB J.* **2002,** *16,* 1792-1798. (d) Bailey, T. S.; Pluth, M. D. *J. Am. Chem. Soc.* **2013,** *135,* 16697-16704. (b) Szabo, C. *Nat. Rev. Drug Discov.* **2007,** *6,* 917-935. (c) Boehning, D.; Synder, S. H. *Annu. Rev. Nurosci.* **2003,** *26,* 105-135.

(4) (a) Li, L.; Rose, P.; Moore, P. K. *Annu. Rev. Pharmacol. Toxicol.* **2011,** *51,* 169-187. (b) Lin, V. S., Lippert, A. R.; Chang, C. J. *Proc. Natl. Acad. Sci. U.S.A.* **2013,** *110,* 7131-7135. (c) Liu, J.; Sun, Y.-Q.; Zhang, J.; Yang, T.; Cao, J.; Zhang, L.; Guo, W. *Chem. Eur. J.* **2013,** *19,* 4717-4722. (d) Wu, P.; Zhang, J.; Wang, S.; Zhu, A.; Hou, X. *Chem. Eur. J.* **2014,** *20,* 952-956.

(5) (a) Yang, G.; Wu, L.; Jiang, B.; Yang, W.; Qi, J.; Cao, K.; Meng, Q.; Mustafa, A. K.; Mu, W.; Zhang, S.; Snyder, S. H.; Wang, R. *Science* **2008,** *322,* 587-590. (b) Zhao, Y.; Biggs, T. D.; Xian, M. *Chem. Commun.* **2014,** *50,* 11788-11805.

(6) Eto, K.; Asada, T.; Arima, K.; Makifuchi, T.; Kimura, H. *Bio-chem. Biophys. Res. Commun.* **2002,** *293,* 1485-1488.

(7) Kamoun, P.; Belardinelli, M.-C.; Chabli, A.; Lallouchi, K.; Chadefaux-Vekemans, B. *Am. J. Med. Genet.* **2003,** *116A,* 310-311.

(8) Yang, W.; Yang, G.; Jia, X.; Wu, L.; Wang, R. *J. Physiol.* **2005,** *569,* 519-531.

(9) Szabo, C.; Coletta, C.; Chao, C.; Modis, K.; Szczesny, B.; Papapetropoulos, A.; Hellmich, M. R. *Proc. Natl. Acad. Sci. U.S.A.* **2013,** *110,* 12474-12479.

(10) (a) Mao, G.-J.; Wei, T.-T.; Wang, X.-X.; Huan, S.-y.; Lu, D.-Q.; Zhang, J.; Zhang, X.-B.; Tan, W.; Shen, G.-L.; Yu, R.-Q. *Anal. Chem.* **2013,** *85,* 7875-7881. (b) Peng, H.; Chen, W.; Burroughs, S.; Wang, B. *Curr. Org. Chem.* **2013,** *17,* 641-653.

(11) Liu, C.; Pan, J.; Li, S.; Zhao, Y.; Wu, L. Y.; Berkman, C. E.; Whorton, A. R.; Xian, M. *Angew. Chem. Int. Ed.* **2011,** *50,* 10327-10329.

(12) Yu,F.; Hanab, X.; Chen, L. *Chem. Commun.* **2014,** *50,* 12234-12249.

(13) (a) Eddaoudi, M.; Kim, J.; Rosi, N.; Vodak, D.; Wachter, J.; Okeeffe, M.; Yaghi, O. M. *Science* **2002,** *295,* 469-472. (b) Takashima, Y.; Martinez, V. M.; Furukawa, S.; Konda, M.; Shimomura, S.; Uehara, H.; Nakahama, M.; Sugimoto, K.; Kitagawa, S. *Nat. Commun.* **2011,** 2:168 doi: 10.1038/ncomms1170. (c) Kreno, L. E.; Leong, K.; Farha, O. K.; Allendorf, M.; Duyne, R. P.; Hupp, J. T. *Chem. Rev.* **2012,** *112,* 1105-1125. (d)

Horcajada, P.; Gref, R.; Baati, T.; Allan, P. K.; Maurine, G.; Couvreur, P.; Ferey, G.; Morris, R.; Serre, C. *Chem. Rev.* **2012,** *112,* 1232-1268. (e) Kupller. R. J.; Timmons, D. J.; Fang, Q.-R.; Li, J. R.; Makal, T. A.; Young, M. D.; Yuan, D.; Zhao, D.; Zhuang, W.; Zhou, H.-C. *Coord. Chem. Rev.* **2009,** *253,* 3042-3066. (f) Nagarkar, S. S.; Desai, A. V.; Ghosh, S. K. *Chem. Asian J.* **2014,** *9,* 2358-2376. (g) Diring, S.; Wang, D. O.; Kim, C.; Kondo, M.; Chen, Y.; Kitagawa, S.; Kamei, K.-i.; Furukawa, S. *Nat. Commun.* **2013,** 4:2684 doi: 10.1038/ncomms3684. (h) Yoon, M.; Suh, K.; Natarajan, S.; Kim, K. *Angew. Chem. Int. Ed.* **2013,** *52,* 2688-2700.

(14) (a) Xiong, R.; Odbadrakh, K.; Michalkova, A.; Luna, J. P.; Petrova, T.; Keffer, D. J.; Nicholson, D. M.; Fuentes-Cabrera, M. A.; Lewis, J. P.; Leszczynski, J. *Sens. and Actuators B* **2010,** *148,* 459-468. (b) Wang, Z.; Cohen, S. M. *Chem. Soc. Rev.* **2009,** *38,* 1315-1329.

(15) (a) Hamon, L.; Serre, C.; Devic, T.; Loiseau, T.; Millange, F.; Férey, G.; Weireld, G. D. *J. Am. Chem. Soc.* **2009,** *131,* 8775-8777. (b) Petit, C.; Mendoza, B.; Bandosz, T. J. *ChemPhysChem* **2010,** *11,* 3678-3684. (c) Petit, C.; Bandosz, T. J. *Dalton Trans.* **2012,** *41,* 4027-4035. (d) Allan, P. K.; Wheatley, P. S.; Aldous, D.; Infas Mohideen, M.; Tang, C.; Hriljac, J. A.; Megson, I. L.; Chapman, K. W.; Weireld, G. D.; Vaesen, S.; Morris, R. E. *Dalton Trans.* **2012,** *41,* 4060-4066. (e) Gutierrez-Sevillano, J. J.; Martin-Calvo, A.; Dubbeldam, D.; Calero, S.; Hamad, S. *RSC Adv.* **2013,** *3,* 14737-14749. (f) Chavan, S.; Bonino, F.; Valenzano, L.; Civalleri, B.; Lamberti, C.; Acerbi, N,; Cavka, J. H.; Leistner, M.; Bordiga, S. *J. Phys. Chem. C* **2013,** *117,* 15615-15622. (g) Nickerl, G.; Leistner, M.; Helten, S.; Bon, V.; Senkovska, I.; Kaskel, S. *Inorg. Chem. Front.* **2014,** *1,* 325-330. (h) Liu, B.; Chen, Y. *Anal. Chem.* **2013,** *85,* 11020-11025. (i) Li, H.; Feng, X.; Guo, Y.; Chen, D.; Li, R.; Ren, X.; Jiang, X.; Dong, Y.; Wang, B. *Sci. Rep.* **2014,** 4, doi:10.1038/srep04366. (j) Liu, J.; Yee, K.-K.; Lo, K. K.-W.; Zhang, K. Y.; To, W.-P.; Che, C.-M.; Xu, Z. *J. Am. Chem. Soc.* **2014,** *136,* 2818-2824.

(16) Nagarkar, S. S.; Saha, T.; Desai, A. V.; Talukdar, P.; Ghosh, S. K. *Sci. Rep.* **2014,** DOI: 10.1038/srep07053.

(17) Montoya, L. A.; Pluth, M. D. *Chem. Commun.* **2012,** *48,* 4767-4769.

(18) (b) Kandiah, M.; Nilsen. M. H.; Usseglio, S.; Jakobsen, S.; Olsbye, U.; Tilset, M.; Larabi, C.; Quadrelli, E. A.; Bonino, F.; Lillerud, K. P. *Chem. Mater*. **2010,** *22*, 6632-6640. (b) Cavka, J. H.; Jakobsen, S.; Olsbye, U.; Guillou, N.; Lamberti, C.; Bordiga, S.; Lillerud, K. P. *J. Am. Chem. Soc.* **2008,** *130*, 13850-13851

(19) Garibay, S. J.; Cohen, S. M. *Chem. Commun.* **2010,** *46*, 7700-7702.

(20) Chen, Y.; Zhu, C.; Yang, Z.; Chen, J.; He, Y.; Jiao, Y.; He, W.; Qiu, L.; Cen, J.; Guo, Z. *Angew. Chem. Int. Ed.* **2013,** *52*, 1688-1691.

Appendix

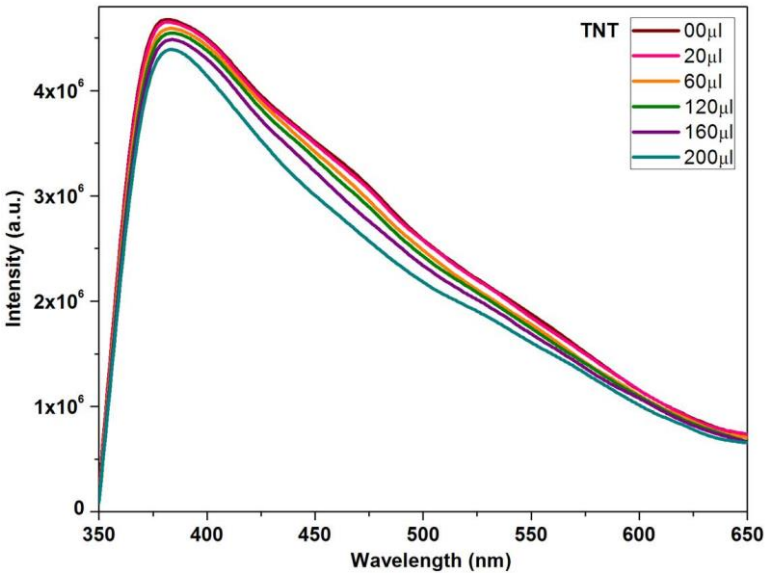

Figure 2.A1: Emission spectra of **1'** dispersed in MeCN upon incremental addition of TNT solution (1mM) in MeCN.

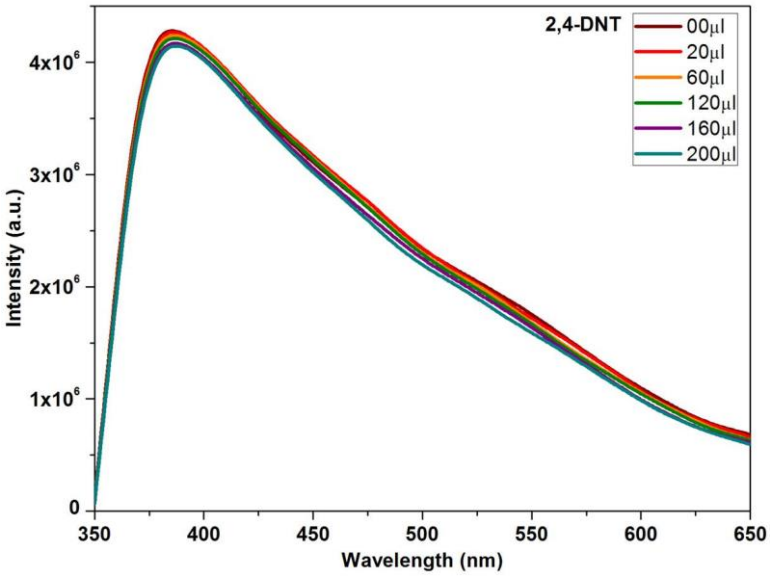

Figure 2.A2: Emission spectra of **1'** dispersed in MeCN upon incremental addition of 2,4-DNT solution (1mM) in MeCN.

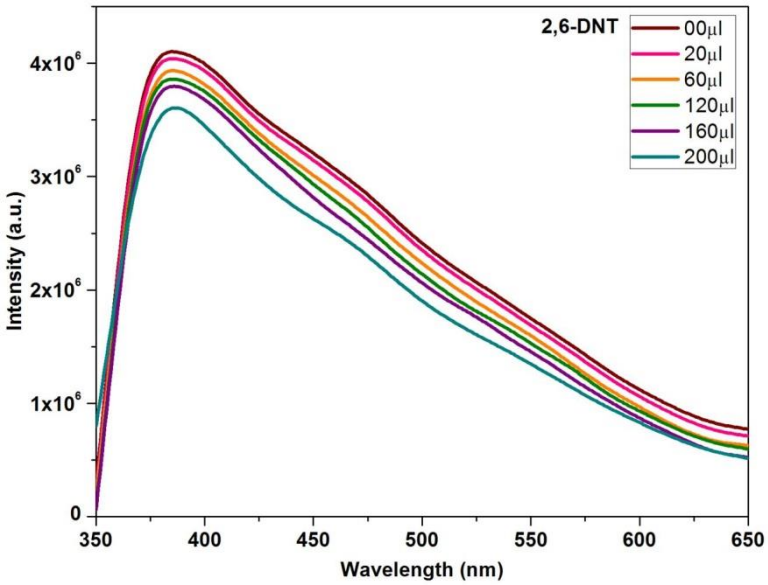

Figure 2.A3: Emission spectra of **1'** dispersed in MeCN upon incremental addition of 2,6-DNT solution (1mM) in MeCN.

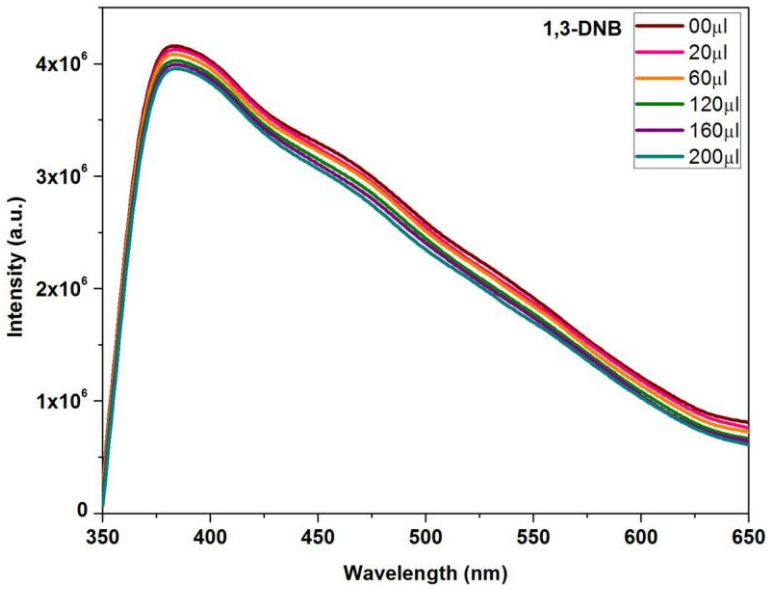

Figure 2.A4: Emission spectra of **1'** dispersed in MeCN upon incremental addition of 1,3-DNB solution (1mM) in MeCN.

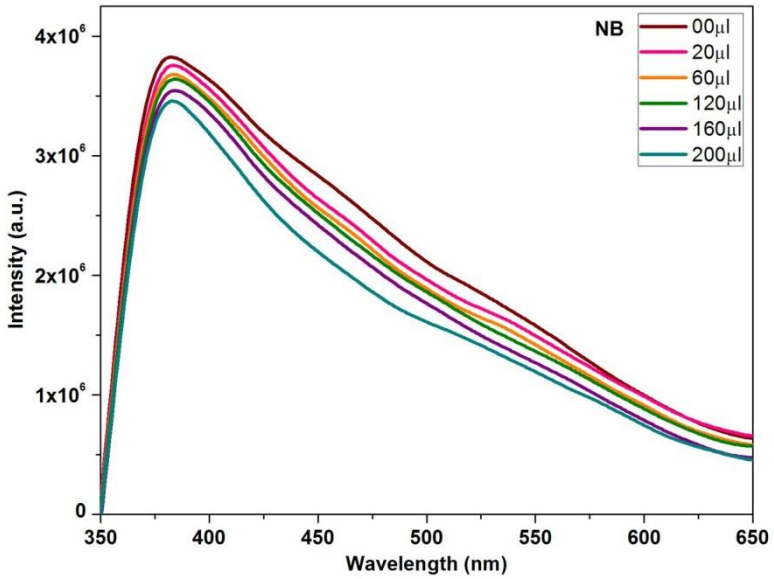

Figure 2.A5: Emission spectra of **1'** dispersed in MeCN upon incremental addition of NB solution (1mM) in MeCN.

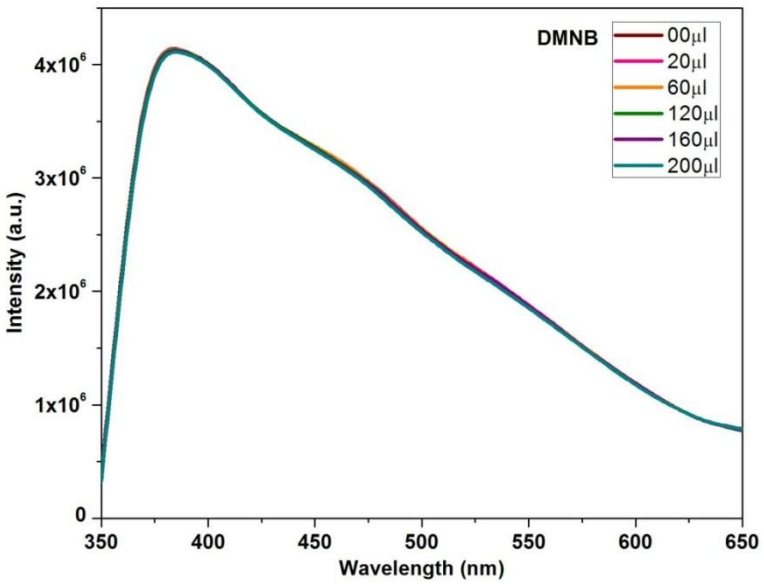

Figure 2.A6: Emission spectra of **1'** dispersed in MeCN upon incremental addition of DMNB solution (1mM) in MeCN.

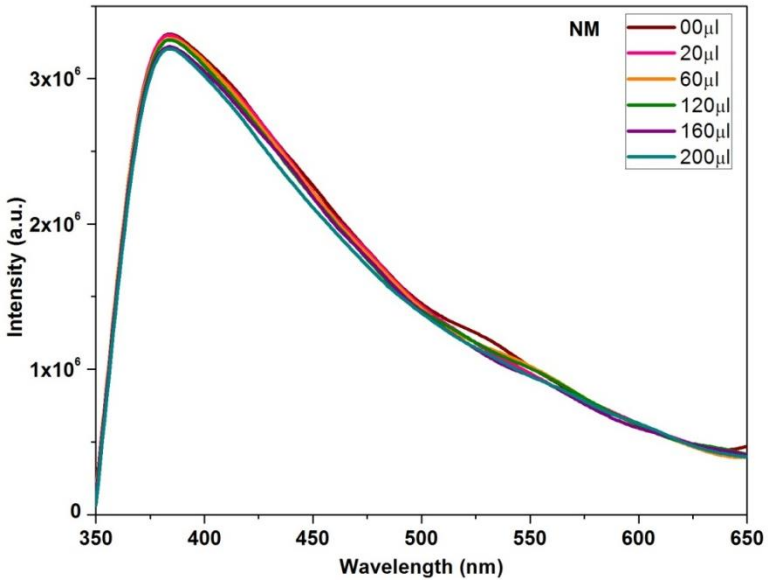

Figure 2.A7: Emission spectra of **1'** dispersed in MeCN upon incremental addition of NM solution (1mM) in MeCN.

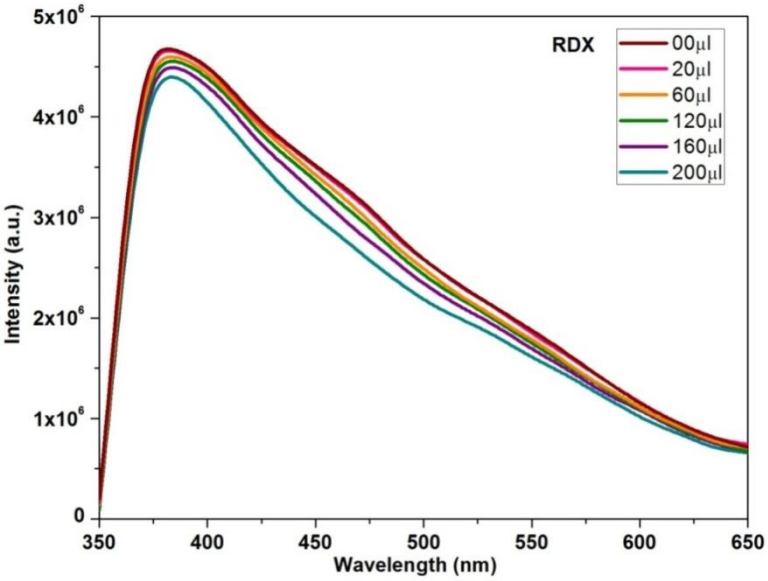

Figure 2.A8: Emission spectra of **1'** dispersed in MeCN upon incremental addition of RDX solution (1mM) in MeCN.

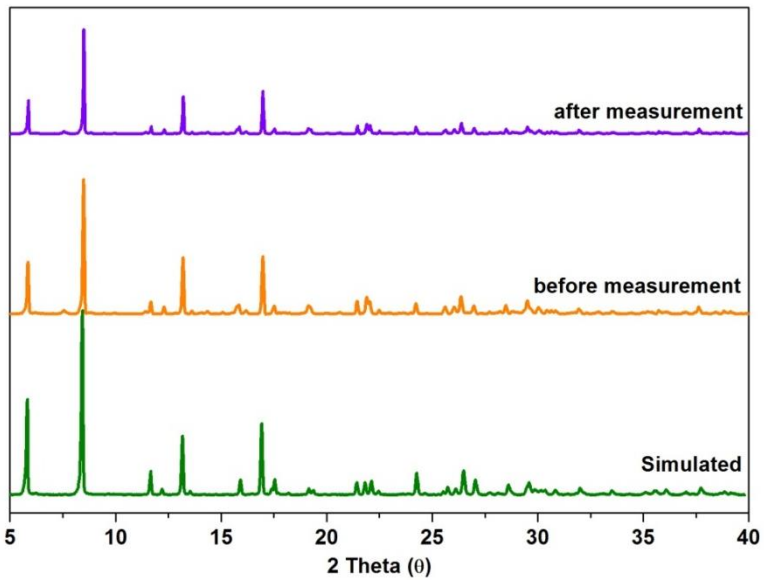

Figure 2.A9: PXRD pattern before and after water addition to **1'** dispersed in MeCN.

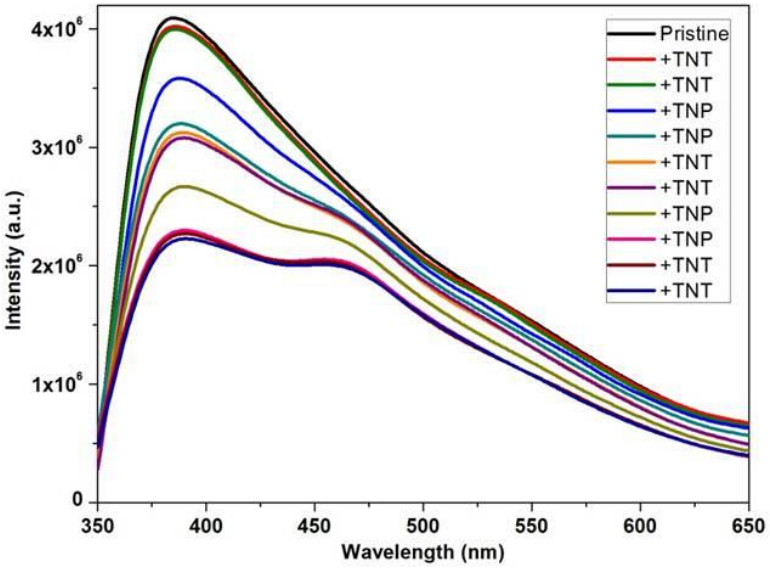

Figure 2.A10: Emission spectrum of **1'** in MeCN upon addition of aqueous solution of TNT followed by TNP (20µl addition each time).

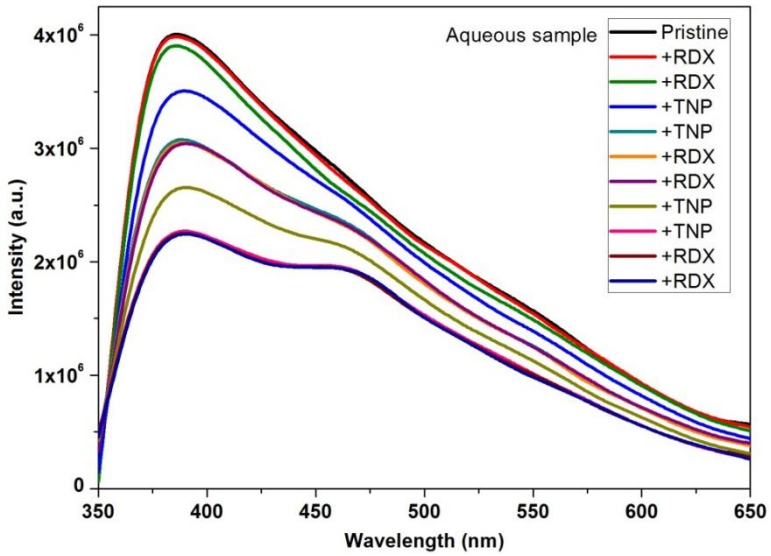

Figure 2.A11: Emission spectrum of **1'** in MeCN upon addition of aqueous solution of RDX followed by TNP (20µl addition each time).

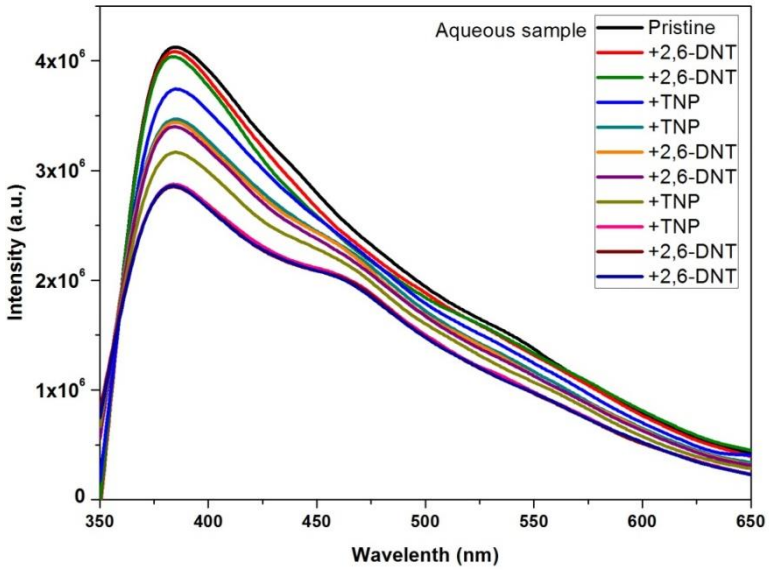

Figure 2.A12: Emission spectrum of **1'** in MeCN upon addition of aqueous solution of 2,6-DNT followed by TNP (20µl addition each time).

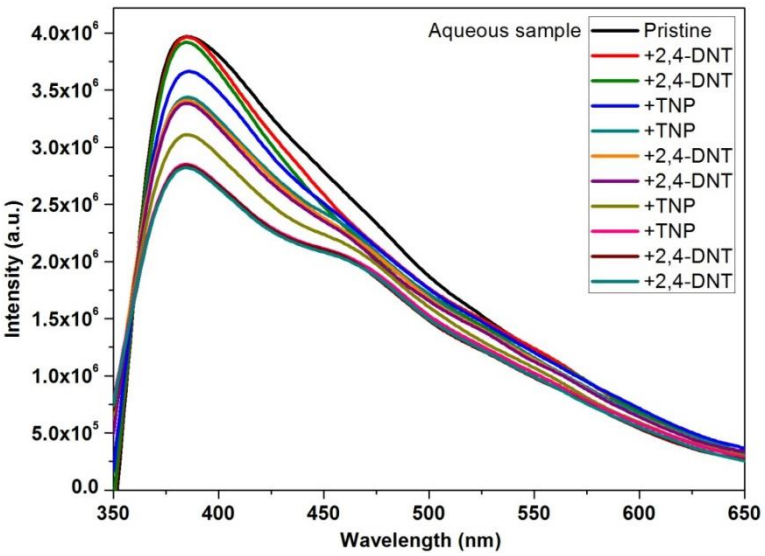

Figure 2.A13: Emission spectrum of **1'** in MeCN upon addition of aqueous solution of 2,4-DNT followed by TNP (20µl addition each time).

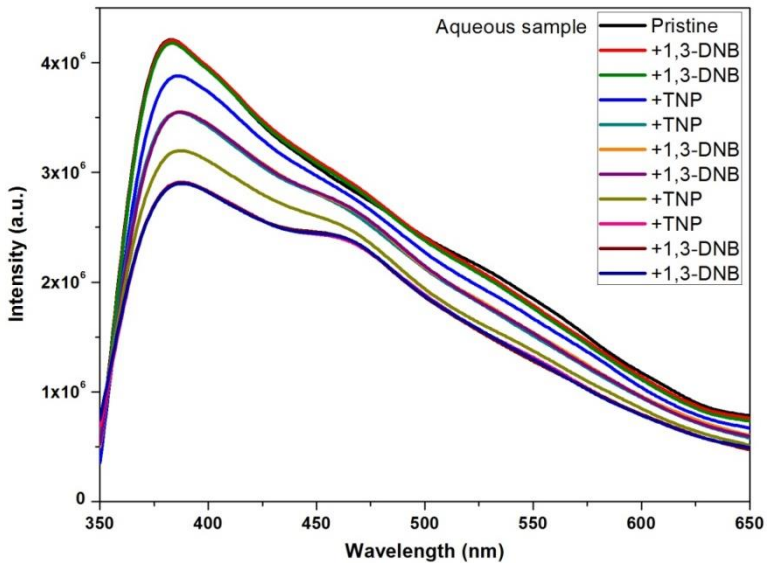

Figure 2.A14: Emission spectrum of **1'** in MeCN upon addition of aqueous solution of 1,3-DNB followed by TNP (20µl addition each time).

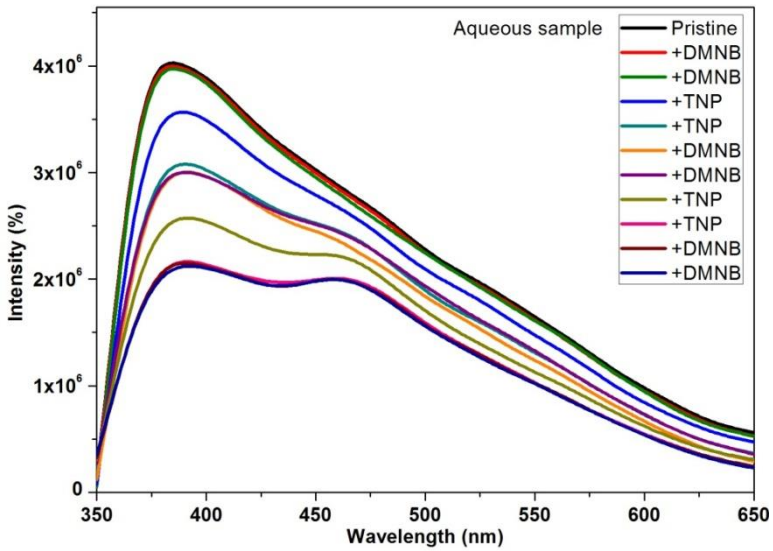

Figure 2.A15: Emission spectrum intensity of **1'** in MeCN upon addition of aqueous solution of DMNB followed by TNP (20µl addition each time).

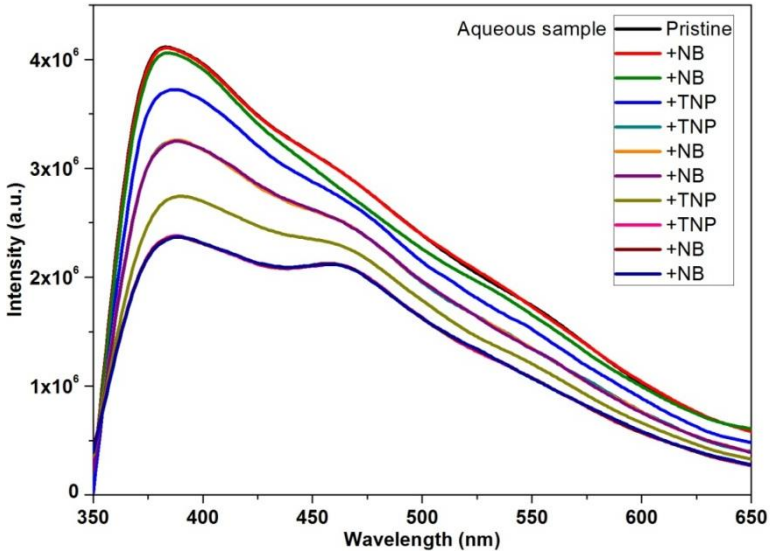

Figure 2.A16: Emission spectrum intensity of **1'** in MeCN upon addition of aqueous solution of NB followed by TNP (20µl addition each time).

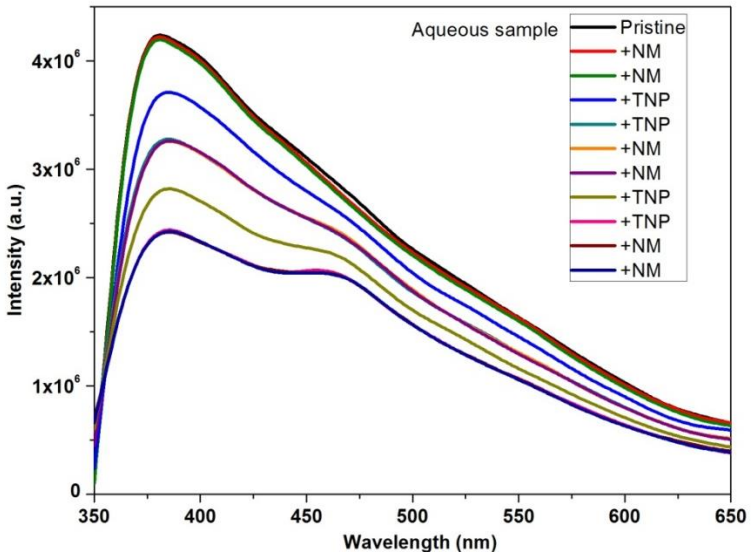

Figure 2.A17: Emission spectrum of **1'** in MeCN upon addition of aqueous solution of NM followed by TNP (20µl addition each time).

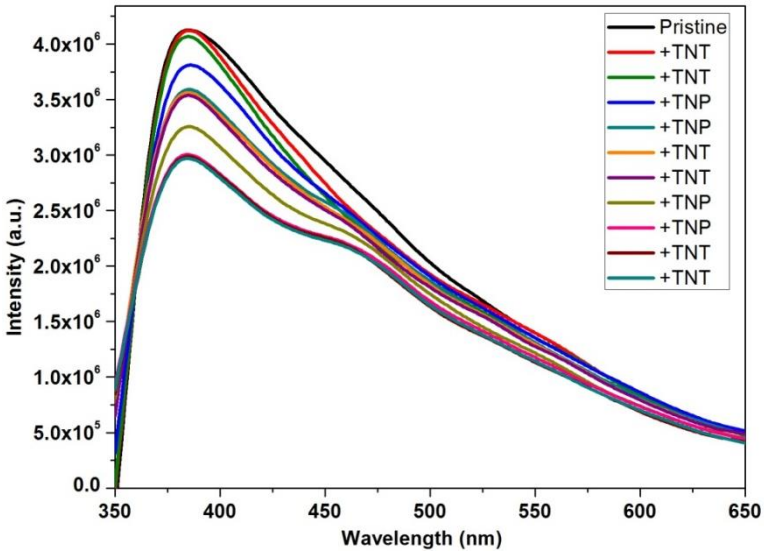

Figure 2.A18: Emission spectrum of **1'** in MeCN upon addition of MeCN solution of TNT followed by TNP (20µl addition each time).

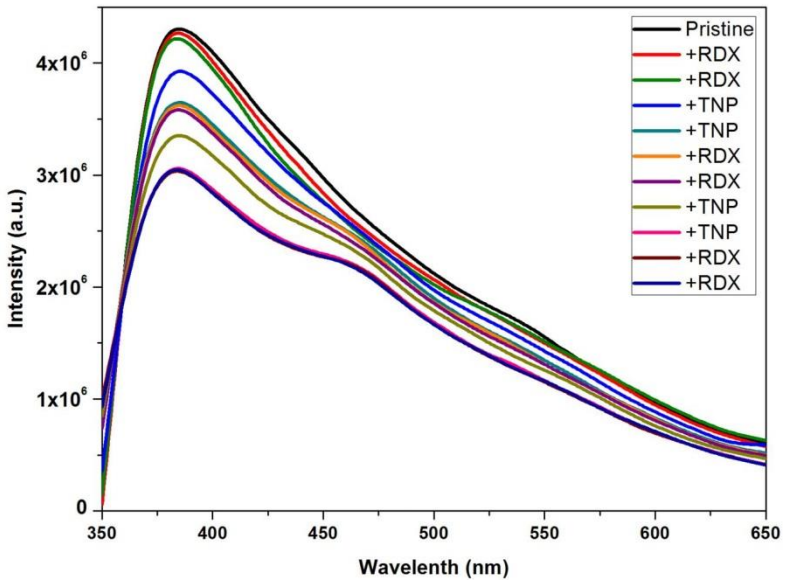

Figure 2.A19: Emission spectrum of **1'** in MeCN upon addition of MeCN solution of RDX followed by TNP (20µl addition each time).

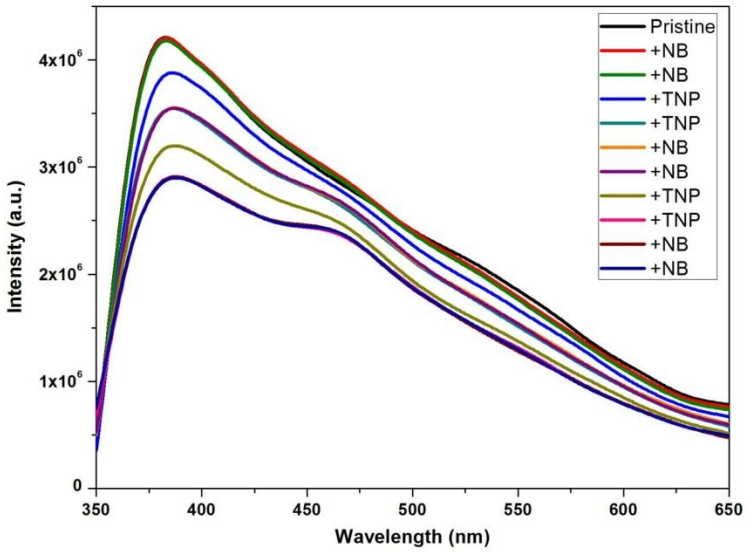

Figure 2.A20: Emission spectrum of **1'** in MeCN upon addition of MeCN solutions of NB followed by TNP (20µl addition each time)

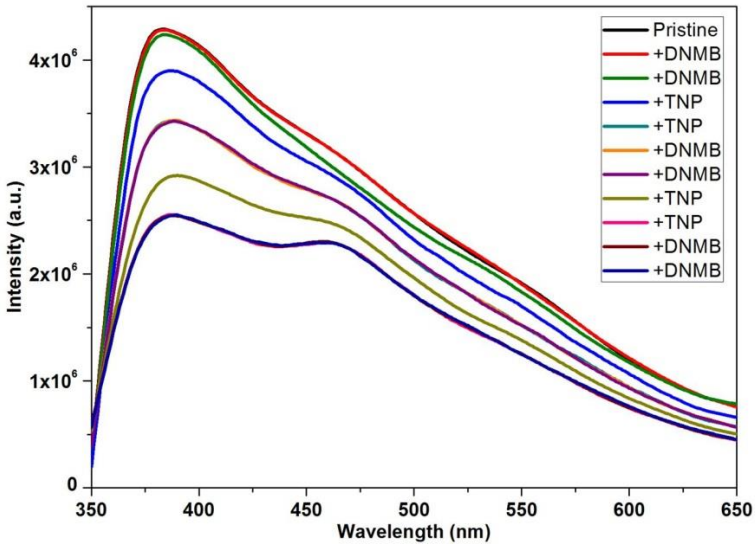

Figure 2.A21: Emission spectrum of **1'** in MeCN upon addition of MeCN solution of DMNB followed by TNP (20µl addition each time).

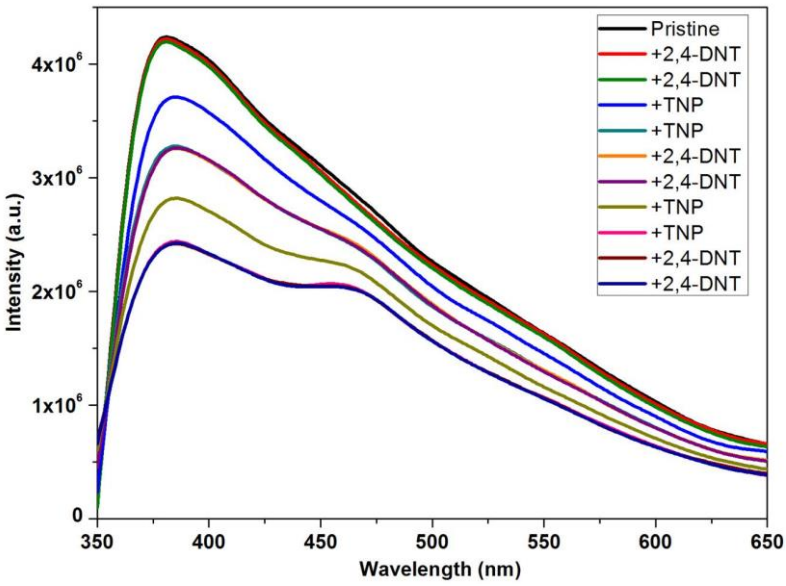

Figure 2.A22: Emission spectrum of **1'** in MeCN upon addition of MeCN solution of 2,4-DNT followed by TNP (20µl addition each time).

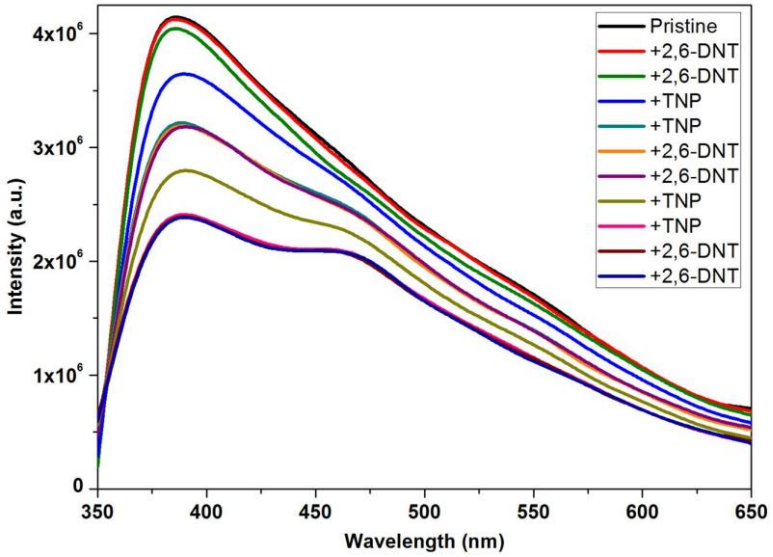

Figure 2.A23: Emission spectrum of **1'** in MeCN upon addition of MeCN solution of 2,6-DNT followed by TNP (20µl addition each time).

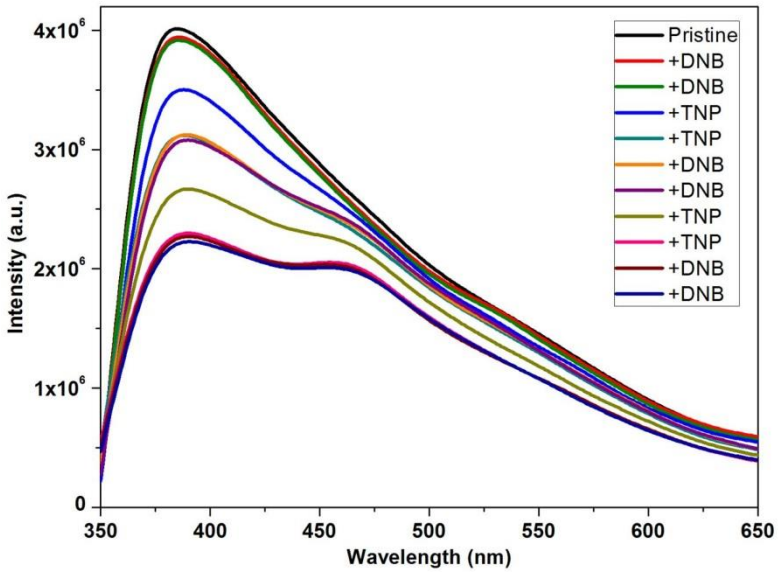

Figure 2.A24: Emission spectrum of **1'** in MeCN upon addition of MeCN solution of 1,3-DNB followed by TNP (20µl addition each time).

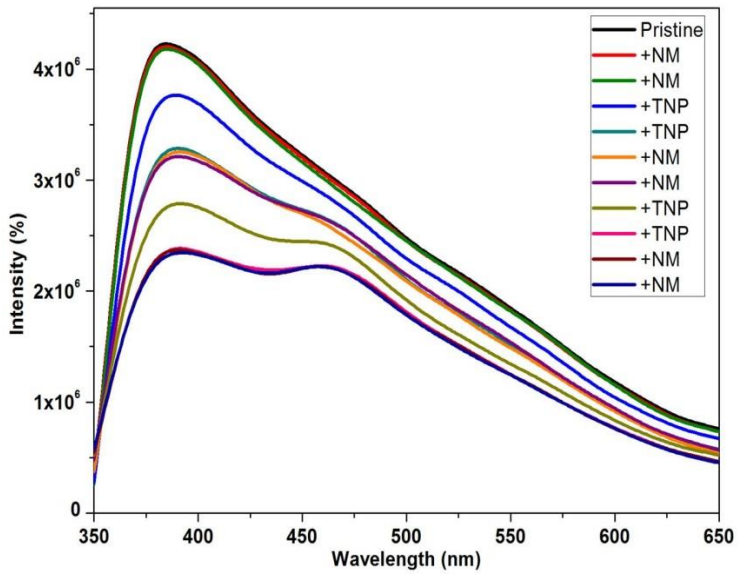

Figure 2.A25: Emission spectrum of **1'** in MeCN upon addition of MeCN solutions of NM followed by TNP (20µl addition each time).

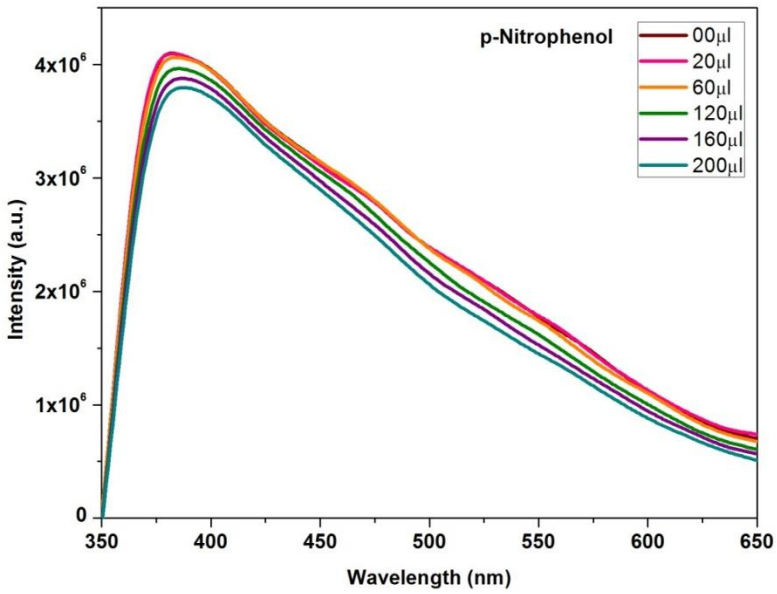

Figure 2.A26: Emission spectra of **1'** dispersed in MeCN upon incremental addition of NP solution (1mM) in MeCN.

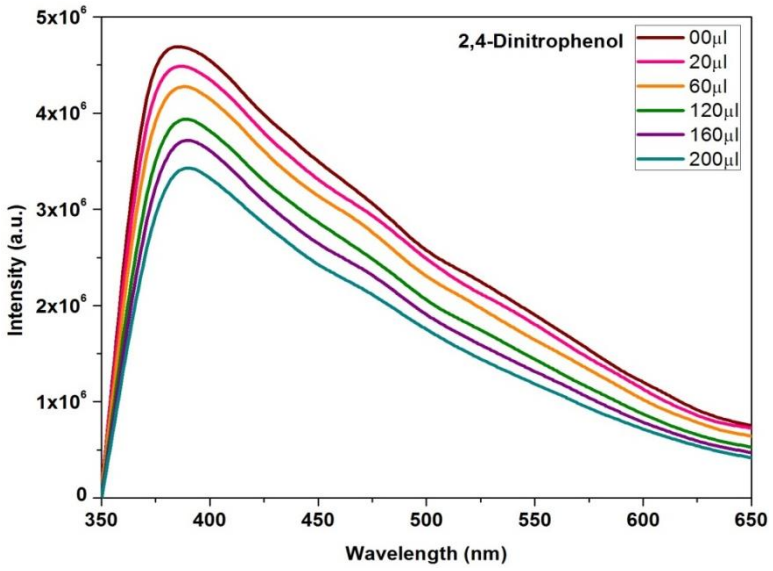

Figure 2.A27: Emission spectra of **1'** dispersed in MeCN upon incremental addition of 2,4-DNP solution (1mM) in MeCN.

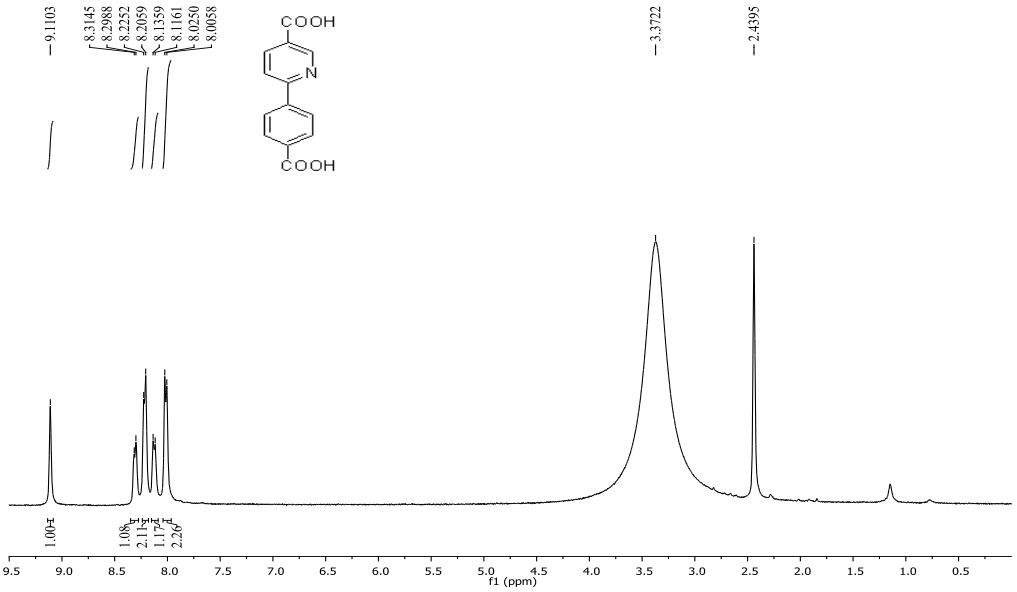

Figure 3A.A1: ^{1}H NMR of $H_2\mathbf{L_3}$ in DMSO-d^{6}.

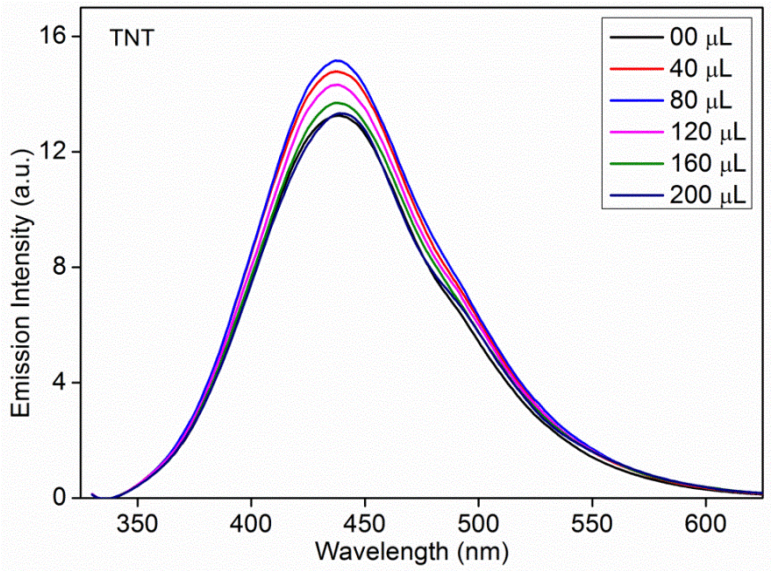

Figure 3A.A2: Emission spectra of **2'** dispersed in water upon incremental addition of TNT solution (1mM) in water.

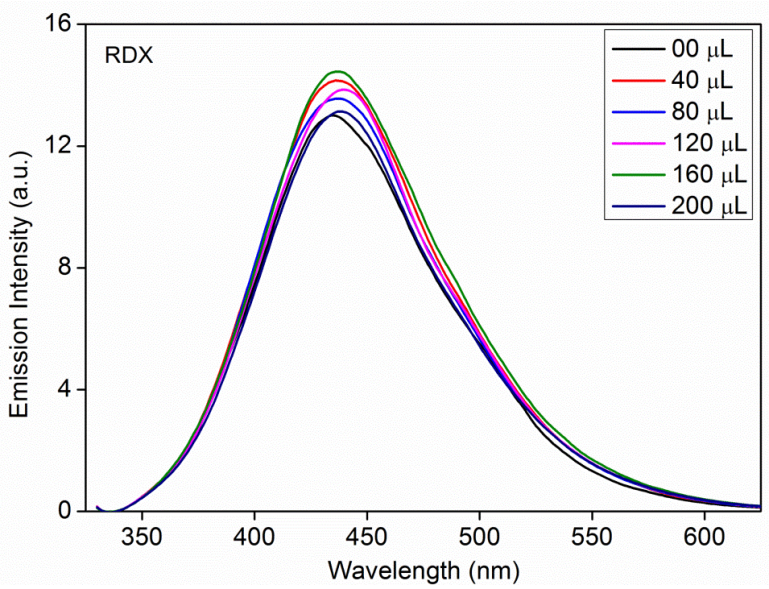

Figure 3A.A3 Emission spectra of **2'** dispersed in water upon incremental addition of RDX solution (1mM) in water.

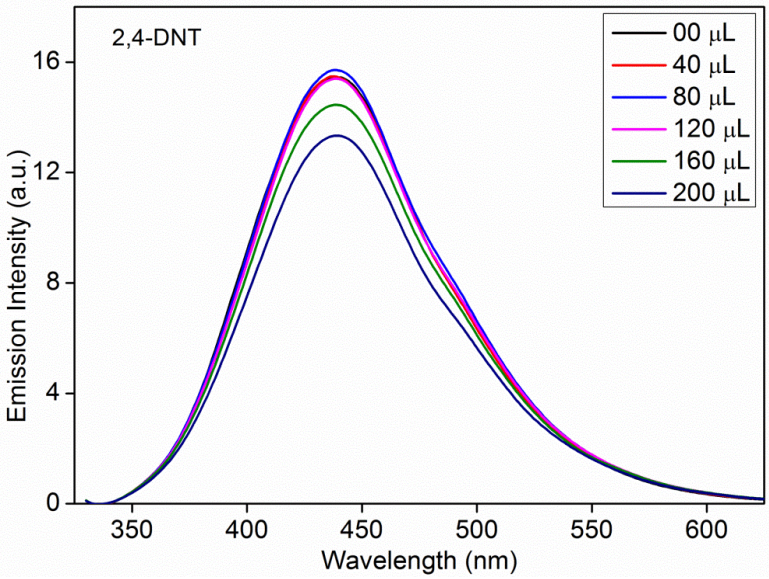

Figure 3A.A4: Emission spectra of **2'** dispersed in water upon incremental addition of 2,4-DNT solution (1mM) in water.

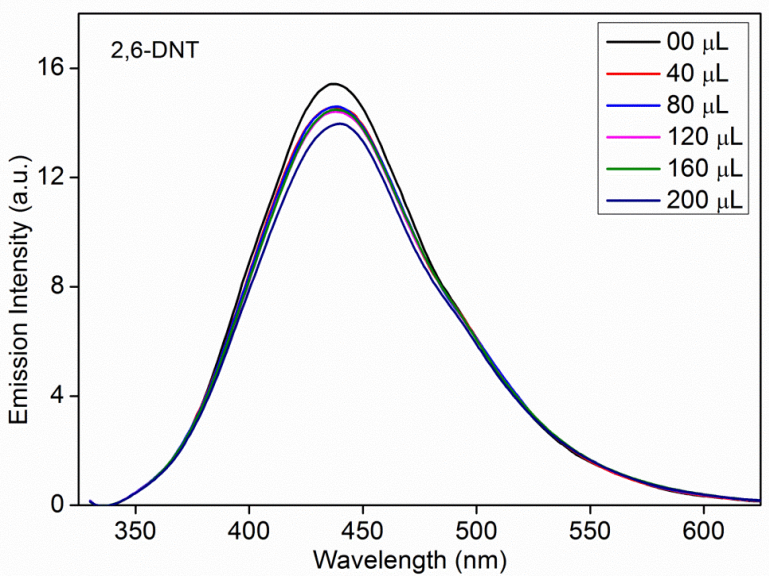

Figure 3A.A5: Emission spectra of **2'** dispersed in water upon incremental addition of 2,6-DNT solution (1mM) in water.

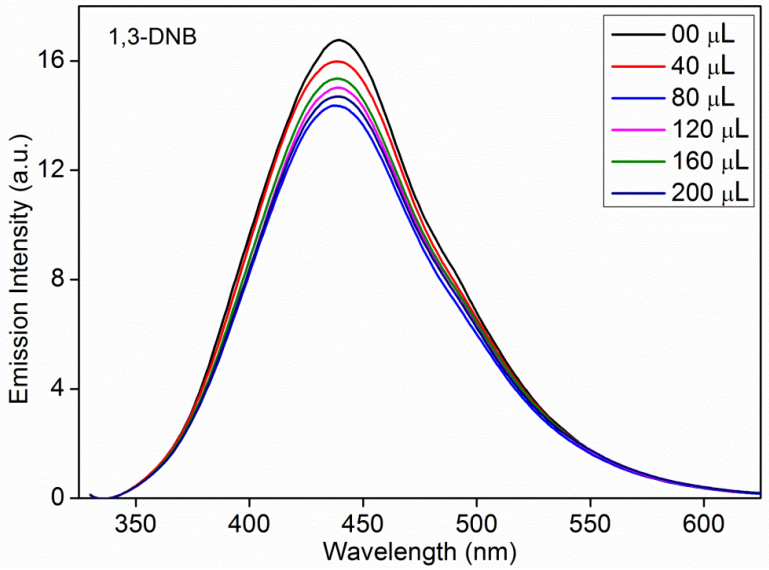

Figure 3A.A6: Emission spectra of **2'** dispersed in water upon incremental addition of 1,3-DNB solution (1mM) in water.

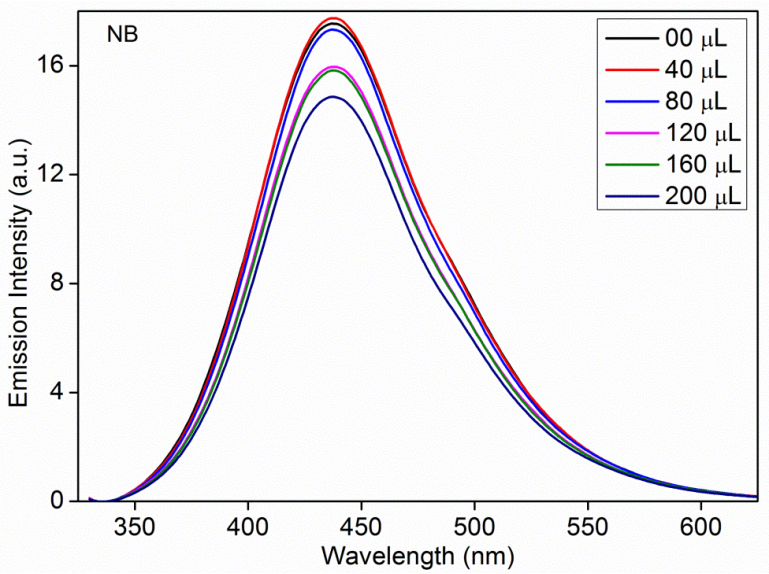

Figure 3A.A7: Emission spectra of **2'** dispersed in water upon incremental addition of NB solution (1mM) in water.

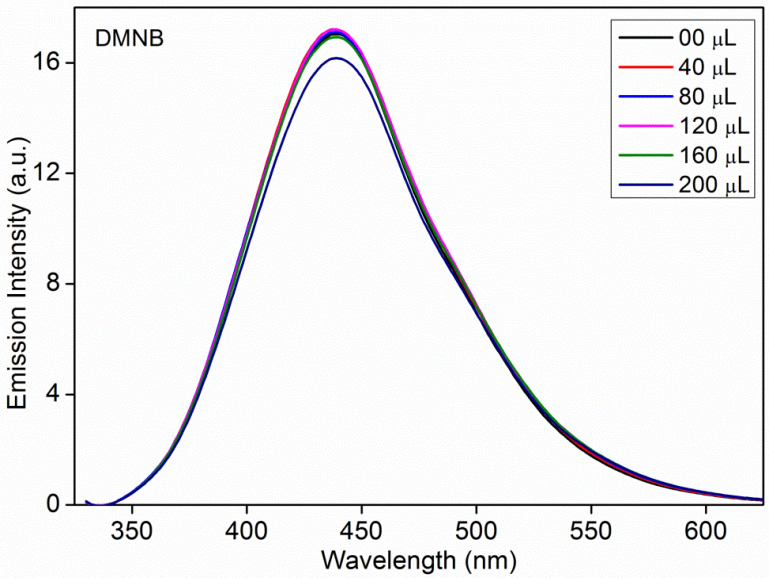

Figure 3A.A8: Emission spectra of **2'** dispersed in water upon incremental addition of DMNB solution (1mM) in water.

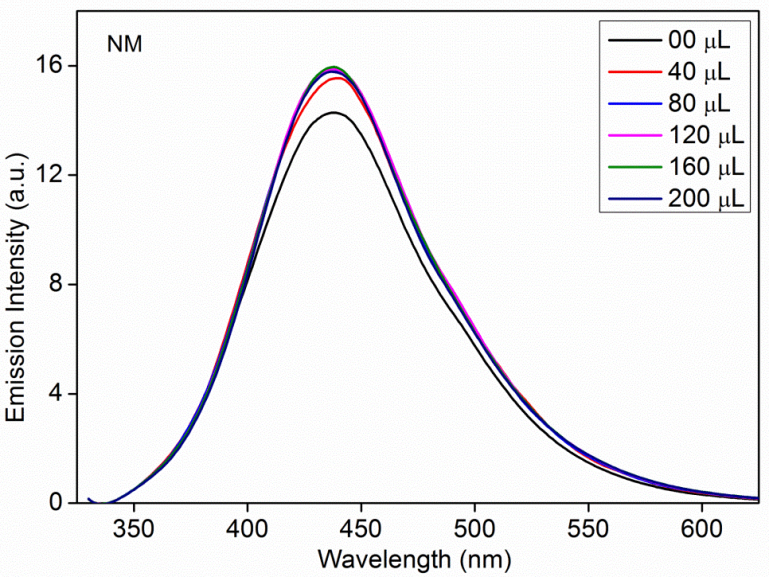

Figure 3A.A9: Emission spectra of **2'** dispersed in water upon incremental addition of NM solution (1mM) in water.

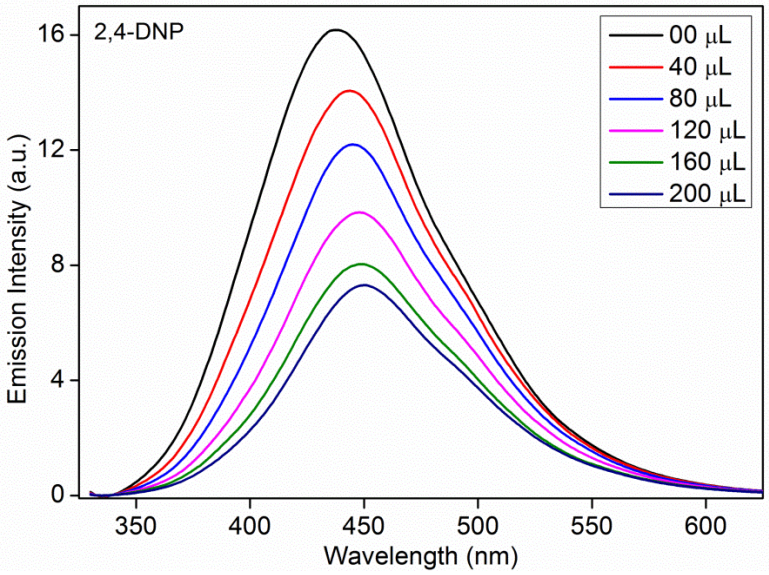

Figure 3A.A10: Emission spectra of **1'** dispersed in water upon incremental addition of 2,4-DNP solution (1mM) in water.

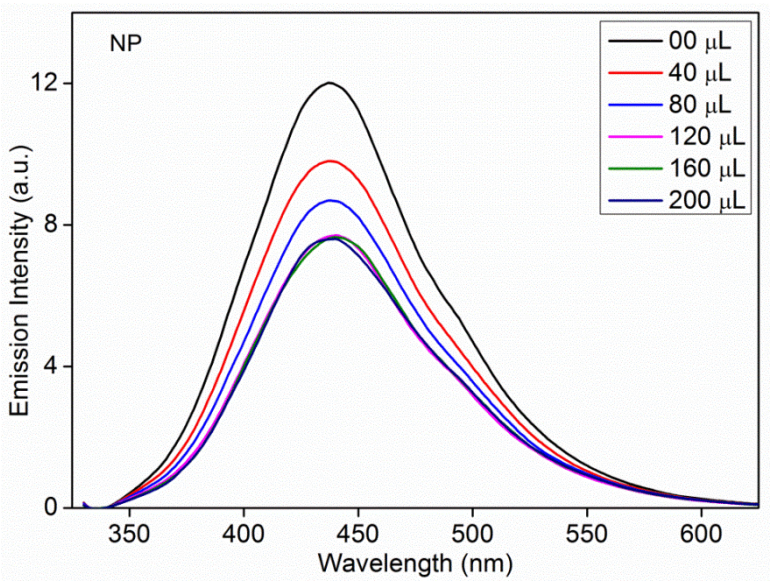

Figure 3A.A11: Emission spectra of **1'** dispersed in water upon incremental addition of NP solution (1mM) in water.

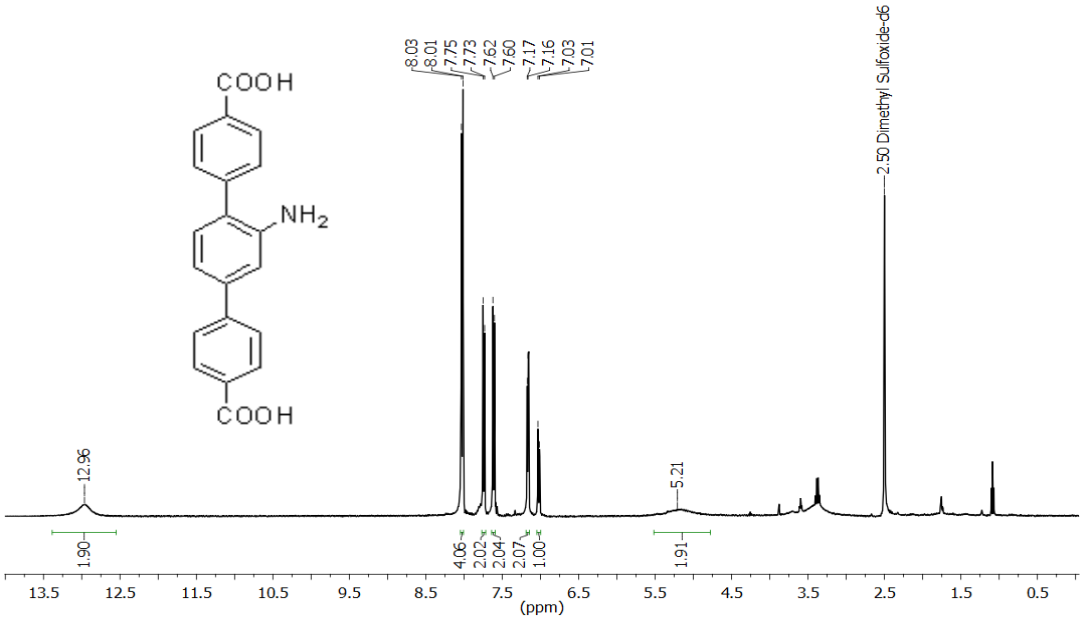

Figure 3B.A1: ^{1}H NMR of ligand $H_2\mathbf{L_4}$ in DMSO-d^{6}.

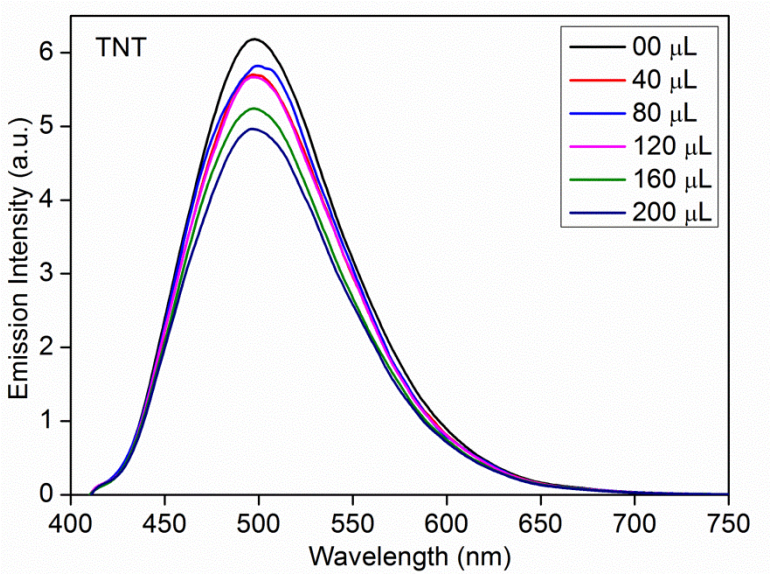

Figure 3B.A2: Emission spectra of **3'** dispersed in water upon incremental addition of TNT solution (1mM) in water.

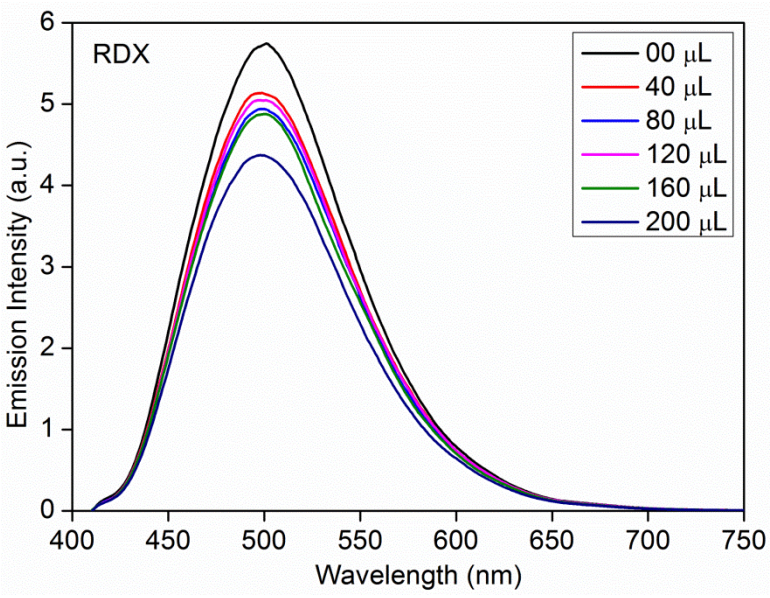

Figure 3B.A3: Emission spectra of **3'** dispersed in water upon incremental addition of RDX solution (1mM) in water.

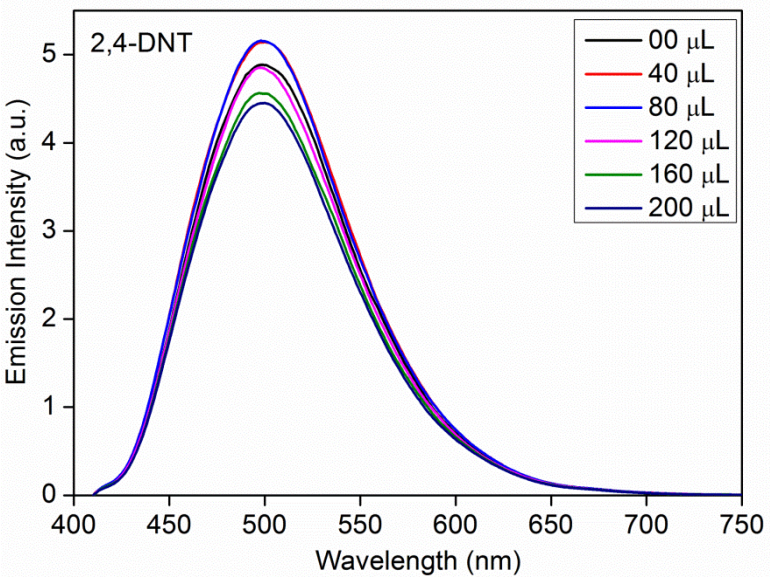

Figure 3B.A4: Emission spectra of **3'** dispersed in water upon incremental addition of 2,4-DNT solution (1mM) in water.

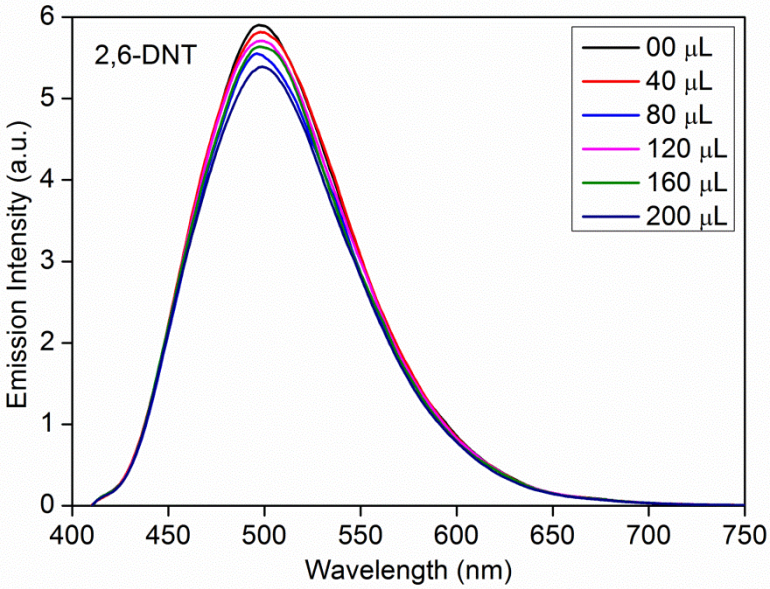

Figure 3B.A5: Emission spectra of **3'** dispersed in water upon incremental addition of 2,6-DNT solution (1mM) in water.

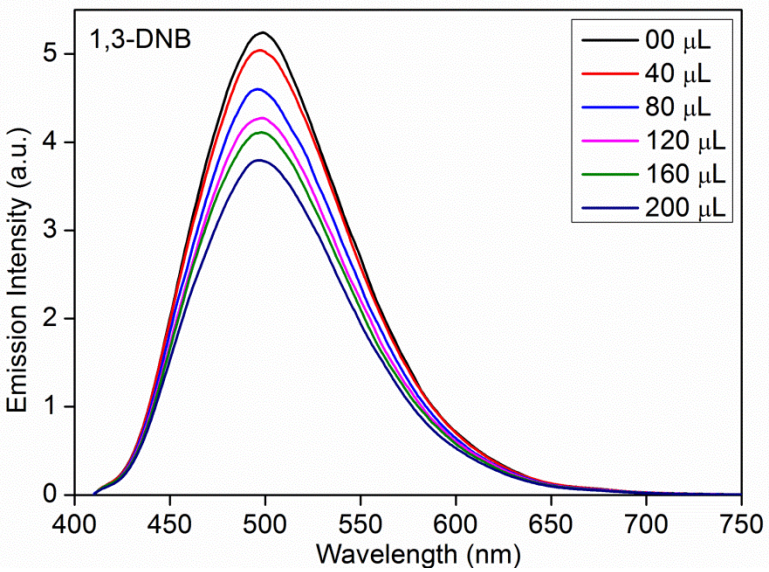

Figure 3B.A6: Emission spectra of **3'** dispersed in water upon incremental addition of 1,3-DNB solution (1mM) in water.

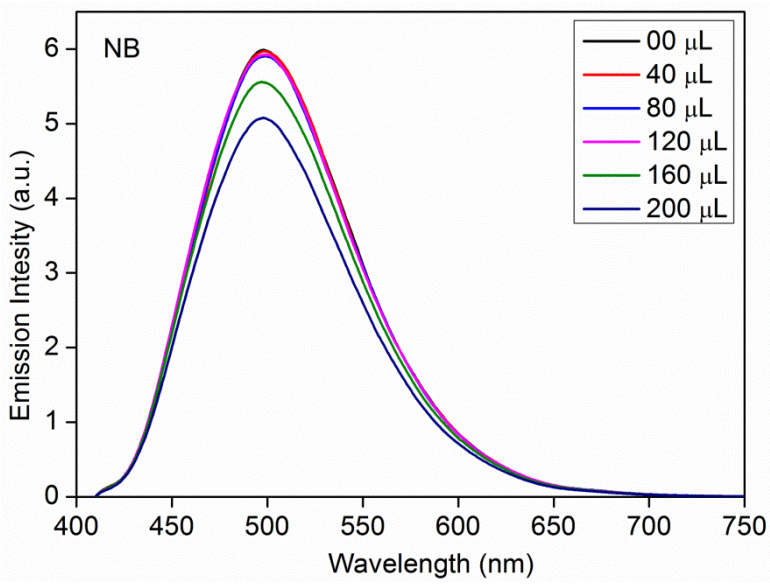

Figure 3B.A7: Emission spectra of **3'** dispersed in water upon incremental addition of NB solution (1mM) in water.

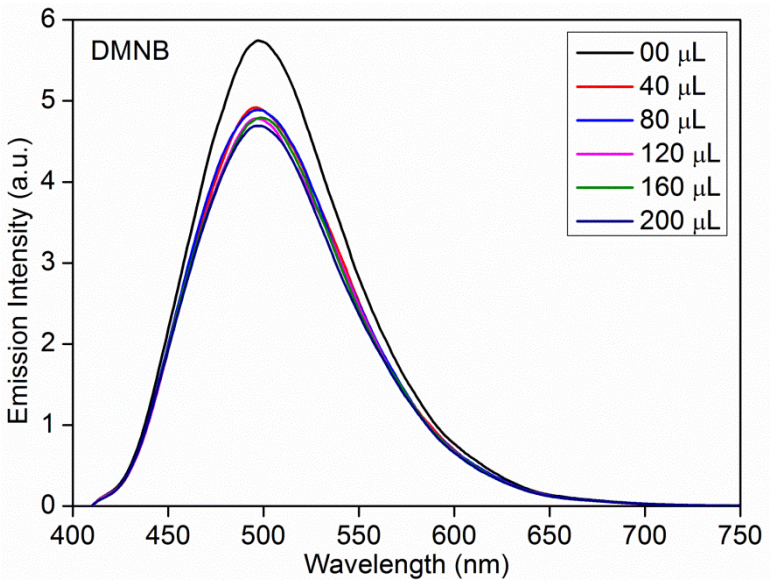

Figure 3B.A8: Emission spectra of **3'** dispersed in water upon incremental addition of DMNB solution (1mM) in water.

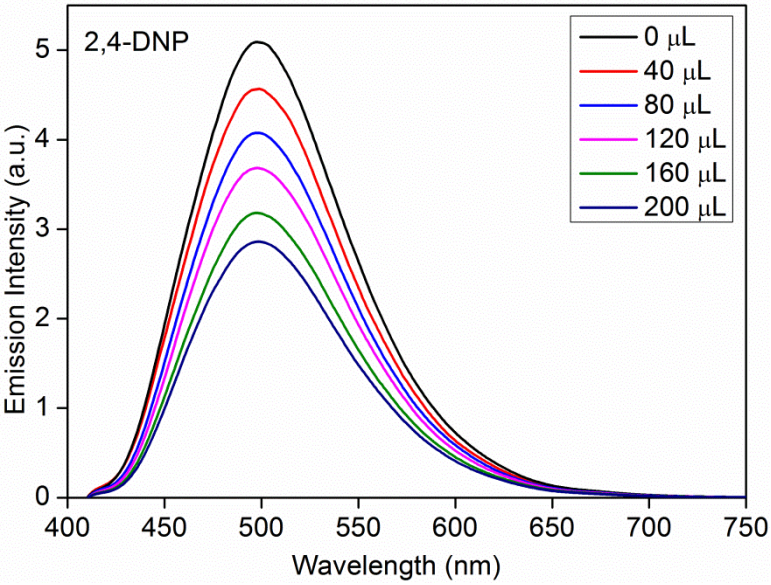

Figure 3B.A9: Emission spectra of **3'** dispersed in water upon incremental addition of 2,4-DNP solution (1mM) in water.

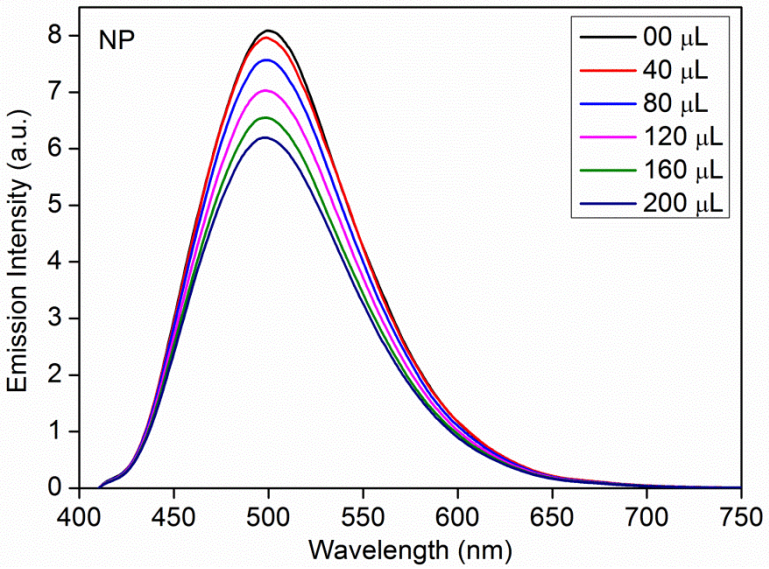

Figure 3B.A10: Emission spectra of **3'** dispersed in water upon incremental addition of NP solution (1mM) in water.

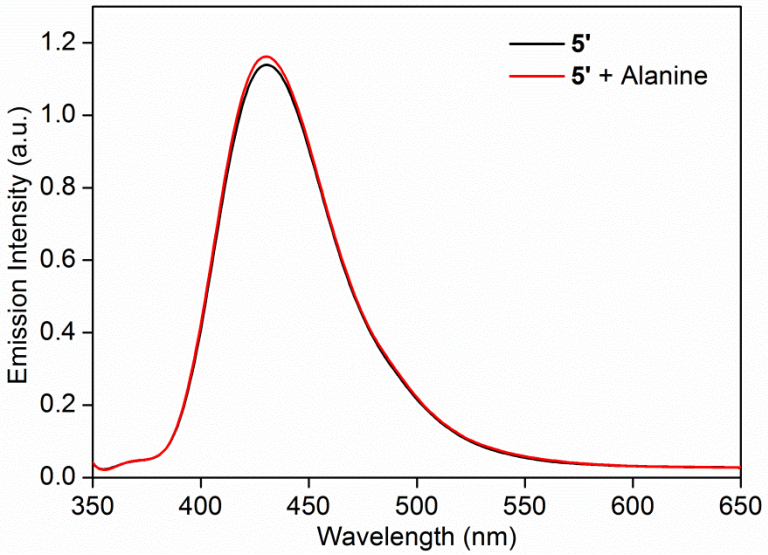

Figure 4A.A1: Fluorescence response of **5'** before and after addition of Alanine.

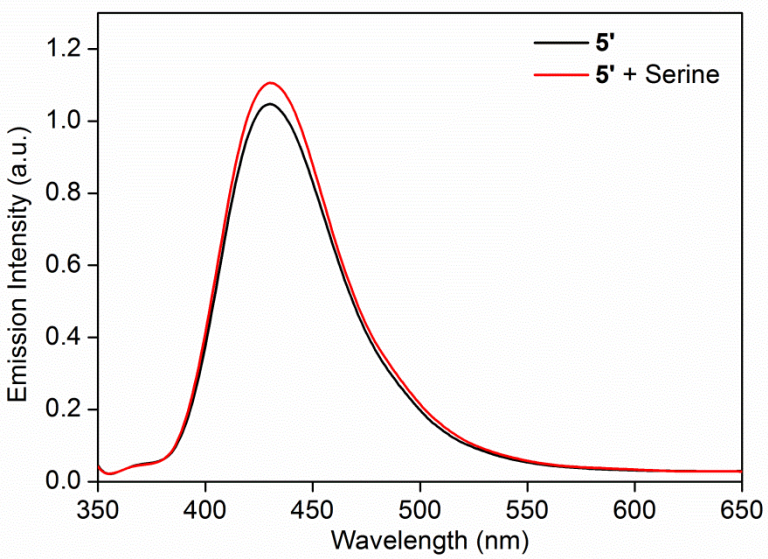

Figure 4A.A2: Fluorescence response of **5'** before and after addition of Serine.

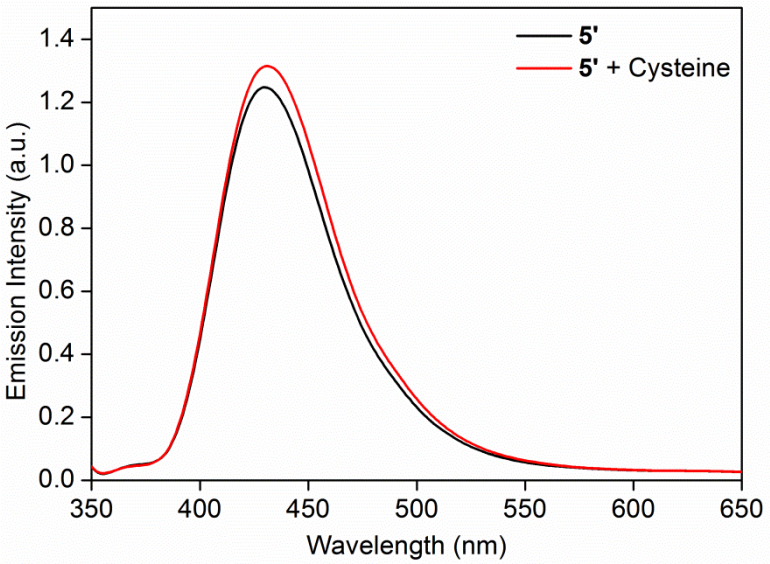

Figure 4A.A3: Fluorescence response of **5'** before and after addition of Cysteine.

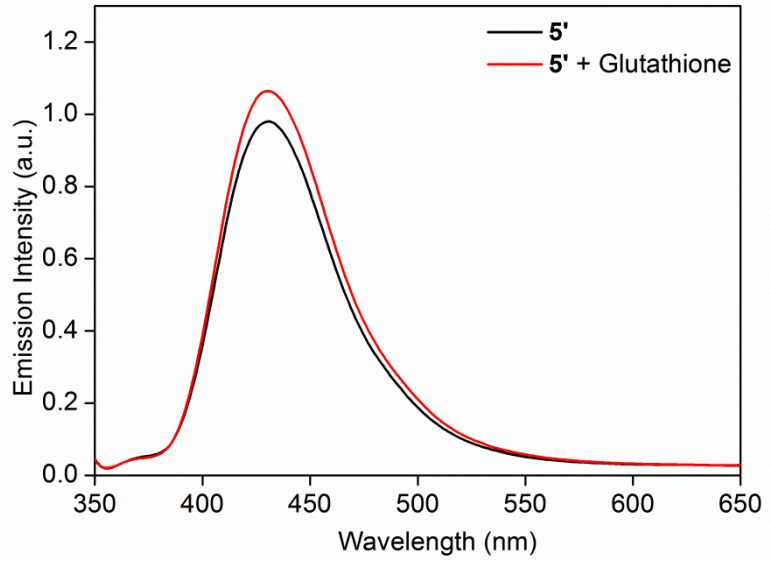

Figure 4A.A4: Fluorescence response of **5'** before and after addition of Glutathione.

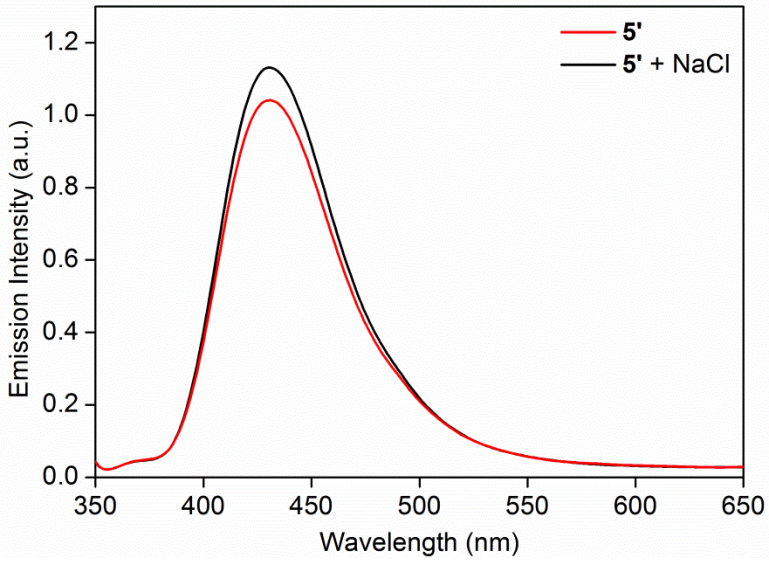

Figure 4A.A5: Fluorescence response of **5'** before and after addition of NaCl.

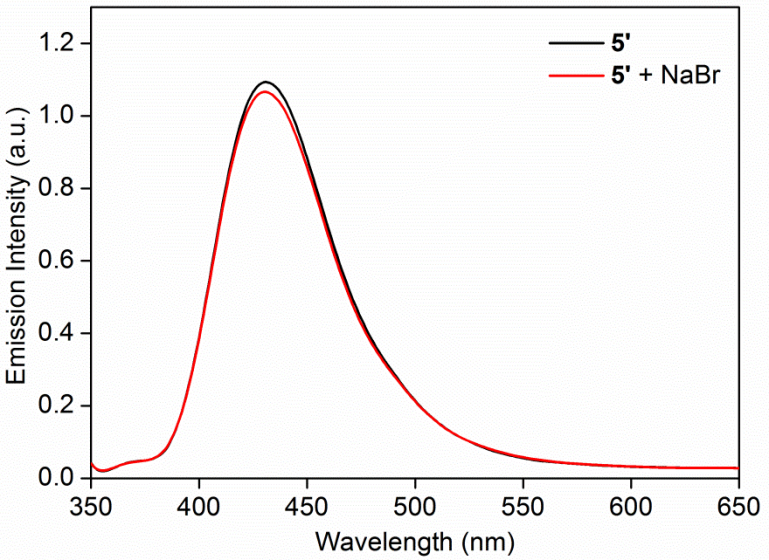

Figure 4A.A6: Fluorescence response of **5'** before and after addition of NaBr.

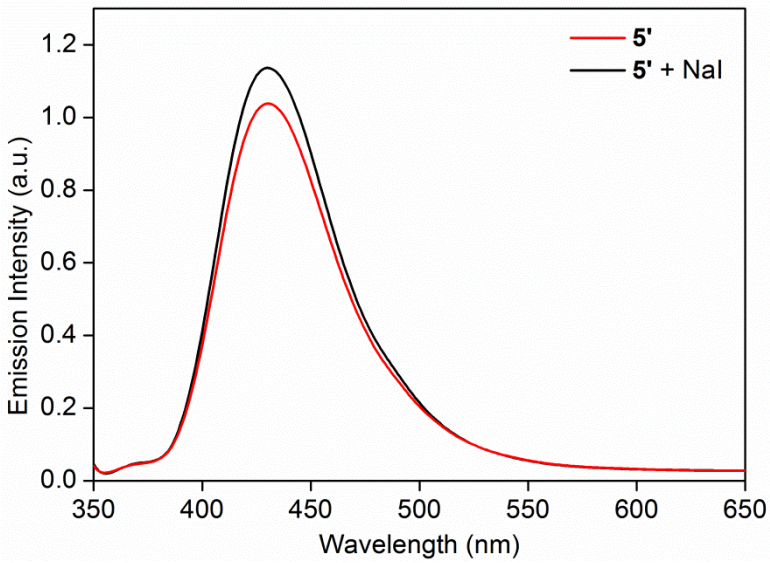

Figure 4A.A7: Fluorescence response of **5'** before and after addition of NaI.

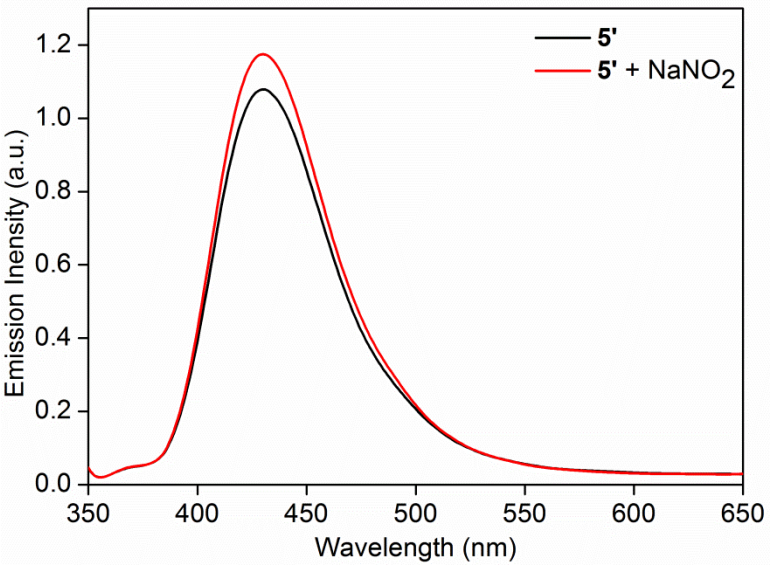

Figure 4A.A8: Fluorescence response of **5'** before and after addition of $NaNO_2$.

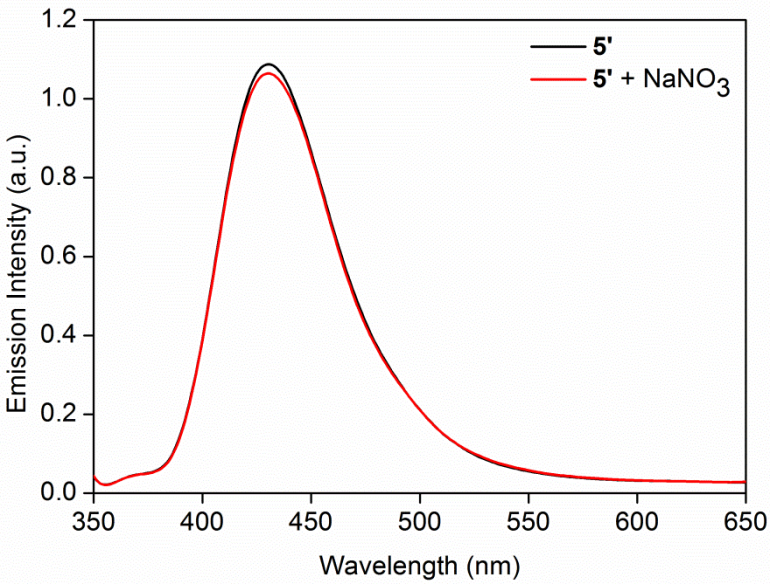

Figure 4A.A9: Fluorescence response of **5'** before and after addition of $NaNO_3$.

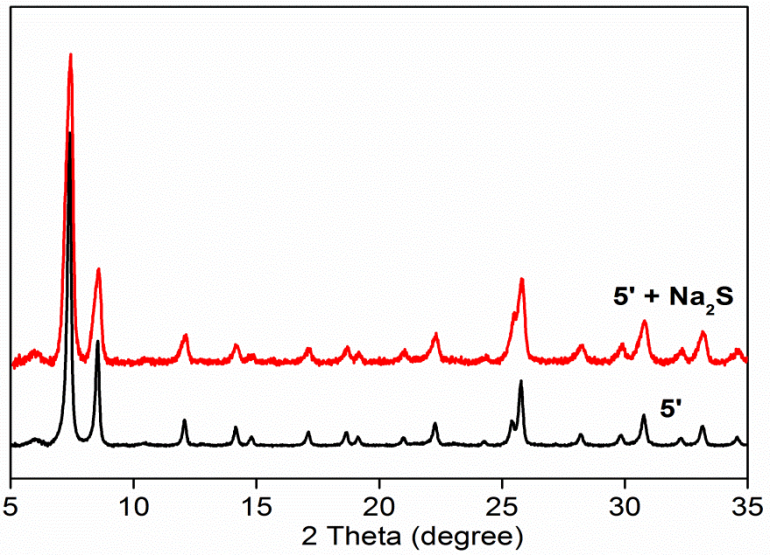

Figure 4A.A10: Comparison of PXRD patterns of **5'** and **5'** upon treatment with Na_2S.

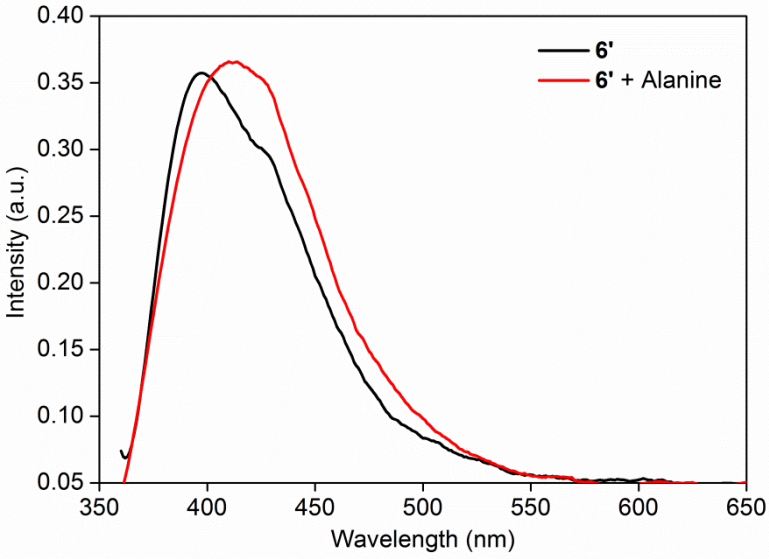

Figure 4B.A1: Fluorescence response of **6'** before and after addition of Alanine.

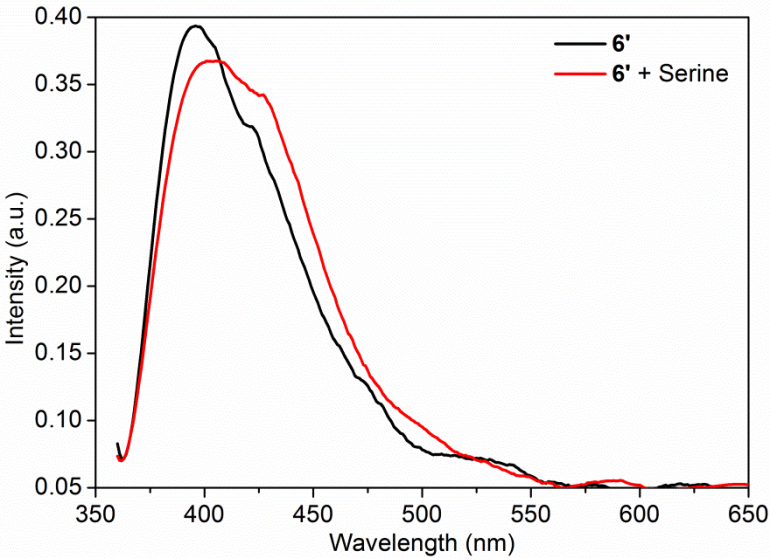

Figure 4B.A2: Fluorescence response of **6'** before and after addition of Serine.

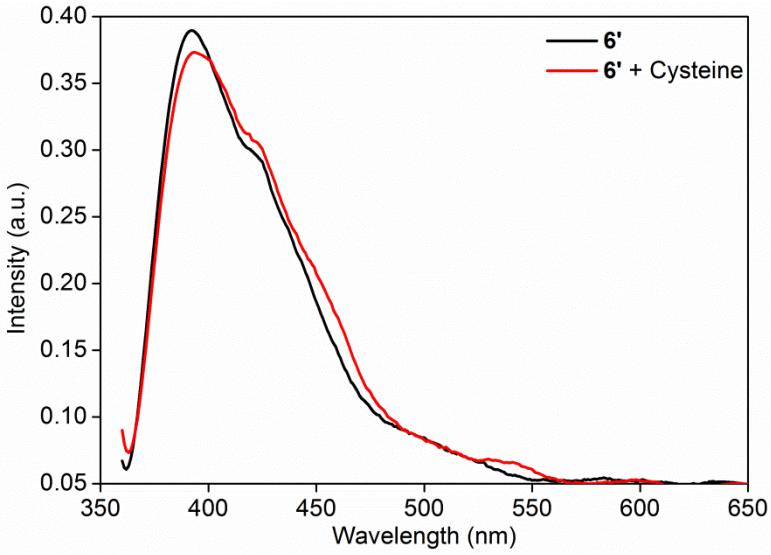

Figure 4B.A3: Fluorescence response of **6'** before and after addition of Cysteine.

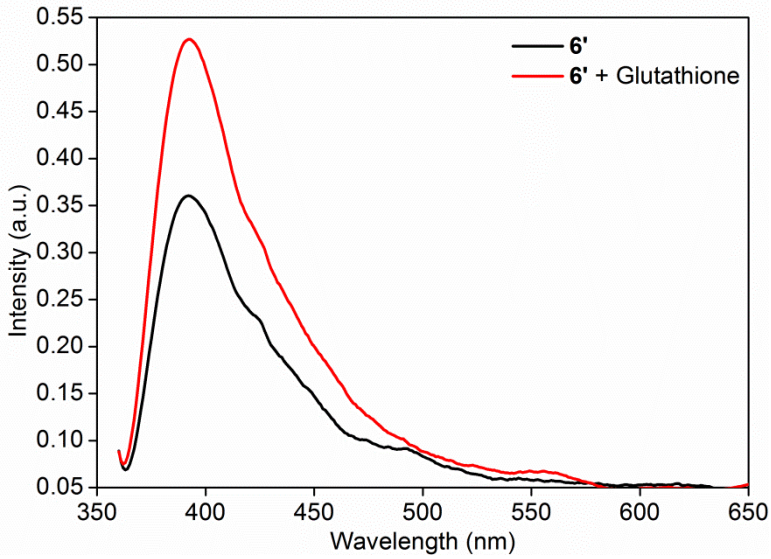

Figure 4B.A4: Fluorescence response of **6'** before and after addition of Glutathione.

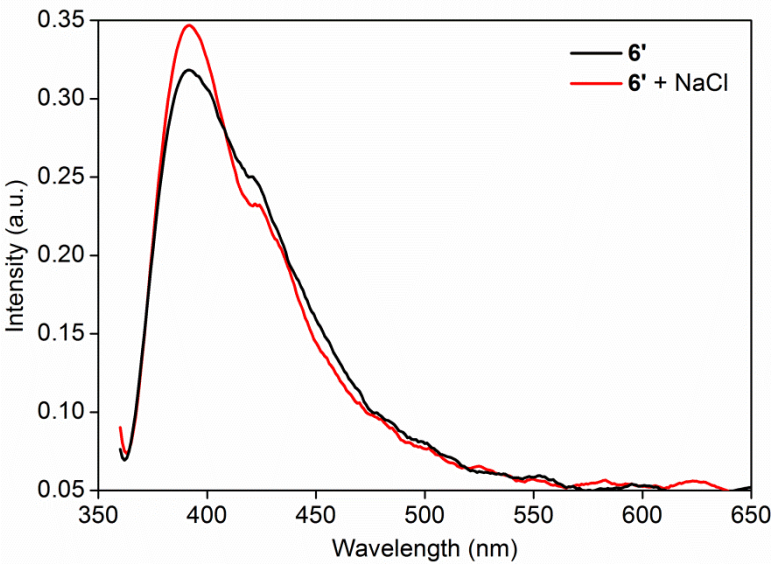

Figure 4B.A5: Fluorescence response of **6'** before and after addition of NaCl.

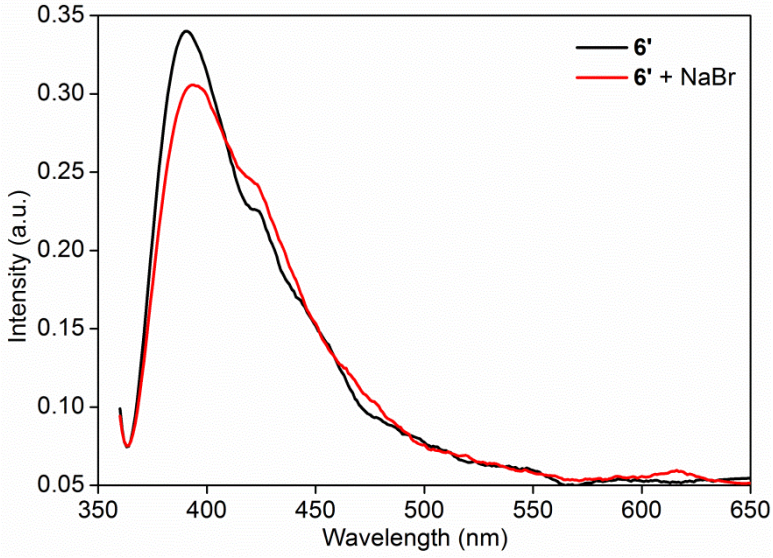

Figure 4B.A6: Fluorescence response of **6'** before and after addition of NaBr.

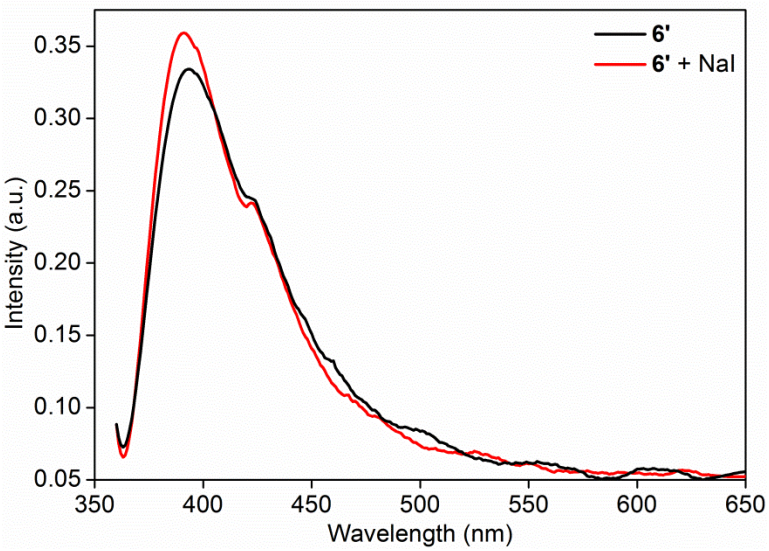

Figure 4B.A7: Fluorescence response of **6'** before and after addition of NaI.

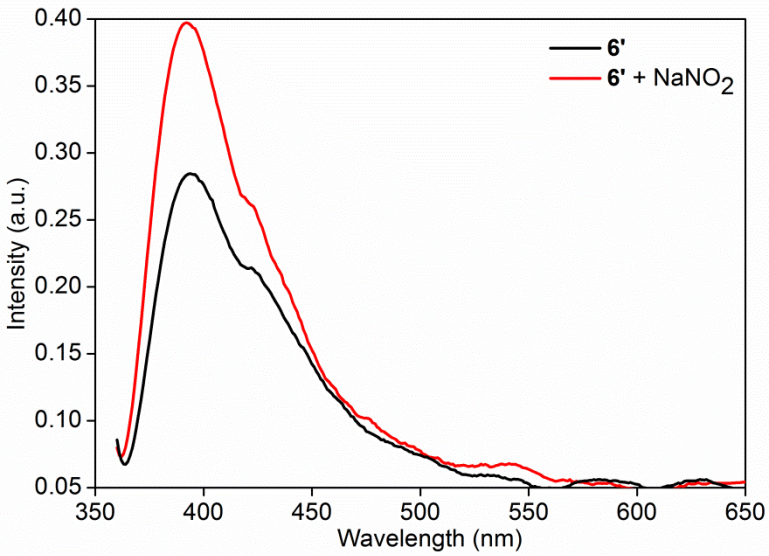

Figure 4B.A8: Fluorescence response of **6'** before and after addition of $NaNO_2$.

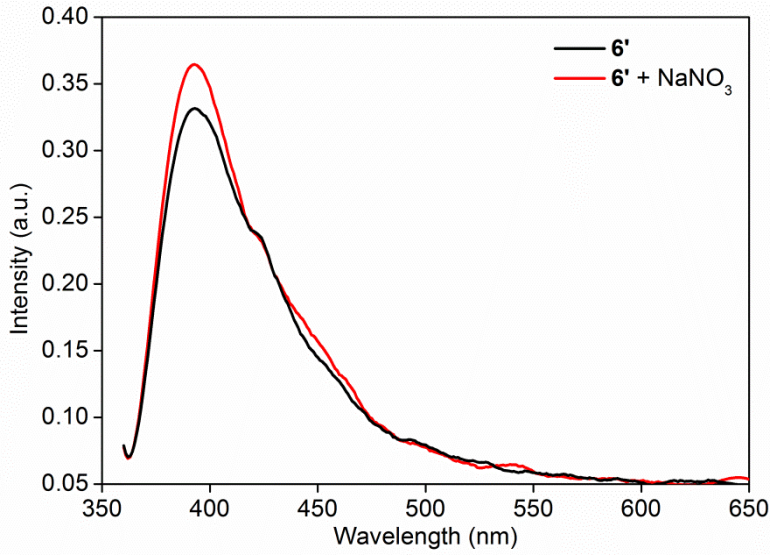

Figure 4B.A9: Fluorescence response of **6'** before and after addition of $NaNO_3$.

Table 2.A1: Crystallographic data for compound **1.**

Identification code	Compound 1
Empirical formula	C12 H7 Cd N O4
Formula weight	341.59
Temperature	150(2) K
Wavelength	0.71073 Å
Crystal system, space group	Monoclinic, $P2_1/c$
Unit cell dimensions	a = 15.385(6) Å
	b = 14.237(5) Å β = 96.622(8) deg.
	c = 6.918(3) Å
Volume	1505.2(10) $Å^3$
Z, Calculated density	4, 1.507 mg/m^3
Absorption coefficient	1.454 mm^{-1}
F(000)	664
Crystal size	0.12 x 0.09 x 0.08 mm
Theta range for data collection	1.95 to 28.84 deg.
Limiting indices	-20<=h<=20, -19<=k<=19, -9<=l<=9
Reflections collected / unique	13633 / 3851 [R(int) = 0.0421]
Completeness to theta = 28.84	97.7 %
Max. and min. transmission	0.8925 and 0.8448
Refinement method	Full-matrix least-squares on F^2
Data / restraints / parameters	3851 / 0 / 163
Goodness-of-fit on F^2	0.938
Final R indices [I>2sigma(I)]	R1 = 0.1483, wR2 = 0.3883
R indices (all data)	R1 = 0.1592, wR2 = 0.3921
Largest diff. peak and hole	14.200 and -7.308 $e.Å^{-3}$

Table 2.A2: HOMO and LUMO energies calculated for explosive analytes (at B3LYP/6-31G* level of theory.

Analytes	HOMO (ev)	LUMO (eV)	Band gap (eV)
TNP	-8.2374	-3.8978	4.3396
TNT	-8.4592	-3.4926	4.9666
1,3-DNB	-7.9855	-3.4311	4.5544
2,6-DNT	-7.6448	-3.2877	4.3571
2,4-DNT	-7.7645	-3.2174	4.5471
RDX	-8.245	-2.531	5.7140
NB	-7.5912	-2.4283	5.1629
DNMB	-8.2298	-2.3875	5.8423
NM	-8.026	-1.8994	6.1266

Permissions

1) **Chapter 1:** Partly adapted with permission from (*Chem. Asian J.* **2014,** *9,* 2358-2376). Copyright (2015) John Wiley and Sons.

2) **Chapter 2:** Partly adapted with permission from (*Inorg. Chem.* **2012,** *51,* 572-576). Copyright (2012) American Chemical Society.

3) **Chapter 2:** Adapted with permission from (*Angew. Chem. Int. Ed.* **2013,** *52,* 2881-2885). Copyright (2013) John Wiley and Sons.

4) **Chapter 3A:** Adapted with permission from (*Chem. Commun.* **2014,** *50,* 8915-8918). Copyright (2014) The Royal Society of Chemistry.

5) **Chapter 3B:** Adapted with permission from (*Dalton Trans.* **2015,** doi: 10.1039/C5DT00397K.). Copyright (2015) The Royal Society of Chemistry.

6) **Chapter 4A:** Adapted with permission from (*Sci. Rep.* **2014,** doi:10.1038/srep07053). Copyright (2014) Nature Publishing Group.